



STScI | SPACE TELESCOPE
SCIENCE INSTITUTE

Instrument Science Report HST+COS 2018-XX

Cycle 20–24 HST+COS Target Acquisition Monitoring

Steven V. Penton

April 18, 2018

ABSTRACT

This ISR documents the Cosmic Origins Spectrograph (COS) Target Acquisition (TA) annual monitoring programs for HST Cycles 20–24, with additional information about COS TA performance determined from data of the C17–C23 FGS-to-SI alignment programs. During this period, NUV exposures were obtained at the nominal (LP1) position, and FUV exposures were executed at Lifetime Positions LP2 and LP3. These programs were designed to monitor numerous aspects of both imaging and spectroscopic TAs, including checking the TA subarrays, the NUV SIAF entries, the telescope slew distances, and evaluating the accuracy of numerous COS flight software (FSW) patchable constants required for TA. This project verified that all three COS TA modes (FUV spectroscopic, NUV spectroscopic, and NUV imaging) were, on large, behaving nominally in Cycle 20–24, and determined that no SIAF or FSW parameter updates were required during this time, with the exception of changes to MIRRORB ACQ/IMAGE in 2014. These changes included a changing of the lamp current from LOW to MEDIUM, an adjustment of the LTACAL exposure time, and a modification of both the MIRRORB WCA and PSA/BOA ACQ/IMAGE TA subarrays.

Contents

1	Introduction	5
1.1	Introductory Notes and Conventions	6
1.2	COS TA Monitoring Program History	9
1.3	COS centroid measurements	9
1.4	ISR Organization	11
2	COS TA Operations Summary	12
2.1	COS TA Centering Requirements	13
3	Program Descriptions	15
3.1	FGS-to-SI Programs	15
3.2	COS TA Monitoring Program Structure	16
3.3	Differences between C20–C24 HST+COS TA monitoring programs	17
3.4	Exposure Lists	20
4	Verifying the TA (ACQ/) Subarrays	28
4.1	COS NUV Imaging TA subarrays	29
4.2	COS NUV Spectroscopic TA Subarrays	29
4.3	COS FUV Spectroscopic TA Subarrays	32
4.4	Trimming of COS FUV TA subarrays due to FUVB “Hot-Spot”.	33
5	NUV Imaging TA verification	37
5.1	Baseline Bootstrapping of ACQ/ IMAGE Modes	37
5.2	Co-alignment of ACQ/ IMAGE Configurations	39
5.3	WCA Lamp Images (aka, Lamp Family Portraits)	43
6	SIAF Verification	50
6.1	COS SIAF History	50
6.2	C17–C23 COS to SIAF Alignment	53
7	COS TA Slew Accuracy	57
8	Spectroscopic TA Verification	59
8.1	NUV Spectroscopic TA verification	59
8.2	FUV Spectroscopic TA verification	60
9	Results and Conclusion	63
10	Acknowledgements	64
11	Change History for COS ISR 2018-XX	64
12	References	66

List of Figures

1	C21 WCA Lamp ‘Family Portrait’	47
2	C22 WCA Lamp ‘Family Portrait’	48
3	C23 WCA Lamp ‘Family Portrait’	48
4	C24 WCA Lamp ‘Family Portrait’	49
5	Illustration of COS SIAF Entries	53
6	COS Aperture Orientation	56

List of Tables

1	ACQ/ to LTA Conversion Table	8
2	ACQ/IMAGE Measurement Uncertainties	10
3	COS TA Centering Requirements	14
4	Historical List of FGS-to-SI proposals used for COS TA Monitoring.	16
5	COS/NUV TA Monitoring Imaging Exposures - PSA	22
6	COS/NUV TA Monitoring Imaging Exposures - BOA	23
7	COS/NUV TA Monitoring Imaging Exposures - WCA only	24
8	COS Cross-Dispersion (XD) Aperture Positions (<i>APERXPOS</i>)	25
9	NUV Spectroscopic TA Monitoring Exposures	26
10	FUV TA Monitoring Exposures	27
11	2009–2011.016 ACQ/IMAGE and ACQ/SEARCH Subarrays.	29
12	2011.017–Present COS ACQ/SEARCH TA Subarrays.	30
13	2011.017–2014.299 ACQ/IMAGE Subarrays.	30
14	2014.300–Present ACQ/IMAGE Subarrays.	30
15	FITS Reported TA ACQ/IMAGE Subarrays	31
16	NUV Spectroscopic ACQ/SEARCH and PEAKD Target Subarrays	32
17	NUV ACQ/PEAKXD Subarray “XC”s	32
18	FUV WCA Subarrays for LP1–4	33
19	FUVA SA Subarrays for LP1–4	34
20	FUVB PSA/BOA Subarrays for LP1–4	35
21	PCTA-[X,Y]IMCALTARGETOFFSET Values	38
22	C17–C20 PSA ACQ/IMAGE Co-alignment Measurements	39
23	C21–24 ACQ/IMAGE Bootstrapping Results	40
24	ACQ/IMAGE Bootstrapping Measurements Sorted by Configuration	41
25	ACQ/IMAGE Co-alignment Measurements	44
26	Initial ACQ/IMAGE Co-alignment Measurements	45
27	C20–C24 ACQ/IMAGE Co-Alignment Results	46
28	History of COS SIAF Changes and FGS Alignment Activities	51
29	Active COS SIAF ^a Entries	52
30	C17–C23 FGS-to-SI Program Initial Pointing Determinations	54
31	C17–C23 SIAF vs PSA×MIRA ACQ/IMAGE Residuals	55
32	C17–23 FGS-to-SI Program Pointing Accuracy	58
35	NUV Spectroscopic ACQ/PEAKXD Monitoring	61

Instrument Science Report HST+COS 2018-XX

36 FUV Spectroscopic ACQ/PEAKXD Monitoring	62
--	----

1 Introduction

Preliminary results of the Hubble Space Telescopes' (HST) Cosmic Origins Spectrograph (COS) annual target acquisition (TA) monitoring programs reviewed here were previously reported in the following COS ISRs:

- COS ISR 2015-02 (Summary of the COS Cycle 20 Calibration Program)
- COS ISR 2015-06 (Summary of the COS Cycle 21 Calibration Program)
- COS ISR 2016-03 (Summary of the COS Cycle 22 Calibration Program)
- COS ISR 2016-09 (Cycle 22 COS Target Acquisition Monitor Summary)
- COS ISR 2017-18 (Cycle 23 COS Target Acquisition Monitor Summary)
- COS ISR 2018-09 (Cycle 24 COS Target Acquisition Monitor Summary)

The information in this ISR supersedes any previous preliminary results or conclusions.

This ISR provides details on the following HST+COS calibration programs:

- P13124 (COS Imaging TA and Spectroscopic WCA-PSA/BOA offset verifications, Cycle 20)
- P13526 (COS Imaging TA and Spectroscopic WCA-PSA/BOA offset verifications, Cycle 21)
- P13972 (COS Imaging TA and Spectroscopic WCA-PSA/BOA offset verifications, Cycle 22)
- P14440 (COS Imaging TA and Spectroscopic WCA-PSA/BOA offset verifications, Cycle 23)
- P14857 (COS Imaging TA and Spectroscopic WCA-PSA/BOA offset verifications, Cycle 24)

In many ways, this ISR is a followup to the initial on-orbit COS TA ISR (COS ISR 2010-14; Keyes & Penton, 2011) and TIR (COS TIR 2010-03; Penton & Keyes, 2011). We will refer to these documents where appropriate, and will follow the naming conventions in these documents as described in § 1.1.

1.1 Introductory Notes and Conventions

There are a few COS conventions to be established before discussing the TA monitoring in detail.

1. COS TAs are performed in raw or “detector” coordinates, not the “user” coordinate system of calibrated COS files. To avoid confusion over the different coordinate systems, we will use along-dispersion (AD) and cross-dispersion (XD) whenever possible. All references to the coordinates “ X_{DET} ” and “ Y_{DET} ” are in the detector coordinate system unless otherwise specified. In NUV detector coordinates, $+X_{DET}$ is -XD and $+Y_{DET}$ is -AD. In FUV detector coordinates, $+X$ is -AD and $+Y$ is +XD. The transformations between user and detector coordinates are:

$$\text{NUV} : X_{USER} = 1023 - Y_{DET} \quad (1)$$

$$\text{NUV} : Y_{USER} = 1023 - X_{DET} \quad (2)$$

$$\text{FUV} : X_{USER} = 16383 - X_{DET} \quad (3)$$

$$\text{FUV} : Y_{USER} = Y_{DET} \quad (4)$$

2. When referencing NUV pixels, we will abbreviate pixel as p. For the FUV, we use rows or columns to reference the FUV digital elements, as the FUV detector does not have physical pixels.
3. When discussing the various subarrays used during COS TA, boxes will be specified by giving the lowest valued corner (C) and full size (S) for both X and Y. A box is fully specified by giving its XC, XS, YC & YS. In this ISR, these will always be given in detector coordinates as these are how they are implemented in the HST ground commanding.
4. To clarify the names and locations of TA parameters, the following convention will be used:
 - COS TA modes and their Astronomers Proposal Tool (APT) optional parameters will be in *Courier* (e.g., ACQ/IMAGE and NUM_POS).
 - Keywords in FITS headers will be in *ITALICIZED ALL CAPITALS* (e.g., ACQSLEWY).
 - Flight SoftWare (FSW) parameters and routines will be in *SIMALL CAPITALS*. All TA FSW patchable constants begin with “PCTA_” (e.g., PCTA_CALTARGETOFFSET). In this ISR, this prefix is considered implied after the initial introduction of a PCTA_paramater, and will not always be included. FSW patchable constants relating to mechanism positions begin with PCMECH_ and will always be included in references.
 - Archived COS files are in FITS (.fits) format. FITS filenames, or portions of a file-name, will be in *sans-serif* (e.g., ld9mg2nrq_rawtag.fits or _spt.fits). COS filenames are in the form IPPPSSOOT_*extension*.fits. The HST naming convention breaks down for COS as I=Instrument=“L”, PPP=Program ID, SS=Visit ID, OO=Exposure ID, and T=“Q” for nominally recorded observations. See the COS Data Handbook (DHB, Fox et al. 2015) for a full breakdown of the HST IPPPSSOOT naming conventions. COS TA files have the *extension* of rawacq, and additional information useful for TA analysis is contained in the IPPPSSOOT_spt.fits files known as the support file, and in the IPPPSSOOT_jit/f.fits files known as the jitter files.

5. COS contains numerous FUV and NUV central wavelength settings, which are defined in the FSW by the OSM1 or OSM2 rotation positions. In this ISR, the term *CENWAVE*, which is also the FITS keyword name, will be used to mean any of the pre-defined OSM1 + OSM2 rotation settings that uniquely define a central wavelength setting.
6. COS *CENWAVE*s are named for the (predicted) lowest wavelength that lands on the FUVA detector segment for *FP-POS*=3. For convenience, when referring to a specific *CENWAVE* we will either call out the grating and *CENWAVE* in use as *GRATING/CENWAVE* (e.g. G130M/1222), or just use a leading “C” to identify a particular *CENWAVE* (e.g., C1222) in the same manor as “G” is used for *GRATING* (e.g., G130M). Note that the FITS header keyword equivalent of *GRATING* is *OPT_ELEM*.
7. Unless specified, all spectroscopic exposures were taken at *FP-POS*=3.
8. When referring to an HST program number, we will use either “HST PID” or a leading “P” in a similar fashion an “C=*CENWAVE*” and “G=*GRATING*”.
9. The COS FUV detector has two independent segments, Segment-A and Segment-B. In this ISR, they will be referred to as FUVA & FUVB.
10. ACQ/IMAGE can use either of two “MIRROR” modes, MIRRORA or MIRRORB. In this ISR, they will sometimes be referred to as MIRA & MIRB to save space, mainly in tables and captions.
11. Following the conventions used in APT and the Phase II Proposal Instructions (Rose et al., 2017), NUV ACQ/PEAKXD exposures will specify which STRIPE¹ is used during TA. In this ISR, we will always use the APT default (STRIPE=DEF) for a given *CENWAVE*. This default is STRIPE=MEDIUM (or STRIPE=B) for all *CENWAVE*s, except G230L/3360 where it is STRIPE=SHORT (STRIPE=A).
12. When referring to a particular day, we will use YEAR.DAY. For example, day 60 of 2010 will be referred to as 2010.060.
13. HST observations are grouped in approximately annual “cycles”. ‘C##’ will be used as shorthand for “HST Cycle ##” (e.g., Cycle 19 = C19).
14. Unit abbreviations:
 - Milli-arcseconds (0.001") will be abbreviated as mas.
 - Milli-amperes (0.001 A) will be abbreviated as mA.
 - Counts per second will be abbreviated as cps.
15. COS has two internal PtNe wavelength calibrations lamps that send light through the Wavelength Calibration Aperture (WCA) and onto the detectors. The two PtNe lamps are referred to in this ISR as **P1** and **P2**. Each lamp has three current settings, LOW, MEDIUM (MED) or HIGH. The **P1** lamp is used for spectroscopic lamp flashes during science exposures

¹STRIPE is the optional parameter name in APT, therefore the Courier font is used.

Table 1. ACQ/ to LTA Conversion Table

ACQ/ Mode	FSW	Comments
ACQ/ IMAGE	LTAIMCAL LTAIMAGE	Calibrate Image Aperture Location for LTAIMAGE NUV Image Acquisition
ACQ/ SEARCH	LTASEARCH	Spiral Target Search
ACQ/ PEAKD	LTAPKD	Peakup in the Dispersion Direction (AD)
ACQ/ PEAKXD (NUM_POS=1)	LTACAL LTAPKXD	Calibrate Aperture Location for LTAPKXD Peakup in the Cross-Dispersion Direction (XD)
ACQ/ PEAKXD (NUM_POS>1)	LTAPKD	Peakup in the Dispersion Direction, but modified in LV54 for XD

Note. — LV54 is the COS FSW Version 4.16 update. GSFC SCRC#352 adapted LTAPKD for XD use in LV54 and was installed on HST on 2014.133.

(“TAGFLASH”es), while the **P2** lamp is used for all TA exposures. Both lamps have MED current settings of 10 mA, but the **P1** lamp has LOW/HIGH current settings of 6/18 mA. The **P2** lamp has LOW/HIGH current settings of 3/14 mA. COS lamp output generally scales as current² ($P = I^2 R$).

16. STScI uses a problem reporting (PR) system to track HST changes. Where applicable, these STScI PR identifying numbers will be included as *PR#*.
17. Goddard Spaceflight Center (GSFC) use a Software Change Request (SCR) system to document HST FSW changes. COS requests are identified by their SCRC#.
18. Each COS ACQ/ mode calls one or more FSW routines which interact with HST+COS to perform the TA. The FSW routine names begin with LTA. The FSW routines called by each ACQ/ mode are given in Table 1.
19. We use the FSW NUV imaging plate scales values² of 0.02352"/p (AD) and 0.02362"/p (XD) as these are in agreement with the SMOV results of Goudfrooij et al., 2010. We also assume the NUV detector orientation as described in Goudfrooij et al., 2010 (a 0.52° rotation between the NUV detector coordinates and the APT POS_TARG system).

²The C25 COS IHB (Fox et al., 2017) does not differentiate between AD and XD NUM imaging plate scales, and lists 0.0235 "/p for both AD and XD.

1.2 COS TA Monitoring Program History

After the installation of COS into HST in 2009 (STS-125), and the servicing mission orbital verification (SMOV) phase, a series of calibration programs in NUV imaging mode carefully determined the two-dimensional offset from the COS WCA to the center of the Primary Science Aperture (PSA) when observed with MIRA. A target was then centered using a PSA×MIRA ACQ/ IMAGE, and a target image was taken along with a MIRB image of the WCA image. These images were used to determine the AD and XD offsets of the PSA×MIRB image target and WCA centroids. This bootstrapping procedure was repeated with the BOA×MIRA and BOA×MIRB ACQ/ IMAGE modes until all four ACQ/ IMAGE modes were co-aligned.

The FGS-to-SI programs perform a PSA×MIRA ACQ/ IMAGE on a target that should be approximately centered in the aperture. After some post-processing analysis of the spacecraft telemetry, the PSA×MIRA ACQ/ IMAGE can be used to estimate the accuracy of the NUV PSA aperture position in the SIAF³.

1.3 COS centroid measurements

The COS FSW uses either a mean or a median to calculate spectral XD locations and imaging wavelength lamp center centers. On the NUV channel, medians are always used, while for FUV, a mean is always used. This behavior is controlled by the following FSW patchable constants :

1. pcta_UseMedian4CAL4FUV

Description: Flag to indicate whether to use “median” or “mean” for the calculation of the cross-dispersion coordinate of the wavelength calibration lamp spectrum in the phase LTACAL for the FUV detector.

Format: Boolean

Limits/Ranges: TRUE = use median; FALSE = use mean

Current Value⁴: FALSE (use mean)

2. pcta_UseMedian4CAL4NUV

Description: Flag to indicate whether to use ‘median’ or ‘mean’ for the calculation of the cross-dispersion coordinate of the cal lamp spectrum in the phase LTACAL for the NUV detector.

Format: Boolean

Limits/Ranges: TRUE = use median; FALSE = use mean

Current Value : TRUE (use median)

3. pcta_UseMedian4PKXD4FUV

Description: Flag to indicate whether to use ‘median’ or ‘mean’ for the calculation of the cross-dispersion coordinate of the target spectrum in the phase LTAPKXD for the FUV detector.

Format: Boolean

Limits/Ranges: TRUE = use median; FALSE = use mean

Current Value : FALSE (use mean)

4. pcta_UseMedian4PKXD4NUV

Description: Flag to indicate whether to use ‘median’ or ‘mean’ for the calculation of the cross-dispersion coordinate of the target spectrum in the phase LTAPKXD for the NUV detector.

Format: Boolean

³Science Instrument Aperture File (Mallo, 2008)

Limits/Ranges: TRUE = use median; FALSE = use mean

Current Value : TRUE (use median)

During COS TA, all ACQ/ procedures operate in ACCUM mode (no individual photon events, no pulse-height information, and no calibrations) and operate using integer values only. For ACQ/IMAGE, the WCA lamp image location is determined using a median in each coordinate. Therefore, a ± 0.5 p uncertainty is present during each LTAIMCAL measurement when determining the center of the SA position for the LTAIMAGE portion of the ACQ/IMAGE. The target location phase of ACQ/IMAGE (LTAIMAGE) uses a flux-weighted centroid over a 9×9 checkbox, which is described in detail in the COS IHB (C25, Fox et al., 2017: Section 8.4, “ACQ/IMAGE Acquisition Mode”) and in § 4.2 of COS TIR 2010-03 (Penton & Keyes, 2010). A point source in a PSA \times MIRA image produces an approximately Gaussian image with a FWHM of ~ 2.5 p. The 9×9 checkbox considers the majority of the target ($> 70\%$ ⁵) light while minimizing background contamination,⁶ and should find the target center to within $\pm \frac{1}{3}$ p. Combined LTAIMCAL and LTAIMAGE TA stages have a combined uncertainty of $\sqrt{\frac{1}{2}^2 + \frac{1}{3}^2}$ p = 0.6 p. ACQ/IMAGE relies upon the WCA-to-SA offset, which was measured in a similar way and has the same uncertainty. Therefore, the total uncertainty of a PSA \times MIRA ACQ/IMAGE is $\sqrt{2} \cdot 0.6$ p = 0.85 p in each direction ($\sim 0.020''$). As the ACQ/IMAGE configurations were bootstrapped from the PSA \times MIRA configuration, their uncertainties follow an identical derivation and are given in Table 2.

Additionally, the COS aperture mechanism is repeatable in the XD direction to ± 1 motor step (0.053''), as reported by the header keyword *APERYPOS*. In addition, the WCA location phase of the ACQ/IMAGE (LTAIMCAL), which uses the median integer pixel location as the lamp location, cannot measure the WCA position to better than $\frac{1}{2}$ pixel in either AD or XD. On the NUV detector, an imaging pixel is 0.02352'' (AD) and 0.02362'' (XD), so there is an intrinsic radial uncertainty of $\sim 0.017''$ after each LTAIMCAL. Occasionally, the motion from the PSA to the BOA misses by up to ± 2 *APERYPOS* steps. However, in the data of this ISR, this was not observed, and this uncertainty is not included in our error estimates.

Table 2 ACQ/ IMAGE Measurement Uncertainties

Configuration	WCA-to-SA Offset Uncertainty	ACQ/ IMAGE WCA+SA Measurement Uncertainty	Total ACQ/ IMAGE Uncertainty
PSA \times MIRA	$\sqrt{\frac{1}{2}^2 + \frac{1}{3}^2}$ p = 0.6 p	0.6 p	$\sqrt{2} \cdot 0.6$ p = 0.85 p ($\sim 0.020''$)
PSA \times MIRB	$\sqrt{2} \cdot 0.6$ p = 0.85 p	0.6 p	$\sqrt{3} \cdot 0.6$ p = 1.04 p ($\sim 0.024''$)
BOA \times MIRA	$\sqrt{3} \cdot 0.6$ p = 1.04 p	0.6 p	$\sqrt{4} \cdot 0.6$ p = 1.20 p ($\sim 0.028''$)
BOA \times MIRB	$\sqrt{4} \cdot 0.6$ p = 1.20 p	0.6 p	$\sqrt{5} \cdot 0.6$ p = 1.34 p ($\sim 0.032''$)

For NUV ACQ/PEAKXD, the same ± 0.5 p uncertainty is present in both the spectral and target locations portions of the LTAPKXD. Combined in quadrature, this implies that an LTAPKXD has an inherent XD centering accuracy of no less than $\sqrt{2} \cdot 0.5$ p = 0.7 p = 0.017''. For FUV LTAP-KXD, a mean is used to measure both the WCA lamp spectrum XD location and the target XD

⁵PSA \times MIRB, BOA \times MIRA, and BOA \times MIRB 9×9 checkbox fractions are $\sim 51\%$, 38% , and 28% , respectively.

⁶As of April, 2018, the average NUV detector background was $\sim 8.2E-4$ cps.

location. For FUV LP1–3, uncorrected geometric and thermal distortions can cause targets with different spectral energy distributions (SEDs) to center differently. This effect has been measured (Penton & Keyes, 2010) to be as large at ± 2 rows or $\sim 0.2''$.⁷

1.4 ISR Organization

In § 2 we will discuss the concepts involved in the TA monitoring strategy along with a basic review of COS TA operations and centering requirements (§ 2.1).

In § 3 we discuss the programs discussed in this ISR. § 3.2 discusses the details of the individual COS TA monitoring programs and, the annual HST FGS-to-SI alignment programs and their connection to the COS TA monitoring programs are discussed in § 3.1. In § 3.4 we list and discuss the individual program exposures.

In § 4 we discuss the numerous detektor subarrays used in COS TA, and their verification by the programs in this ISR. The NUV imaging subarrays are discussed in § 4.1, and the NUV and FUV spectroscopic subarrays are discussed in § 4.2, and § 4.3, respectively.

In § 5 we discuss the verification co-alignment of the four COS ACQ/IMAGE configurations.

In § 6 we discuss the relationship and history of the COS SIAF (Science Instrument Aperture File), and discuss the verification of the C17–C24 NUV entries (§ 6.2).

In § 7 we use information from the FGS-to-SI programs to estimate the accuracy of COS TA slews.

In § 8 we discuss the verification of the FSW parameters, lamp operations, and subarrays associated with COS spectroscopic TAs.

Results and Conclusions are presented in § 9.

⁷At FUV LP4 this effect is even more pronounced and prohibits LTAPKXD (NUM_POS=1 ACQ/PEAKXD) from achieving the centering requirement of $\pm 0.3''$. For this reason, the ACQ/PEAKD FSW routine LTAPKD was enabled for XD usage in FSW version LV58 (installed 2014.132 and initially tested on-orbit on 2014.300 in P13636).

2 COS TA Operations Summary

There are three modes of Target Acquisition (TA) for the Cosmic Origins Spectrograph (COS); NUV imaging, NUV spectroscopic, and FUV spectroscopic. There are four COS TA (ACQ/) procedures; ACQ/IMAGE, ACQ/PEAKD, ACQ/PEAKXD, and ACQ/SEARCH. ACQ/PEAKD and ACQ/SEARCH step the telescope through dwell patterns on the sky. As long as the target light falls correctly within the TA detector subarrays, ACQ/PEAKD and ACQ/SEARCH will continue to nominally assist in TA (barring any unforeseen anomalies, such as detector ‘hot-spots’). The ACQ/IMAGE and ACQ/PEAKXD procedures also rely on the subarrays, but also rely on numerous patchable (changeable) constants in the COS flight software (FSW) which assist in target centering.

In both ACQ/IMAGE and ACQ/PEAKXD, the internal wavelength calibration lamp is flashed to locate the center of the wavelength calibration aperture (WCA). From this location, the center of the science aperture (SA) in use, which could be the PSA or BOA, can be predicted by applying the FSW constants that give the SA offset compared to the WCA center. For ACQ/IMAGE, the offset is in both detector ‘ X_{DET} ’ (along-dispersion, AD) and ‘ Y_{DET} ’ (cross-dispersion, XD). For ACQ/PEAKXD, which uses dispersed light, this offset is only in the XD direction.

To combat the effects of FUV gain sag, the FUV ACQ/PEAKXD algorithm was modified in C19 to only use the FUVA segment. All FUV ACQ/PEAKXD exposures discussed in this ISR are FUVA-only.⁸

BOA spectroscopic TAs were not supported during C19–C24, accordingly the programs discussed here only verify PSA spectroscopic TAs. WCA-to-PSA offsets are used in ACQ/PEAKXDs, and each COS grating has a different XD offset. These offsets are both grating (*OPT_ELEM*) and lifetime position (LP) dependent.⁹ The programs listed here verify the NUV LP1 as well as FUV LP2¹⁰ and LP3¹¹. FUV LP4 uses a different ACQ/PEAKXD algorithm (NUM_POS>1), and, like ACQ/PEAKD, does not use the WCA-to-SA XD offsets¹².

The initial HST/COS target pointing is based on definitions of the physical locations of the COS apertures in terms of [V2,V3] in the Science Instrument Aperture File (SIAF). The NUV (LP1) SIAF entries are verified in this program (§ 6.2), while the FUV entries are verified in the FUV LP enabling programs and ISRs.

These programs, and this ISR, do not attempt to monitor the AD accuracy of the COS spectroscopic TA modes.¹³ This ISR does not attempt to monitor other aspects of COS TA which require a higher than annual cadence such as lamp count rates and average GO ACQ/ slews (aka, ‘Blind Pointing’).

⁸The change went into effect on April 18, 2011 (2011.101) with PR#67985.

⁹In the COS FSW, these WCA-to-SA XD offsets are stored in the PCTA_CALTARGETOFFSET table.

¹⁰The default COS FUV spectral location for all *CENWAVEs* was moved from LP1 to LP2 on July 23, 2012 (2012.205).

¹¹The default COS FUV spectral location was moved to LP3 on February 15, 2015 (2015.046) for all *CENWAVEs* except G130M/1055 and G130M/1096, which still operate at LP2. On October 2, 2017 (2017.275), the default FUV spectral location was moved to LP4, with additional observing and TA constraints as outlined on the COS2025 website (<http://www.stsci.edu/hst/cos/cos2025>).

¹²All NUV and FUV LP1–3 ACQ/PEAKXD observations use the optional parameter, NUM_POS=1.

¹³For ACQ/PEAKD, short-term fluctuations of the detector background rate due to environmental conditions remains the largest source of AD pointing error.

2.1 COS TA Centering Requirements

The COS TA centering requirements are based upon wavelength accuracy requirements in the AD, and for flux and resolution optimization in the XD.¹⁴ The strictest [AD,XD] NUV requirements are [0.041, 0.3]”, while for the FUV they are [0.106, 0.3]”.¹⁵ Since the AD requirement is in units of km s^{-1} , it is detector, grating, and wavelength dependent as defined, generally, in Equation 5, and specifically for each grating in Equations 6–12. Wavelengths assigned to COS data are required to have an absolute uncertainty of less than $\pm 15 \text{ km/s}$ in the medium resolution modes, $\pm 150 \text{ km/s}$ in G140L mode and $\pm 175 \text{ km/s}$ in G230L mode. In the XD direction, the requirement is to be centered to within $\pm 0.3”$, however, our goal is $\pm 0.1”$ for FUV flat-fielding purposes. Since the AD requirement is in units of km/s, it is detector and wavelength dependent shown in Equation 5.

$$\Delta AD(\text{\AA}) = \frac{\text{velocity requirement} \cdot \lambda}{c \cdot \text{dispersion } (\text{\AA}/p) \cdot \text{platescale } (p/”)} \quad (5)$$

$$\Delta AD(G185M@1825\text{\AA}) = \frac{15 \text{ km s}^{-1} \cdot 1825\text{\AA}}{c \cdot 0.037\text{\AA}/p \cdot 42.47p/”} = 0.058” \quad (6)$$

$$\Delta AD(G225M@2250\text{\AA}) = \frac{15 \text{ km s}^{-1} \cdot 2250\text{\AA}}{c \cdot 0.035\text{\AA}/p \cdot 42.47p/”} = 0.076” \quad (7)$$

$$\Delta AD(G285M@2850\text{\AA}) = \frac{15 \text{ km s}^{-1} \cdot 2850\text{\AA}}{c \cdot 0.040\text{\AA}/p \cdot 42.47p/”} = 0.084” \quad (8)$$

$$\Delta AD(G230L@2450\text{\AA}) = \frac{175 \text{ km s}^{-1} \cdot 2450\text{\AA}}{c \cdot 0.390\text{\AA}/p \cdot 42.47p/”} = 0.086” \quad (9)$$

$$\Delta AD(G130M@1300\text{\AA}) = \frac{15 \text{ km s}^{-1} \cdot 1300\text{\AA}}{c \cdot 0.00997\text{\AA}/p \cdot 43.5p/”} = 0.150” \quad (10)$$

$$\Delta AD(G160M@1600\text{\AA}) = \frac{15 \text{ km s}^{-1} \cdot 1600\text{\AA}}{c \cdot 0.01223\text{\AA}/p \cdot 42.9p/”} = 0.153” \quad (11)$$

$$\Delta AD(G140L@1800\text{\AA}) = \frac{150 \text{ km s}^{-1} \cdot 1800\text{\AA}}{c \cdot 0.08030\text{\AA}/p \cdot 45.4p/”} = 0.247” \quad (12)$$

Assuming that the wavelength error budget is split evenly between the COS TA and wavelength scale accuracies, the error budgets for the COS gratings, in arc-seconds (“), are given in Table 2.1. By “evenly” we mean that when added in quadrature the total error budget is that given by the second column of Table 2.1. Setting the TA error budget equal to the wavelength scale accuracy, the AD TA requirement given in the third column is the second column divided by $\sqrt{2}$.

¹⁴The COS requirements are documented in the CEI (Contract End Item) Specification (Smith et. al., 2004).

¹⁵While the XD requirement for all TAs is $\pm 0.3”$, our 1σ goal is $\pm 0.1”$. This goal ensures that spectra fall on a consistent XD location on the the detector, which aids in extraction and calibration accuracy.

Table 3. COS TA Centering Requirements

<i>OPT_ELEM</i>	Total AD Error Budget	AD TA Requirement ^a	XD TA Requirement ^x
(1)	(2)	(3)	(4)
NUV			
G185M	0.058"	0.041"	0.3 (0.1)"
G225M	0.076"	0.054"	0.3 (0.1)"
G285M	0.084"	0.059"	0.3 (0.1)"
G230L	0.086"	0.061"	0.3 (0.1)"
FUV			
G130M	0.150"	0.106"	0.3 (0.1)"
G160M	0.153"	0.108"	0.3 (0.1)"
G140L	0.247"	0.175"	0.3 (0.1)"

^aAssuming the total AD error budget (column 2) is split equally between TA centering and wavelength scale accuracy, the AD TA requirements (column 3) are $1/\sqrt{2}$ of the total AD error budget (equations 6–12).

^xThe XD requirement is 0.3", but our 1σ goal is 0.1".

3 Program Descriptions

COS ACQ/IMAGE has four commonly used combinations of two Science Apertures (SAs), the Primary Science Aperture (PSA) and the Bright Object Aperture (BOA), and two mirror modes, MIRA and MIRB. During the 2009 servicing mission orbital verification (SMOV) phase, a series of C17 calibration programs in NUV imaging mode (P11469, P11473, & P11471) carefully determined the two-dimensional offset from the COS WCA to the center of the PSA when observed with MIRA. These AD (Y_{DET}) and XD (X_{DET}) offsets were loaded in the FSW TA parameters¹⁶. A target was then centered using a PSA×MIRA ACQ/IMAGE, then a target image was taken along with a MIRB image of the WCA image. These images were used to determine the AD and XD offsets of the image target and WCA centroids. These values were uploaded in the FSW paramters. This bootstrapping procedure was repeated with the BOA×MIRA and BOA×MIRB modes until all four ACQ/IMAGE modes were co-aligned.

In the COS TA Monitoring programs described in this ISR, we re-use this bootstrapping strategy to test the co-alignment of all four ACQ/IMAGE modes¹⁷. In addition to COS calibration programs listed above, and described in detail in § 1.2–3.4, COS ACQ/IMAGE exposures obtained in the C17–C23 visits of the “Focal Plane Calibration (SI-FGS Alignment)” series were used in the monitoring discussed in this ISR. These programs were developed by the HST Telescope’s division (PIs Cox and/or Lallo) for Fine Guidance Sensor (FGS) to Science Instrument (SI) alignment, and are described in § 3.1.

All data for a given cycle were intentionally taken contemporaneously to avoid any long-term detector or spacecraft effects from affecting our results. Our requirement was that all data for a given cycles’ TA monitoring were taken within 45 days of each other. There were minor differences in the specific exposures in each cycles TA monitoring program, these are discussed in § 3.3.

All programs verify that the TA subarrays in use for the given cycle were proper for the ACQ/and spectroscopic modes tested, verify the WCA-to-SA offsets, and monitor, as much as possible, the performance of COS TAs.

3.1 FGS-to-SI Programs

From C17–C23, an FGS-to-SI program was executed with COS visits twice a year. These programs contained COS exposures designed to assist in the monitoring of the COS NUV alignent to HST. These programs used the same two target stars with COS in visits spaced six months apart. Both visits observed the astrometric open cluster M35, at orientations that were 180° apart. The two stars observed were 206W3 (in the Fall) and 427W3 (in the Spring). Due to orbital time constraints, the exact content of the COS visits in these programs varied from year to year. The COS TA Monitoring programs were timed to execute within 45 days of the Fall observations of 206W3.

The COS portion of each program begins with a PSA×MIRA ACQ/IMAGE on a target should be approximately centered due to observations with other instruments earlier in the visit. Post-

¹⁶In the COS FSW, these WCA-to-SA offsets are stored as patchable constants in the PCTA_XIMCALTARGETOFFSET (XD) and PCTA_YIMCALTARGETOFFSET (AD)

¹⁷The underlying assumption of these programs is that the PSA×MIRA ACQ/IMAGE centering relative to the aperture center has not changed since SMOV. This includes the assumption that the WCA-to-SA offsets have remained stable over C17–C24.

Table 4. Historical List of FGS-to-SI proposals used for COS TA Monitoring.

PID	Cycle	Summary of Contents
P11878	C17	2 sets of PSA ACQ/ IMAGES, Target+Lamp TT images, & G230L Spectra
P12399	C18	2 sets of PSA ACQ/ IMAGES, 1 set of Target+Lamp TT images + G230L Spectrum (427W3)
P12781	C19	2 sets of PSA ACQ/ IMAGES
P13171	C20	2 sets of PSA ACQ/ IMAGES
P13616	C21	2 sets of PSA ACQ/ IMAGES
P14035	C22	2 sets of PSA ACQ/ IMAGES
P14452	C23	2 sets of PSA ACQ/ IMAGES, with Lamp-Only TT images after each ACQ/ IMAGE

observation telemetry data¹⁸, and the results of the ACQ/ IMAGE, are used to refine this assumption. This process verifies the COS NUV PSA aperture position¹⁹ as described in § 6.2.

After this PSA×MIRA ACQ/ IMAGE, a PSA×MIRB ACQ/ IMAGE is then performed (together, a “set”). This bootstraps the PSA×MIRB centering to the PSA×MIRA (a measure of COS TA precision) and to the SIAF verification (a measure of its accuracy relative to HSTs’ definition of the COS aperture center). This allows us to monitor the properties of the PSA×MIRB image in a controlled way on a centered target. Due to the nature of the FGS-to-SI alignment program, it was not practical to place the COS exposures into ‘non-interruptible’ sequences. As discussed in § 6.2, this had some minor impacts on some of the PSA×MIRB ACQ/ IMAGES.

The historical list of FGS-to-SI proposals, HST cycles (C##), and content are given in Table 4. Where possible, time-tag (TT) images of the lamps and/or targets, along with NUV G230L spectra were acquired.

3.2 COS TA Monitoring Program Structure

Each cycles TA monitoring program contains three single-orbit visits. The number of visits is mandated by the bootstrapping technique between the four different ACQ/ IMAGE SA×MIR configurations.

Each visit begins with a comparison of the centering of two ACQ/ IMAGE modes out of the possible four science apertures (SA, PSA or BOA) × (MIRA or MIRB). This back-to-back process allows us to test that all ACQ/ IMAGE modes are centering the target to the same point in the aperture. This comparison involves not only the ACQ/ IMAGES, but NUV detector images of the PtNe lamp (WCA) image and, if possible, coeval target images. These direct lamp+target comparisons are only available for the PSA modes. For the BOA modes, the WCA lamp images and target images are taken consecutively. The lamp+target exposures are interleaved throughout the visit and are available to measure and verify the imaging WCA-to-SA offsets are still accurate for each HST Cycle. Images will usually use the PtNe#2 (**P2**) lamp, as it is the primary TA lamp, but some images will use PtNe#1 (**P1**) to monitor both lamps in imaging mode.

¹⁸The [V2,V3] positions reported in the telemetry have an uncertainty of ∼ 10 mas (Cox, private communication).

¹⁹Specifically, the *LFPSAA* SIAF entry.

In its generic format, the three, one-orbit, visits are configured as follows:

- The 1st orbit on each program is designed to test the co-alignment of the PSA×MIRA and PSA×MIRB ACQ/IMAGE configurations. However, this exact configuration of ACQ/IMAGE occurs at the end of each semi-annual visit in the FGS-to-SI alignment programs (see § 3.1). This visit was usually treated as an on-hold contingency visit in case, for whatever reason, the fall visit of the program did not execute in a given cycle. The target for this contingency visit is 206W3, the same target as the Fall visit of the FGS-to-SI alignment program. In one case, (C22, P13972), this visit was re-purposed to verify a change to the MIRBACQ/IMAGE configuration required due to the increasing background (see PR#78749).
- The 2nd orbit of each program takes back-to-back PSA×MIRB and BOA×MIRA ACQ/IMAGEs and target (WD1657+343) TIME-TAG images (with lamp flashes). A second PSA×MIRB ACQ/IMAGE is then performed to provide a second measurement of the offset. Additionally, NUV and FUV spectra are acquired to test their WCA-to-PSA offsets.
- The 3rd orbit of each program takes back-to-back BOA×MIRA and MIRB ACQ/IMAGEs and target (HIP66578) TIME-TAG images (with lamp flashes). As in the 2nd orbit, a second BOA×MIRA ACQ/IMAGE is then performed to provide a second measurement of the offset. Additional NUV and FUV spectra are acquired to the remaining WCA-to-PSA offsets not tested in the 2nd orbit.
- All visits were executed in APT 3-Gyro mode (3GOBAD) with the BASE1B3 guide star requirement set in APT.

The exact configuration of which gratings and CENWAVEs were spectroscopically tested varied with each cycle as the programs evolved. Specifically, with the 2015 change in OSM2 home position²⁰, NUV spectra were re-ordered for efficiency and some NUV CENWAVEs were changed to those that are known to have strong STRIPE=B WCA spectra against the increasing detector background (Fix, 2018) and declining NUV sensitivity (Taylor, 2017). In C21–C24, we took G160M/1600 exposures offset in XD by $\pm 0.7''$ ²¹ to test for the effects of gain sag induced ‘Ywalk’ on FUV spectra. In addition, one visit of each program, usually the second visit, performed an annual “family portrait” of all the P1/P2 MIRA/MIRB WCA lamp images to track any drifting of the centroids, or changes in the lamps with time. The ‘Family Portrait’ lamp images are discussed in § 5.3. Further details on the differences between the programs is provided in § 3.3.

3.3 Differences between C20–C24 HST+COS TA monitoring programs

There are several important differences between the various versions of the COS TA monitoring programs:

- In the initial, C20, version of the TA monitoring program (P13124), the PSA×MIRB + BOA×MIRA ACQ/IMAGE visit (‘01’, 24-Oct-2013), contained G230L/3000, G285M/2850,

²⁰In May 2015, the “home” position of the COS Optic Select Mechanism #2 (OSM2, the NUV grating wheel) was changed from G185M/1850 to the MIRA position to reduce wear on the OSM, increase observing efficiency, and reduce mechanism drift and position offsets during ACQ/IMAGE TAs. (see PR#80893 and PR#80894).

²¹Offsets set by using APT exposure level POS_TARGS.

G130M/1309 & G140L/1280. The BOA×MIRA + BOA×MIRB ACQ/ IMAGE visit ('02', 01-Nov-2013) contained G185M/1890, G225M/2306, and both BOA and PSA G160M/1623 spectra. A 2×2 ACQ/ SEARCH proceeded the BOA×MIRA ACQ/ IMAGE in visit '02' due to some uncertainty in the rather large (> 400 mas/yr) proper motion of the target (HIP66578).

- In the C21 TA monitoring program (P13526), the 2×2 ACQ/ SEARCH present in the beginning of Visit '02' was removed after further verification of the proper motion. Confirming ACQ/ IMAGES of the initial configuration (config#1) were added after the test configuration (config#2) in all visits. Also, the G160M BOA spectrum was dropped in favor of the $\pm 0.7''$ POS_TARG exposures to monitor gain sag induced 'Ywalk' at LP2 in Visit '02' (17-Nov-2014). In addition, a 'family portrait' of the **P1** and **P2** PtNe lamps were acquired using both MIRA and MIRB NUV imaging. The MIRA lamp images were taken for both the **P1** and **P2** lamps at LOW current, while for MIRB image the **P1** lamp image was taken at LOW current and the **P2** lamp was at MED current. Additionally, the C21, P13526, contingency visit '03' was activated to verify the count rates associated with the re-configuration of the the MIRB ACQ/ IMAGE lamp flash of the MIRB LTACAL exposures for **P2** from LOW to MED current. All MIRB lamp images in the C21 program were also taken at MED current, as compared to LOW for the C20 program. Further details on the MIRB ACQ/ IMAGE adjustments are given in § ??.

The optional parameter WAVECAL=YES in the BOA×MIRA target+Lamp image of the C20 program was discovered to not have taken the expected internal lamp image in the LC6601RYQ.rawtag.fits exposure. Correcting this inconsistency would have required significant APT, TRANS, and commanding changes. As this internal calibration exposure combination is rarely executed, the C21 program included separate TARGET=WAVE companion lamp exposures for the target BOA exposure²². A second MIRA lamp image was added directly after the BOA×MIRA ACQ/ IMAGE, to verify the repeatability of the WCA lamp location when moving the BOA into and out of position. To create time for the new exposures, the exposure times of the spectroscopic observations were scaled back, but still achieved the required S/N to measure the XD spectral locations.

- In the C22 TA monitoring program (P13972), the G185M and G285M exposures were changed from C2850 to C2676 and from C1890 to C1913, respectively, as the WCA lamp spectra much stronger in the latter STRIPE=B bandpasses. Beginning with C22, GOs were discouraged from using the G285M for spectroscopic ACQ/PEAKXD TAs, and the CEN-WAVEs for the other NUV gratings were highlighted in section 2.6 (NUV Spectroscopic Acquisitions) of the C25 COS Instrument Handbook (Fox, 2017) and C25 Phase II Proposal Instructions (Rose, et al., 2017). Prior to C25, GOs were contacted directly by their Contact Scientists (CS) to ensure the success of their NUV spectroscopic ACQ/PEAKXDs. The contingency visit ('03') was not executed in C22.

²²The COS apertures are physically configured such that WCA light lands on the detector(s) when the PSA in place, but does not when the BOA is in place (INSERT REF). Therefore, whenever lamp images are required to verify BOA ACQ/ IMAGE exposures, the BOA is replaced by the PSA so that WCA light falls on the detector at the same location as it would fall for a PSA image.

- In the C23 TA monitoring program (P14440), each of the one-orbit visits was placed in a non-interruptible sequence to prevent guide-star (GS) re-acquisitions (reacqs) from changing the telescope pointing during a visit. None of the previous visits encountered this situation, but the use of the non-interruptible sequences in APT requires this to be true for this, and all subsequent programs. The lamp ‘family portrait’ in Visit ‘02’ is contained in a separate non-interruptible sequence from the other exposures in the visit as any GS reacqs would not affect the internal lamp exposures. Some exposures were slightly lengthened to take advantage of the increased efficiency of the modified OSM2 home position.²³ The contingency visit (‘03’) was not executed in C23.
- In the C24 TA monitoring program (P14857), the visit names were changed from ‘01’, ‘02’, and ‘03’ to ‘BA’, ‘BB’, and ‘PB’ to indicate which ACQ/ IMAGE mode was being tested; PB = PSA×MIRB, BA = BOA×MIRA, and BB = BOA×MIRB. Visits ‘BA’ and ‘BB’ of the C24 program are identical to visits ‘01’ and ‘02’ of the C23 program in all other regards. Visit ‘PB’ of the C24 program was noticeably different than the contingency visit ‘03’ in C23 program. The ‘PB’ visit only includes those exposures absolutely required to compare the ACQ/ IMAGE accuracy of PSA×MIRA to PSA×MIRB, while the C23 program also obtained spectra of all three FUV gratings for additional monitoring of spectroscopic TA performance under the assumption that detector ‘Y-walk’ monitoring would benefit from additional observations near the end of the FUV LP3 lifetime. The C24 version of the FGS-to-SI alignment program was replaced with an improved program (P14867²⁴) for aligning the FGSSs which did not allow the inclusion of these ACQ/ IMAGE exposures²⁵. For C24, we activated the contingency ‘PB’ visit to obtain the needed PSA×MIRA to PSA×MIRB ACQ/ IMAGE alignment verification.

²³The OSM2 home position was changed from G185M to MIRA on July 6, 2015 (2015.157).

²⁴HST C24 Focal Plane Calibration (SI-FGS alignment), PI = Edmund Nelan.

²⁵The FGSSs were used as the prime science instrument in this proposal, which precluded the use of COS during the visit as COS is not an allowed parallel HST instrument.

3.4 Exposure Lists

Table 5 gives the operational details of all NUV PSA imaging exposures which opened the external shutter used in this ISR, while Table 6 details the NUV BOA imaging exposures. Table 7 gives the operational details of all NUV imaging WAVECAL exposures. Tables 9 and 10 give the details of all spectroscopic exposures used in this ISR. All tables follow the convention that if an entry was extracted from a FITS header, then the column name will appear in *ITALICIZED ALL CAPITALS*.

The columns of the Table 5 and 6 give:

1. *ROOTNAME* gives the IPPSSOOT of the COS exposure,
2. *PROPOSID* gives the HST program id (PID),
3. *TARNMAME* gives the target name as present in the MAST archive,
4. *OBSMODE* gives the observation mode, where “TT” is used for Time-Tag observations,
5. *EXPTYPE* gives the exposure type, which is either ACQ/ IMAGE or EXT/SCI. EXT/SCI images using *APERATURE* = PSA allow co-eval target and lamp images for direct measurement of their WCA-to-SA offset. ACQ/ IMAGE exposures return before and after target images in OBSTYPE=ACCUM, but do not return lamp images.
6. *EXPTIME* gives the exposure time in seconds. For EXT/SCI PSA images, the lamp time may be different. These lamp times are given in Table ??.
7. gives the PtNe Lamp# gives the wavelength calibration lamp name (**P1** or **P2**) and current setting. The conversion from current setting to current in milli-amps (mA) is given in § 1.1, and in the table footnotes.
8. gives the configuration (*APERTURE*×*OPT_ELEM*) of the SA and grating or MIRROR used as the primary optic.
9. *APERXPOS* gives the AD (*X_{USER}*) aperture position. The default position is *APERXPOS*=22 for all FUV and NUV science and TA exposures.²⁶
10. *APERYPOS* gives the XD (*Y_{USER}*) aperture position. It is not uncommon that the XD aperture location (*APERYPOS*) is ±1 step off from its nominal position during the LTAIMCAL phase. Each *APERYPOS* step is ≈ 0.053'', or about $\frac{1}{6}$ of our XD centering requirement, and $\frac{1}{2}$ of our 1σ XD centering goal. The default NUV and FUV LP1 PSA/BOA positions are *APERYPOS*=126/ – 153, where the WCA has the same XD (*APERYPOS*) position as the PSA. As shown in Table 8, the nominal PSA & WCA *APERYPOS* positions for LP2, LP3, and LP4 are +53, +181, and +234, respectively.²⁷
11. *DATE-OBS* gives the date of the observation in YEAR-MOnth-DAy format.

The columns of the NUV imaging WAVECAL table (Table 7) are similar to those of Tables 5 & 6, with the following exception:

1. All exposures have *TARGNAME*=WAVE, *OBSMODE*=TT, and *EXPTYPE*=WAVECAL, so these columns have been removed.

The columns of the spectroscopic NUV (Table 9) and FUV (Table 10) tables are similar to the columns listed above for Tables 5 & 6, with the following exceptions:

²⁶The trailing ”0.1” is a FITS conversion anomaly present in all aperture positions (*APERXPOS* & *APERYPOS*).

²⁷Due to the known behavior of the XD aperture mechanism to miss by one step in *APERYPOS*, entries in the PCMECH_APMDISPPOSITION FSW table were intentionally offset by ±1 step, depending on travel direction from NUV/FUV LP1, which share the common PCMECH_APMDISPPOSITION (*APERYPOS*) entry of +126.

- All spectroscopic exposures are time-tag (*OBSMODE*=TT) with the PSA, so the configuration column has been removed.
- The ‘Lamp#/Current’ column is not present. In the programs of this ISR, the default **P1** lamp usage for spectroscopic observations was overridden with the use of the USE-LAMP=LINE2 and CURRENT=MEDIUM special commanding in APT to simulate the lamp exposures obtained in LTAPKXD exposures. The APT optional parameter FLASH was used to set **P2** exposures times that provided counts in excess of those expected during the TA exposures. Since all spectra were taken in TT mode, if required, an exact replica of the counts received in an actual LTAPKXD WCA spectrum could be re-produced. The additional counts allow for a better determination of the WCA-to-SA XD offsets discussed in § 8 and § 8.2.
- The *OPT_ELEM* column shows the grating in use, as this is now the primary optic.
- *CENWAVE* now follows the *OPT_ELEM* column, giving the central wavelength setting.
- The LP gives the lifetime position (*LIFE_ADJ*) of the observation. Note that there is only one NUV LP, so all NUV observations are LP1.

The nominal focus value for ACQ/IMAGE exposures is *LOMFSTP*=-88. Minor deviations from this value are expected, and should not impact any results presented in this ISR. For the exposures in this ISR, the $-91 \leq LOMFSTP \leq -86$. For all exposures in this ISR, OSM1 reported the nominal ACQ/IMAGE position of *LOM1STP*, OSM2 also reported all nominal values of *LOM2STP*=8964 for MIRRORA and 9424 for MIRRORB.

Table 5. COS/NUV TA Monitoring Imaging Exposures - PSA

PROP OSID (1)	ROOT NAME (2)	TARG NAME (3)	OBS MODE ^t (4)	EXPTYPE (5)	EXPTIME (s) (6)	PtNe (WCA) Lamp#×Current (7)	APERTURE ×OPT_ELEM (8)	APER XPOS ^x (9)	APER YPOS ^y (10)	DATE-OBS (11)
PSA×MIRA										
P13171	lc6ka1i1q	427W3	ACCUM	ACQ/IMAGE	60	P2 ×Low	PSA×MIRA	22.1	127.1	2013-03-02
P13171	lc6ka2imq	206W3	ACCUM	ACQ/IMAGE	60	P2 ×Low	PSA×MIRA	22.1	127.1	2013-09-01
P13616	lc4ia1dcq	427W3	ACCUM	ACQ/IMAGE	60	P2 ×Low	PSA×MIRA	22.1	127.1	2014-04-03
P13616	lc4ia2e3q	206W3	ACCUM	ACQ/IMAGE	60	P2 ×Low	PSA×MIRA	22.1	127.1	2014-10-27
P13526	lcgq03dbq	206W3	ACCUM	ACQ/IMAGE	15	P2 ×Low	PSA×MIRA	22.1	127.1	2014-10-06
P13526	lcgq03ddq	206W3	TT	EXT/SCI	15	P2 ×Low	PSA×MIRA	22.1	127.1	2014-10-06
P13526	lcgq03drq	206W3	TT	EXT/SCI	12	P2 ×Low	PSA×MIRA	22.1	127.1	2014-10-06
P13526	lcgq03dtq	206W3	ACCUM	ACQ/IMAGE	12	P2 ×Low	PSA×MIRA	22.1	127.1	2014-10-06
P14035	lcsla1i4q	427W3	ACCUM	ACQ/IMAGE	60	P2 ×Low	PSA×MIRA	22.1	125.1	2015-04-14
P14035	lcsla2bhq	206W3	ACCUM	ACQ/IMAGE	60	P2 ×Low	PSA×MIRA	22.1	125.1	2015-10-02
P14452	ld3la1coq	427W3	ACCUM	ACQ/IMAGE	60	P2 ×Med	PSA×MIRA	22.1	125.1	2016-04-01
P14452	ld3la2ojq	206W3	ACCUM	ACQ/IMAGE	60	P2 ×Med	PSA×MIRA	22.1	125.1	2016-10-02
P14857	ldozpbff5q	206W3	ACCUM	ACQ/IMAGE	20	P2 ×Low	PSA×MIRA	22.1	125.1	2017-09-10
P14857	ldozpbff7q	206W3	TT	EXT/SCI	20	P2 ×Low	PSA×MIRA	22.1	125.1	2017-09-10
P14857	ldozpbffq	206W3	TT	EXT/SCI	20	P2 ×Low	PSA×MIRA	22.1	125.1	2017-09-10
P14857	ldozpbfhq	206W3	ACCUM	ACQ/IMAGE	20	P2 ×Low	PSA×MIRA	22.1	125.1	2017-09-10
PSA×MIRB										
P13124	lc6601rrq	WD-1657+343	ACCUM	ACQ/IMAGE	12	P2 ×Med	PSA×MIRB	22.1	127.1	2013-10-24
P13124	lc6601rtq	WD-1657+343	TT	EXT/SCI	20	... ^a	PSA×MIRB	22.1	127.1	2013-10-24
P13124	lc6601s0q	WD-1657+343	TT	EXT/SCI	20	... ^a	PSA×MIRB	22.1	126.1	2013-10-24
P13171	lc6ka1i3q	427W3	ACCUM	ACQ/IMAGE	300	P2 ×Low	PSA×MIRB	22.1	127.1	2013-03-02
P13171	lc6ka2ioq	206W3	ACCUM	ACQ/IMAGE	300	P2 ×Low	PSA×MIRB	22.1	127.1	2013-09-01
P13616	lc4ia1deq	427W3	ACCUM	ACQ/IMAGE	300	P2 ×Low	PSA×MIRB	22.1	127.1	2014-04-03
P13616	lc4ia2e5q	206W3	ACCUM	ACQ/IMAGE	300	P2 ×Med	PSA×MIRB	22.1	127.1	2014-10-27
P13526	lcgq01q5q	WD-1657+343	ACCUM	ACQ/IMAGE	12	P2 ×Med	PSA×MIRB	22.1	127.1	2014-11-19
P13526	lcgq01q7q	WD-1657+343	TT	EXT/SCI	16	P2 ×Med	PSA×MIRB	22.1	127.1	2014-11-19
P13526	lcgq01qhq	WD-1657+343	TT	EXT/SCI	12	P2 ×Med	PSA×MIRB	22.1	126.1	2014-11-19
P13526	lcgq01qjq	WD-1657+343	ACCUM	ACQ/IMAGE	12	P2 ×Med	PSA×MIRB	22.1	126.1	2014-11-19
P13526	lcgq03dfq	206W3	TT	EXT/SCI	160	P2 ×Low	PSA×MIRB	22.1	127.1	2014-10-06
P13526	lcgq03dhq	206W3	TT	EXT/SCI	180	P2 ×Low	PSA×MIRB	22.1	127.1	2014-10-06
P13526	lcgq03dqj	206W3	TT	EXT/SCI	180	P2 ×Med	PSA×MIRB	22.1	127.1	2014-10-06
P13526	lcgq03dlq	206W3	ACCUM	ACQ/IMAGE	160	P2 ×Med	PSA×MIRB	22.1	127.1	2014-10-06
P13526	lcgq03dnq	206W3	TT	EXT/SCI	180	P2 ×Med	PSA×MIRB	22.1	127.1	2014-10-06
P13526	lcgq03dpq	206W3	TT	EXT/SCI	160	P2 ×Low	PSA×MIRB	22.1	127.1	2014-10-06
P13972	lcri01fzq	WD-1657+343	ACCUM	ACQ/IMAGE	12	P2 ×Med	PSA×MIRB	22.1	125.1	2015-10-06
P13972	lcri01g1q	WD-1657+343	TT	EXT/SCI	12	P2 ×Med	PSA×MIRB	22.1	125.1	2015-10-06
P13972	lcri01gcq	WD-1657+343	TT	EXT/SCI	14	P2 ×Med	PSA×MIRB	22.1	126.1	2015-10-06
P13972	lcri01geq	WD-1657+343	ACCUM	ACQ/IMAGE	12	P2 ×Med	PSA×MIRB	22.1	126.1	2015-10-06
P14035	lcsla1i6q	427W3	ACCUM	ACQ/IMAGE	300	P2 ×Med	PSA×MIRB	22.1	125.1	2015-04-14
P14035	lcsla2bjq	206W3	ACCUM	ACQ/IMAGE	300	P2 ×Med	PSA×MIRB	22.1	125.1	2015-10-02
P14452	ld3la1csq	427W3	ACCUM	ACQ/IMAGE	300	P2 ×Med	PSA×MIRB	22.1	125.1	2016-04-01
P14452	ld3la2onq	206W3	ACCUM	ACQ/IMAGE	300	P2 ×Med	PSA×MIRB	22.1	125.1	2016-10-02
P14440	ld3701gtq	WD-1657+343	ACCUM	ACQ/IMAGE	13	P2 ×Med	PSA×MIRB	22.1	125.1	2016-10-18
P14440	ld3701gvq	WD-1657+343	TT	EXT/SCI	16	P2 ×Med	PSA×MIRB	22.1	125.1	2016-10-18
P14440	ld3701h5q	WD-1657+343	TT	EXT/SCI	16	P2 ×Med	PSA×MIRB	22.1	126.1	2016-10-18
P14440	ld3701h7q	WD-1657+343	ACCUM	ACQ/IMAGE	13	P2 ×Med	PSA×MIRB	22.1	126.1	2016-10-18
P14857	ldozbadhq	WD-1657+343	ACCUM	ACQ/IMAGE	13	P2 ×Med	PSA×MIRB	22.1	125.1	2017-09-04
P14857	ldozbadjs	WD-1657+343	TT	EXT/SCI	16	P2 ×Med	PSA×MIRB	22.1	125.1	2017-09-04
P14857	ldozbadtq	WD-1657+343	TT	EXT/SCI	16	P2 ×Med	PSA×MIRB	22.1	126.1	2017-09-04
P14857	ldozbadvq	WD-1657+343	ACCUM	ACQ/IMAGE	13	P2 ×Med	PSA×MIRB	22.1	126.1	2017-09-04
P14857	ldozpbffq	206W3	TT	EXT/SCI	220	P2 ×Med	PSA×MIRB	22.1	125.1	2017-09-10
P14857	ldozpbfbq	206W3	ACCUM	ACQ/IMAGE	220	P2 ×Med	PSA×MIRB	22.1	125.1	2017-09-10
P14857	ldozpbfdq	206W3	TT	EXT/SCI	220	P2 ×Med	PSA×MIRB	22.1	125.1	2017-09-10

^aThe intended PtNe lamp flashes of P13124 did not occur as expected. This was corrected in all other programs.^tTT = TIME-TAG.^xAPERYPOS, the AD aperture mechanism positions, are stored in the FSW in PCMECH_APMDISPPOSITION. The trailing “0.1” reported in the FITS headers is a conversion anomaly that is present in all aperture positions (APERXPOS & APERYPOS).^yIt is not uncommon that the XD aperture location (APERXPOS) is ±1 step off from its nominal position. The XD aperture mechanism positions are stored in the FSW in PCMECH_APMDISPPOSITION (see Table 8).

Table 6. COS/NUV TA Monitoring Imaging Exposures - BOA

PROP OSID	ROOT NAME	TARG NAME	OBS MODE ^t	EXPTYPE	EXPTIME (s)	PtNe (WCA) Lamp#×Current	APERTURE ×OPT_ELEM	APER XPOS ^x	APER YPOS ^y	DATE-OBS (11)
BOA×MIRRORA										
P13124	lc6601rvq	WD-1657+343	ACCUM	ACQ/IMAGE	150	P2 ×Med	BOA×MIRA	22.1	-153.1	2013-10-24
P13124	lc6601ryq	WD-1657+343	TT	EXT/SCI	150	... ^a	BOA×MIRA	22.1	-153.1	2013-10-24
P13124	lc6602y5q	HIP66578	ACCUM	ACQ/IMAGE	12	P2 ×Med	BOA×MIRA	22.1	-153.1	2013-11-01
P13124	lc6602y7q	HIP66578	TT	EXT/SCI	12	... ^a	BOA×MIRA	22.1	-153.1	2013-11-01
P13526	lcgq02hmq	HIP66578	ACCUM	ACQ/IMAGE	12	P2 ×Low	BOA×MIRA	22.1	-153.1	2014-11-17
P13526	lcgq02i0q	HIP66578	ACCUM	ACQ/IMAGE	12	P2 ×Low	BOA×MIRA	22.1	-153.1	2014-11-17
P13526	lcgq01q9q	WD-1657+343	TT	EXT/SCI	150	P2 ×Med	BOA×MIRA	22.1	-153.1	2014-11-19
P13526	lcgq01qdq	WD-1657+343	ACCUM	ACQ/IMAGE	150	P2 ×Low	BOA×MIRA	22.1	-153.1	2014-11-19
P13972	lcri01g3q	WD-1657+343	TT	EXT/SCI	150	P2 ×Med	BOA×MIRA	22.1	-153.1	2015-10-06
P13972	lcri01g7q	WD-1657+343	ACCUM	ACQ/IMAGE	150	P2 ×Low	BOA×MIRA	22.1	-153.1	2015-10-06
P13972	lcri02h8q	HIP66578	ACCUM	ACQ/IMAGE	12	P2 ×Low	BOA×MIRA	22.1	-153.1	2015-10-06
P13972	lcri02hmq	HIP66578	ACCUM	ACQ/IMAGE	12	P2 ×Low	BOA×MIRA	22.1	-153.1	2015-10-06
P14440	ld3701gxq	WD-1657+343	TT	EXT/SCI	150	P2 ×Med	BOA×MIRA	22.1	-153.1	2016-10-18
P14440	ld3701h1q	WD-1657+343	ACCUM	ACQ/IMAGE	150	P2 ×Low	BOA×MIRA	22.1	-153.1	2016-10-18
P14440	ld3702mzq	HIP66578	ACCUM	ACQ/IMAGE	16	P2 ×Low	BOA×MIRA	22.1	-153.1	2016-10-19
P14440	ld3702nhq	HIP66578	ACCUM	ACQ/IMAGE	16	P2 ×Low	BOA×MIRA	22.1	-153.1	2016-10-19
P14857	ldozbadlq	WD-1657+343	TT	EXT/SCI	150	P2 ×Med	BOA×MIRA	22.1	-153.1	2017-09-04
P14857	ldozbadpq	WD-1657+343	ACCUM	ACQ/IMAGE	150	P2 ×Low	BOA×MIRA	22.1	-153.1	2017-09-04
P14857	ldozbbgleq	HIP66578	ACCUM	ACQ/IMAGE	16	P2 ×Low	BOA×MIRA	22.1	-153.1	2017-09-06
P14857	ldozbbqlsq	HIP66578	ACCUM	ACQ/IMAGE	16	P2 ×Low	BOA×MIRA	22.1	-153.1	2017-09-06
BOA×MIRRORA										
P13124	lc6602y9q	HIP66578	ACCUM	ACQ/IMAGE	175	P2 ×Med	BOA×MIRB	22.1	-153.1	2013-11-01
P13124	lc6602ycq	HIP66578	TT	EXT/SCI	175	... ^a	BOA×MIRB	22.1	-153.1	2013-11-01
P13124	lc6602yxq	HIP66578	TT	EXT/SCI	12	... ^a	BOA×MIRB	22.1	-153.1	2013-11-01
P13526	lcgq02hqxq	HIP66578	TT	EXT/SCI	181	P2 ×Low	BOA×MIRB	22.1	-153.1	2014-11-17
P13526	lcgq02huq	HIP66578	ACCUM	ACQ/IMAGE	181	P2 ×Med	BOA×MIRB	22.1	-153.1	2014-11-17
P13972	lcri02hcq	HIP66578	TT	EXT/SCI	181	P2 ×Low	BOA×MIRB	22.1	-153.1	2015-10-06
P13972	lcri02hgq	HIP66578	ACCUM	ACQ/IMAGE	181	P2 ×Med	BOA×MIRB	22.1	-153.1	2015-10-06
P14440	ld3702n4q	HIP66578	TT	EXT/SCI	183	P2 ×Low	BOA×MIRB	22.1	-153.1	2016-10-19
P14440	ld3702n9q	HIP66578	ACCUM	ACQ/IMAGE	183	P2 ×Med	BOA×MIRB	22.1	-153.1	2016-10-19
P14857	ldozbbliq	HIP66578	TT	EXT/SCI	183	P2 ×Low	BOA×MIRB	22.1	-153.1	2017-09-06
P14857	ldozbbmlq	HIP66578	ACCUM	ACQ/IMAGE	183	P2 ×Med	BOA×MIRB	22.1	-153.1	2017-09-06

^aThe intended PtNe lamp flashes of P13124 did not occur as expected. This was corrected in all other programs.

^tTT = TIME-TAG.

^xAPERYPOS, the AD aperture mechanism positions, are stored in the FSW in PCMECH_APMDISPPOSITION. The trailing "0.1" reported in the FITS headers is a conversion anomaly that is present in all aperture positions (APERXPOS & APERYPOS).

^yIt is not uncommon that the XD aperture location (APERXPOS) is ±1 step off from its nominal position. The XD aperture mechanism positions are stored in the FSW in PCMECH_APMXDISPPOSITION (see Table 8).

Note. — PSA EXPTYPE=EXT/SCI exposures contain coeval target and PtNe lamp TT images.

Table 7. COS/NUV TA Monitoring Imaging Exposures - WCA only

<i>PROP OSID</i> (1)	<i>ROOT NAME</i> (2)	<i>EXPTIME (s)</i> (3)	PtNe (WCA) Lamp#×Current (4)	<i>APERTURE ×OPT_ELEM</i> (5)	<i>APER XPOS^x</i> (6)	<i>APER YPOS^y</i> (7)	<i>DATE-OBS</i> (8)
WCA×MIRRORA							
P13523	lcgp01byq	20	P2 ×Low	WCA×MIRA	22.1	127.1	2013-11-11
P13523	lcgp01c3q	20	P1 ×Low	WCA×MIRA	22.1	127.1	2013-11-11
P13526	lcgq01qbq	7	P2 ×Low	WCA×MIRA	22.1	126.1	2014-11-19
P13526	lcgq01lqfq	7	P2 ×Low	WCA×MIRA	22.1	126.1	2014-11-19
P13526	lcgq02hoq	7	P2 ×Low	WCA×MIRA	22.1	126.1	2014-11-17
P13526	lcgq02hyq	10	P2 ×Low	WCA×MIRA	22.1	126.1	2014-11-17
P13526	lcgq02icq	10	P1 ×Low	WCA×MIRA	22.1	127.1	2014-11-17
P13526	lcgq02ieq	10	P2 ×Low	WCA×MIRA	22.1	127.1	2014-11-17
P13972	lcri01g5q	10	P2 ×Low	WCA×MIRA	22.1	126.1	2015-10-06
P13972	lcri01g9q	10	P2 ×Low	WCA×MIRA	22.1	126.1	2015-10-06
P13972	lcri02haq	14	P2 ×Low	WCA×MIRA	22.1	126.1	2015-10-06
P13972	lcri02hkq	14	P2 ×Low	WCA×MIRA	22.1	126.1	2015-10-06
P13972	lcri02hyq	14	P1 ×Low	WCA×MIRA	22.1	125.1	2015-10-06
P13972	lcri02i0q	24	P2 ×Low	WCA×MIRA	22.1	125.1	2015-10-06
P14452	ld3la1cqq	10	P2 ×Low	WCA×MIRA	22.1	125.1	2016-04-01
P14452	ld3la2olq	10	P2 ×Low	WCA×MIRA	22.1	125.1	2016-10-02
P14440	ld3701gzq	9	P2 ×Low	WCA×MIRA	22.1	126.1	2016-10-18
P14440	ld3701h3q	10	P2 ×Low	WCA×MIRA	22.1	126.1	2016-10-18
P14440	ld3702n1q	14	P2 ×Low	WCA×MIRA	22.1	126.1	2016-10-19
P14440	ld3702neq	14	P2 ×Low	WCA×MIRA	22.1	126.1	2016-10-19
P14440	ld3702o1q	14	P1 ×Low	WCA×MIRA	22.1	125.1	2016-10-19
P14440	ld3702o3q	24	P2 ×Low	WCA×MIRA	22.1	125.1	2016-10-19
P14857	ldozbadnq	9	P2 ×Low	WCA×MIRA	22.1	126.1	2017-09-04
P14857	ldozbadrq	10	P2 ×Low	WCA×MIRA	22.1	126.1	2017-09-04
P14857	ldozbbllq	14	P2 ×Low	WCA×MIRA	22.1	126.1	2017-09-06
P14857	ldozbbllqq	14	P2 ×Low	WCA×MIRA	22.1	126.1	2017-09-06
P14857	ldozbbm4q	16	P1 ×Low	WCA×MIRA	22.1	125.1	2017-09-06
P14857	ldozbbm6q	26	P2 ×Low	WCA×MIRA	22.1	125.1	2017-09-06
WCA×MIRRORB							
P13523	lcgp01bpq	40	P2 ×Low	WCA×MIRB	22.1	127.1	2013-11-11
P13523	lcgp01bsq	40	P1 ×Low	WCA×MIRB	22.1	127.1	2013-11-11
P13526	lcgq02hsq	12	P2 ×Med	WCA×MIRB	22.1	126.1	2014-11-17
P13526	lcgq02hwq	12	P2 ×Med	WCA×MIRB	22.1	126.1	2014-11-17
P13526	lcgq02igq	30	P1 ×Low	WCA×MIRB	22.1	127.1	2014-11-17
P13526	lcgq02iiq	20	P2 ×Med	WCA×MIRB	22.1	127.1	2014-11-17
P13972	lcri02heq	24	P2 ×Med	WCA×MIRB	22.1	126.1	2015-10-06
P13972	lcri02hiq	24	P2 ×Med	WCA×MIRB	22.1	126.1	2015-10-06
P13972	lcri02i2q	30	P1 ×Low	WCA×MIRB	22.1	125.1	2015-10-06
P13972	lcri02i4q	24	P2 ×Med	WCA×MIRB	22.1	125.1	2015-10-06
P14452	ld3la1cuq	20	P2 ×Med	WCA×MIRB	22.1	125.1	2016-04-01
P14452	ld3la2opq	20	P2 ×Med	WCA×MIRB	22.1	125.1	2016-10-02
P14440	ld3702n7q	24	P2 ×Med	WCA×MIRB	22.1	126.1	2016-10-19
P14440	ld3702nbq	24	P2 ×Med	WCA×MIRB	22.1	126.1	2016-10-19
P14440	ld3702o5q	30	P1 ×Low	WCA×MIRB	22.1	125.1	2016-10-19
P14440	ld3702o7q	24	P2 ×Med	WCA×MIRB	22.1	125.1	2016-10-19
P14857	ldozbbblk	24	P2 ×Med	WCA×MIRB	22.1	126.1	2017-09-06
P14857	ldozbbloq	24	P2 ×Med	WCA×MIRB	22.1	126.1	2017-09-06
P14857	ldozbbm8q	32	P1 ×Low	WCA×MIRB	22.1	125.1	2017-09-06
P14857	ldozbbmaq	26	P2 ×Med	WCA×MIRB	22.1	125.1	2017-09-06

^xAPERYPOS, the AD aperture mechanism positions are stored in the FSW in PCMECH_APMDISPOSITION. The trailing "0.1" reported in the FITS headers is a conversion anomaly present in all reported aperture positions (APERXPOS & APERYPOS).

^yIt is not uncommon that the XD aperture location (APERXPOS) is ±1 step off from its nominal position.

Note. — All exposures in this table are *TARGNAME*=WAVE, time-tag (TT) *EXPTYPE*=WAVECAL (target = WAVE) exposures and contain only PtNe lamp (WCA) images at the indicated MIRROR position (*OPT_ELEM*).

Table 8. COS Cross-Dispersion (XD) Aperture Positions (*APERXPOS*)

<i>LIFE_ADJ</i> (LP)	NUV		FUV	
	PSA ^a /WCA ^b (1)	BOA ^c /FCA ^d (2)	PSA/WCA (4)	BOA/FCA (5)
LP1	126	-153	126	153
LP2	53	-226
LP3	181	-98
LP4	234	-45

^aPSA=Primary Science Aperture^bWCA=Wavelength Calibration Aperture^cBOA=Bright Object Aperture^dFCA=Flat-field Calibration Aperture

Note. — COS XD aperture positions (*APERXPOS*) are stored in the PCMECH_APMDISPPOSITION FSW table. Although LP1–8 are defined in that table for both NUV and FUV, only the NUV LP1 and FUV LP1–4 here have been used for science observations. Values used for FCA calibration observations are different from those listed here, and are commanded via APT special commanding (e.g., during the semi-annual FUV Gain Map programs). AD values (*APERYPOS*) are stored in the PCMECH_APMDISPPOSITION FSW table. All COS apertures and LPs use *APERYPOS*=22.

Table 9. NUV Spectroscopic TA Monitoring Exposures

<i>PROPOSID</i>	<i>ROOTNAME</i>	<i>TARGNAME</i>	<i>EXPTIME</i> (s)	<i>OPT.ELEM</i>	<i>CENWAVE</i>	<i>LP</i>	<i>APER</i> <i>XPOS</i>	<i>APER</i> <i>YPOS</i> ^a	<i>DATE-OBS</i>
(1)	(2)	(3)	(4)	(5)	(6)	(7)	(8)	(9)	(10)
P13124	lc6602yzq	HIP66578	35	G185M	1890	1	22.1	126.1	2013-11-01
P13124	lc6602z1q	HIP66578	53	G125M	2306	1	22.1	126.1	2013-11-01
P13124	lc6601s2q	WD-1657+343	30	G230L	3000	1	22.1	126.1	2013-10-24
P13124	lc6601s4q	WD-1657+343	334	G285M	2850	1	22.1	126.1	2013-10-24
P13526	lcgq02i2q	HIP66578	40	G185M	1890	1	22.1	126.1	2014-11-17
P13526	lcgq02i4q	HIP66578	52	G225M	2306	1	22.1	126.1	2014-11-17
P13526	lcgq01qlq	WD-1657+343	20	G230L	3000	1	22.1	126.1	2014-11-19
P13526	lcgq01r6q	WD-1657+343	151	G285M	2850	1	22.1	126.1	2014-11-19
P13972	lcri01ggq	WD-1657+343	20	G230L	3000	1	22.1	126.1	2015-10-06
P13972	lcri01giq	WD-1657+343	151	G285M	2676	1	22.1	126.1	2015-10-06
P13972	lcri02hoq	HIP66578	52	G225M	2306	1	22.1	126.1	2015-10-06
P13972	lcri02hqq	HIP66578	40	G185M	1913	1	22.1	126.1	2015-10-06
P14440	ld3701h9q	WD-1657+343	21	G230L	3000	1	22.1	126.1	2016-10-18
P14440	ld3701hbq	WD-1657+343	151	G285M	2676	1	22.1	126.1	2016-10-18
P14440	ld3702nmq	HIP66578	53	G225M	2306	1	22.1	126.1	2016-10-19
P14440	ld3702noq	HIP66578	40	G185M	1913	1	22.1	126.1	2016-10-19
P14857	ldozbadxq	WD-1657+343	23	G230L	3000	1	22.1	126.1	2017-09-04
P14857	ldozbadzq	WD-1657+343	151	G285M	2676	1	22.1	126.1	2017-09-04
P14857	ldozbblluq	HIP66578	53	G225M	2306	1	22.1	126.1	2017-09-06
P14857	ldozbblwq	HIP66578	40	G185M	1913	1	22.1	126.1	2017-09-06

^aThe NUV (LP1) PSA XD location of the aperture (*APERYPOS*) is 126 in the FSW table `pcmech.ApMXDispPosition`).

Note. — All spectra taken with the PSA at $FP-POS=3$, and executed at the expected aperture position (*APERXPOS* & *APERYPOS*).

Table 10. FUV TA Monitoring Exposures

<i>PROPOSID</i>	<i>ROOTNAME</i>	<i>TARGNAME</i>	<i>EXPTIME</i> (s)	<i>OPT_ELEM</i>	<i>CENWAVE</i>	<i>LP</i>	<i>APER_XPOS</i>	<i>APER_YPOS</i>	<i>DATE-OBS</i>
(1)	(2)	(3)	(4)	(5)	(6)	(7)	(8)	(9)	(10)
P13124	lc6601s7q	WD-1657+343	110	G130M	1309	2	22.1	52.1	2013-10-24
P13124	lc6601s9q	WD-1657+343	30	G140L	1280	2	22.1	52.1	2013-10-24
P13124	lc6602z3q	HIP66578	20	G160M	1623	2	22.1	52.1	2013-11-01
P13124	lc6602z9q ^a	HIP66578	323	G160M	1623	2	22.1	-224.1	2013-11-01
P13124	lc6602zbq ^b	WAVE	12	G160M	1623	2	22.1	51.1	2013-11-01
P13526	lcgq01r8q	WD-1657+343	20	G130M	1309	2	22.1	52.1	2014-11-19
P13526	lcgq01r8q	WD-1657+343	20	G130M	1309	2	22.1	52.1	2014-11-19
P13526	lcgq01raq	WD-1657+343	7	G140L	1280	2	22.1	52.1	2014-11-19
P13526	lcgq01raq	WD-1657+343	7	G140L	1280	2	22.1	52.1	2014-11-19
P13526	lcgq02i6q	HIP66578	18	G160M	1600	2	22.1	52.1	2014-11-17
P13526	lcgq02i8q	HIP66578	22	G160M	1600	2	22.1	52.1	2014-11-17
P13526	lcgq02iaq	HIP66578	22	G160M	1600	2	22.1	52.1	2014-11-17
P13972	lcri01gkq	WD-1657+343	20	G130M	1309	3	22.1	182.1	2015-10-06
P13972	lcri01gkq	WD-1657+343	20	G130M	1309	3	22.1	182.1	2015-10-06
P13972	lcri01h6q	WD-1657+343	7	G140L	1280	3	22.1	182.1	2015-10-06
P13972	lcri01h6q	WD-1657+343	7	G140L	1280	3	22.1	182.1	2015-10-06
P13972	lcri02hsq	HIP66578	22	G160M	1600	3	22.1	182.1	2015-10-06
P13972	lcri02huq	HIP66578	25	G160M	1600	3	22.1	182.1	2015-10-06
P13972	lcri02hwq	HIP66578	25	G160M	1600	3	22.1	182.1	2015-10-06
P14440	ld3701hdq	WD-1657+343	25	G130M	1309	3	22.1	182.1	2016-10-18
P14440	ld3701hdq	WD-1657+343	25	G130M	1309	3	22.1	182.1	2016-10-18
P14440	ld3701hfq	WD-1657+343	10	G140L	1280	3	22.1	182.1	2016-10-18
P14440	ld3701hfq	WD-1657+343	10	G140L	1280	3	22.1	182.1	2016-10-18
P14440	ld3702nqq	HIP66578	22	G160M	1600	3	22.1	182.1	2016-10-19
P14440	ld3702nsq	HIP66578	25	G160M	1600	3	22.1	182.1	2016-10-19
P14440	ld3702nuq	HIP66578	25	G160M	1600	3	22.1	182.1	2016-10-19
P14857	ldozbae1q	WD-1657+343	25	G130M	1309	3	22.1	182.1	2017-09-04
P14857	ldozbae1q	WD-1657+343	25	G130M	1309	3	22.1	182.1	2017-09-04
P14857	ldozbae3q	WD-1657+343	10	G140L	1280	3	22.1	182.1	2017-09-04
P14857	ldozbae3q	WD-1657+343	10	G140L	1280	3	22.1	182.1	2017-09-04
P14857	ldozbblyq	HIP66578	22	G160M	1600	3	22.1	182.1	2017-09-06
P14857	ldozbbm0q	HIP66578	27	G160M	1600	3	22.1	182.1	2017-09-06
P14857	ldozbbm2q	HIP66578	27	G160M	1600	3	22.1	182.1	2017-09-06

^aFor C20 only (P13124), a G160M BOA spectrum and WAVECAL were obtained to measure the WCA-to-BOA offset. The BOA was 2 steps off (0.105'') of its LP2 expected *APERYPOS* position of -226 for this exposure. This is similar to the ± 1 step offset often seen during ACQ/IMAGES.

^bThis WAVECAL exposure was used to measure the WCA portion of the WCA-to-BOA offset for the proceeding BOA spectrum, and it off its nominal position of 52.1 by 1 *APERYPOS* step.

Note. — All exposures taken at *FP-POS=3*. All PSA spectra executed at the expected aperture positions (*APERXPOS* & *APERYPOS*), while the indicated BOA spectrum was off by 2 *APERYPOS* steps.

4 Verifying the TA (ACQ/) Subarrays

In this section, we describe the various subarrays used in COS TA. These subarrays are defined by giving the detector coordinate of the lowest valued corner (C) and the full size (S) for both X and Y. A subarray is fully specified by giving its XC, XS, YC, and YS. Unless noted, coordinates are in detector coordinates as this is the system in which COS TAs are performed.

TA subarrays are necessary to remove unwanted detector background or spectral or detector features not associated with the target, such as detector “hot-spots” or Geocoronal emission (see Penton & Keyes, 2011). All COS ACQ/ modes use subarrays, but they different for each mode, detector or detector segment, and *CENWAVE*. The explanation for the sizes and locations of the TA subarrays are beyond the scope of this ISR, but can be found in the TIR COS-2010-03 (Penton & Keyes, 2011), the pre-launch estimates (driven by ray-trace predictions; COS-11-0024A (Penton, 2001), COS-11-0014B (Penton, 2002), & COS-11-0016A (Penton, 2001) and for FUV LP2–4 in their respective enabling ISRs (Penton 2018 (LP2), Penton 2018 (LP3) and Penton & White 2018 (LP4).) The programs discussed in this ISR do not contain any FUV or NUV spectroscopic ACQ/ exposures, therefore, the bulk of the discussion for the TA subarrays for spectroscopic TAs are contained in the respective enabling ISRs. The spectroscopic exposures discussed in this ISR will, however, be used to verify the appropriateness of the XD locations of the subarrays in § 8.1 (NUV) and § 8.2 (FUV).

COS TA subarrays are loaded during the HST ground commanding uniquely for each TA exposure. These are ACQ/ mode, NUV *STRIPE*, *CENWAVE*, FUV *SEGMENT* and LP dependent. Additionally, NUV ACQ/SEARCH has both imaging and spectroscopic modes, which use different subarrays. These subarrays change with time in response to detector (e.g., increasing background or “hot-spots) or mechanism (e.g., secular OSM drift) monitoring. There are two stages to the TA verification, 1) ensuring that the intended subarrays were commanded, and 2) that those subarrays were valid for the entire duration of usage.

Ideally, one would compare the commanded subarrays for all exposures to those reported in the *_rawacq.fits* file. However, due to fits conversion issues²⁸, in this ISR, the subarrays obtained from the telemetry reported in the *_spt.fits* files.

Tables 11, 13, 12, 14 give the TA subarrays for all imaging modes as they has evolved since SMOV. Table 16 gives the subarrays for all NUV spectroscopic ACQ/SEARCH and PEAKD that have executed since SMOV. Table 17 gives the subarrays for all NUV ACQ/PEAKXDs since SMOV, which include subarrays to measure the calibration lamp XD location (WCA) as well as the target spectral location of *STRIPE=B* (MEDIUM)). Table 18 gives the subarrays for the WCA portion of all FUV ACQ/PEAKXDs separated by LP and *CENWAVE*.

Table 19 gives the TA subarrays for the SA portion of all FUV ACQ/s separated by LP and *CENWAVE*. Table 20 gives the TA subarrays for all LPs and *CENWAVEs* for FUVB. Note that TA has not been enabled for all FUV *CENWAVEs*, so only the TA subarrays that are in use are listed. The FUV tables includes subarrays for all four COS LPs even though only the LP2 and LP3 subarrays were monitored in this ISR.

All tables indicate that the intended subarrays are being used for all TA exposures. All spectra were visually inspected to verify that the subarrays would have successfully excluded all known detector hot-spots and the bright Geocoronal emission lines that can negatively affect TAs.

²⁸These issues should be addressed for C26 with the corrections outlined in PR#64849, PR#64874, & PR#66840

Table 11. 2009–2011.016 ACQ/IMAGE and ACQ/SEARCH Subarrays.

Aperture	MIRROR	XC	YC	XS	YS
WCA	MIRA	268	95	200	660
WCA	MIRB	103	361	200	660
PSA or BOA	MIRA	572	108	345	816
PSA or BOA	MIRB	410	200	345	816

Note. — Updated on 2011.017 due to increased NUV background (*PR#67139*, Penton & Keyes, 2011).

4.1 COS NUV Imaging TA subarrays

The original (2009) NUV imaging ACQ/IMAGE and SEARCH TA subarrays are given in Table 11. This table includes entries for the WCA and PSA and both MIRA and MIRB. The COS FSW uses the same subarrays for the PSA and BOA as the offset on the detector between the aperture locations is small ($\Delta[\text{AD},\text{XD}] \sim [11.0, 0.4]\text{p}$).

Due to rising NUV detector background, and supported by an analysis of OSM repeatability, reductions to the SA ACQ/SEARCH and WCA ACQ/IMAGE subarrays sizes were implemented on 2011.017 (*PR#67139*)²⁹. During ACQ/IMAGE, the region of the detector used to determine the source location is small, and is given by the square of the TA parameter PCTA_CHECKBOXSIZE, which is currently set to 9×9 p (81 total pixels). Therefore, no adjustment was warranted for the SA ACQ/IMAGE subarrays. However, during ACQ/SEARCH, the counts in the full subarray are used (currently 345×816 p = 19,376 p). NUV ACQ/SEARCH TAs are therefore much more vulnerable (by a factor of 3500) to contamination from background events and SAA passages (Penton & Keyes, 2011). The updated ACQ/SEARCH values are given in Table 12, and the updated ACQ/IMAGE subarrays are given in Table 13.

4.2 COS NUV Spectroscopic TA Subarrays

The NUV spectroscopic TA subarrays for the ACQ/SEARCH and PEAKD phases are identical, and are given in Table 16. These subarrays are not grating-specific and are large enough to capture the flux from all three stripes (two for G230L; STRIPE=C (LONG) is not used for G230L TA). COS uses the same NUV TA subarrays for the PSA and BOA as the XD offset between the NUV spectra is small ($\Delta\text{XD} \sim 5$ p).

²⁹On-orbit OSM position analysis showed that the WCA LTAIMCAL MIRRORA and MIRRORB lamp image detector locations were fairly repeatable (usually with ± 50 p AD, and ± 10 p XD). As discussed in, the WCA TA ACQ/IMAGE subarrays were reduced by ± 50 p in XD and ± 180 p in AD, and ACQ/SEARCH subarrays were reduced by 125 p AD and 346 p XD (Penton & Keyes (2011)).

Table 12. 2011.017–Present COS ACQ/SEARCH TA Subarrays.

<i>APERTURE</i>	<i>MIRROR</i>	<i>XC</i>	<i>YC</i>	<i>XS</i>	<i>YS</i>
PSA or BOA	MIRA	630	284	220	470
PSA or BOA	MIRB	469	499	220	470

Note. — Updated on 2011.017 (*PR#67139*, Penton & Keyes, 2011).

Table 13. 2011.017–2014.299 ACQ/ IMAGE Subarrays.

Aperture	MIRROR	XC	YC	XS	YS
WCA	MIRA	345	324	50	300
WCA	MIRB	184	539	50	300
PSA or BOA	MIRA	572	108	345	816
PSA or BOA	MIRB	410	200	345	816

Note. — **Bold** values were updated on 2011.017 (*PR#67139*) due to increased detector background (Penton & Keyes, 2011).

Table 14. 2014.300–Present ACQ/ IMAGE Subarrays.

<i>APERTURE</i>	<i>MIRROR</i>	<i>XC</i>	<i>YC</i>	<i>XS</i>	<i>YS</i>
WCA	MIRA	345	324	50	300
WCA	MIRB	187	566	50	300
PSA or BOA	MIRA	572	108	345	816
PSA or BOA	MIRB	410	200	345	816

Note. — Due to errors in determining the WCA AD position due to increased NUV detector background, the **bold** subarrays values were updated on 2014.279 (*PR#78749*). Simultaneously, the MIRB ACQ/ lamp exposure time and current settings (for the **P2** lamp) were changed from 17s @ LOW current to 12s @ MED current (*PR#78749*). FSW WCA-to-SA offsets ([X,Y]IMCALTARGETOFFSET) were adjusted accordingly on 2014.289 (*PR#79116*), prior to use by HST users on 2014.314. The default exposure time and current for the **P1** lamp image “TAGFLASH”s were changed later with *PR#84463*.

Table 15. FITS Reported TA ACQ/ IMAGE Subarrays

PROP OSID (1)	ROOT NAME (2)	APERTURE ×MIRROR (3)	WCA				SA (PSA or BOA)				DATE-OBS (12)
			XC (4)	YC (5)	XS (6)	YS (7)	XC (8)	YC (9)	XS (10)	YS (11)	
MIRA ACQ/ IMAGE Subarrays											
13171	lc6ka1i1q	PSA×MIRA	345	324	50	300	572	108	345	816	2013-03-02
13171	lc6ka2imq	PSA×MIRA	345	324	50	300	572	108	345	816	2013-09-01
13616	lc4a1dcq	PSA×MIRA	345	324	50	300	572	108	345	816	2014-04-03
13616	lc4a2e3q	PSA×MIRA	345	324	50	300	572	108	345	816	2014-10-27
13526	lcgq01qdq	BOA×MIRA	345	324	50	300	572	108	345	816	2014-11-19
13526	lcgq02hmq	BOA×MIRA	345	324	50	300	572	108	345	816	2014-11-17
13526	lcgq02i0q	BOA×MIRA	345	324	50	300	572	108	345	816	2014-11-17
13526	lcgq03dbq	PSA×MIRA	345	324	50	300	572	108	345	816	2014-10-06
13526	lcgq03dtq	PSA×MIRA	345	324	50	300	572	108	345	816	2014-10-06
14035	lcsla1i4q	PSA×MIRA	345	324	50	300	572	108	345	816	2015-04-14
14035	lcsla2bhq	PSA×MIRA	345	324	50	300	572	108	345	816	2015-10-02
14452	lcsla1i4q	PSA×MIRA	345	324	50	300	572	108	345	816	2016-04-01
14452	lcsla2bhq	PSA×MIRA	345	324	50	300	572	108	345	816	2016-10-02
13972	lcri01g7q	BOA×MIRA	345	324	50	300	572	108	345	816	2015-10-06
13972	lcri02h8q	BOA×MIRA	345	324	50	300	572	108	345	816	2015-10-06
13972	lcri02hmq	BOA×MIRA	345	324	50	300	572	108	345	816	2015-10-06
14440	ld3701h1q	BOA×MIRA	345	324	50	300	572	108	345	816	2016-10-18
14440	ld3702mzq	BOA×MIRA	345	324	50	300	572	108	345	816	2016-10-19
14440	ld3702nhq	BOA×MIRA	345	324	50	300	572	108	345	816	2016-10-19
14857	ldozbadpq	BOA×MIRA	345	324	50	300	572	108	345	816	2017-09-04
14857	ldozbbgleq	BOA×MIRA	345	324	50	300	572	108	345	816	2017-09-06
14857	ldozbbqlsq	BOA×MIRA	345	324	50	300	572	108	345	816	2017-09-06
14857	ldozpbfl5q	PSA×MIRA	345	324	50	300	572	108	345	816	2017-09-10
14857	ldozpbhq	PSA×MIRA	345	324	50	300	572	108	345	816	2017-09-10
MIRB ACQ/ IMAGE Subarrays											
13171	lc6ka1i3q	PSA×MIRB	184	539	50	300	411	200	345	816	2013-03-02
13171	lc6ka1i3q	PSA×MIRB	184	539	50	300	411	200	345	816	2013-03-02
13171	lc6ka2ioq	PSA×MIRB	184	539	50	300	411	200	345	816	2013-09-01
13171	lc6ka2ioq	PSA×MIRB	184	539	50	300	411	200	345	816	2013-09-01
13616	lc4a1deq	PSA×MIRB	184	539	50	300	411	200	345	816	2014-04-03
MIRB ACQ/ IMAGE Subarray Size After PR#78749 Update											
13616	lc4a2e5q	PSA×MIRB	187	566	50	300	411	200	345	816	2014-10-27
13526	lcgq01q5q	PSA×MIRB	187	566	50	300	411	200	345	816	2014-11-19
13526	lcgq01qj1	PSA×MIRB	187	566	50	300	411	200	345	816	2014-11-19
13526	lcgq02huq	BOA×MIRB	187	566	50	300	411	200	345	816	2014-11-17
13526	lcgq03dlq	PSA×MIRB	187	566	50	300	411	200	345	816	2014-10-06
13972	lcri01fzq	PSA×MIRB	187	566	50	300	411	200	345	816	2015-10-06
13972	lcri01geq	PSA×MIRB	187	566	50	300	411	200	345	816	2015-10-06
13972	lcri02hgq	BOA×MIRB	187	566	50	300	411	200	345	816	2015-10-06
14035	lcsla1i6q	PSA×MIRB	187	566	50	300	411	200	345	816	2015-04-14
14035	lcsla2bjq	PSA×MIRB	187	566	50	300	411	200	345	816	2015-10-02
14452	ld3la1csq	PSA×MIRB	187	566	50	300	411	200	345	816	2016-04-01
14452	ld3la2onq	PSA×MIRB	187	566	50	300	411	200	345	816	2016-10-02
14440	ld3701gtq	PSA×MIRB	187	566	50	300	411	200	345	816	2016-10-18
14440	ld3701h7q	PSA×MIRB	187	566	50	300	411	200	345	816	2016-10-18
14440	ld3702n9q	BOA×MIRB	187	566	50	300	411	200	345	816	2016-10-19
14857	ldozbadhq	PSA×MIRB	187	566	50	300	411	200	345	816	2017-09-04
14857	ldozbadvq	PSA×MIRB	187	566	50	300	411	200	345	816	2017-09-04
14857	ldozbbilmq	BOA×MIRB	187	566	50	300	411	200	345	816	2017-09-06
14857	ldozpbfbq	PSA×MIRB	187	566	50	300	411	200	345	816	2017-09-10

Note. — As correctly reported in the FITS files, the MIRB subarrays values were updated from [XC,YC]=[184,539] to [187,566] on 2014.279 with PR#78749. Simultaneously, the MIRB ACQ/ lamp exposure time and current settings (for the P2 lamp) TAsubarrays.tex:were changed from 17s @ LOW current to 12s @ MED current (PR#78749). The FSW WCA-to-SA offsets ([X,Y]IMCALTARGETOFFSET) were adjusted accordingly (PR#79116) on 2014.289.

Table 16 NUV Spectroscopic ACQ/SEARCH and PEAKD Target Subarrays¹

<i>OPT_ELEM</i>	XC	YC	XS	YS
G185M	509	0	420	1024
G225M	512	0	420	1024
G285M	499	0	420	1024
G230L	659	0	275	1024

¹ NUV ACQ/SEARCH and ACQ/PEAKD external target (SA) subarrays. NUV ACQ/PEAKXD lamp and SA subarrays are given in Table 17.

² Installed by HST commanding on 2009.200 (PR#63095).

Table 17 NUV ACQ/PEAKXD Subarray “XC”s¹

<i>OPT_ELEM</i>	WCA-A	WCA-B	WCA-C	SCI-A	SCI-B	SCI-C
G185M	418	327	192	794	700	565
G225M	430	327	186	804	703	560
G285M	407	313	180	782	688	555
G230L	433	334	194	807	707	564

¹ XC = X-Corner. For all NUV ACQ/PEAKXD TA subarrays: YC=0, YS=1024, and XS=81; where S=Size. Updated on July 19, 2009 (2009.200) with PR#63095. Some early calibration observations used slightly different values.

The NUV spectroscopic TA SA subarrays for the ACQ/PEAKXD are given in Table 17. These subarrays are large enough to only capture the flux from a single NUV stripe. Stripe-specific subarrays are defined for both the WCA and PSA. If used with an extended source, these subarrays are vulnerable to cross-contamination of stripe light. In this table, only the values of XC are listed. For all NUV ACQ/PEAKXDs, YC=0, YS=1024, and XS=81.

4.3 COS FUV Spectroscopic TA Subarrays

The FUV spectroscopic TA subarrays for the WCA are currently the same for ACQ/SEARCH, ACQ/PEAKD, and ACQ/PEAKXD and are given in Table 18 for both FUVA and FUVB. Only one subarray is used for the WCA for each FUV segment, these are labeled ‘A1’ and ‘B1’. As the data are taken in “detector” coordinates, all FUV TA subarrays values are valid only for the normal operating temperature range of COS. FUVB is not used in G140L TAs. Up to four TA subarrays are possible for each FUV SEGMENT³⁰

The FUV spectroscopic subarrays used for all external targets at LP1–4 for FUVA are given in Table 19 and for FUVB in Table 20. There are two subarrays used for each FUV segment, these are labeled ‘A1’, ‘A2’, ‘B1’, and ‘B2’. The COS FSW uses the same subarrays for the PSA and BOA as the offset between the FUV spectra is small (Δ XD~3p). As with the other HST spectrographs, FUV TAs are susceptible to contamination from geocoronal light, particularly Ly α 1216Å, OI 1302Å, and SiII1304Å (Penton & Keyes, 2010). The FUV TA subarrays outlined in

³⁰Increased from 2 per SEGMENT on 2015.258 with PR#81263

Table 18. FUV WCA Subarrays for LP1–4.

<i>OPT_ELEM</i> (1)	XC (2)	A1 Subarray			B1 Subarray			YS (9)
		YC (3)	XS (4)	YS (5)	XC (6)	YC (7)	XS (8)	
LP1								
G130M	1201	541 ^a	13799	44	1501	585	13799	44
G160M	1201	535 ^a	13799	44	1501	579 ^a	13799	44
G140L	1201	547 ^a	13799	44
G140L	4701	547 ^b	10299 ^b	44
LP2 ^c								
G130M	1201	581	13799	44	1501	630	13799	44
G160M	1201	568	13799	44	1501	617	13799	44
G140L	4701	587	10299	44
LP3 ^d								
G130M	1201	515	13799	44	1501	567	13799	44
G160M	1201	504	13799	44	1501	559	13799	44
G140L	4701	521	10299	44
LP4 ^e								
G130M	1201	483	13799	52	1501	539	13799	52
G160M	1201	475	13799	52	1501	534	13799	52
G140L	4701	491	10299	52

^aThese values were updated on 2009.200 (July 19, 2009) with PR#63095, some very early COS calibration and ERO datasets used slightly different TA subarrays.

^bG140L updates were made on Dec. 4, 2012 (2012.339) with PR#72193 to futher optimize the G140L subarrays.

^cUpdated for LP2 operations on July 18, 2012 (2012.200) with PR#70548.

^dUpdated for LP3 operations on Aug. 26, 2014 (2014.238) with PR#78747.

^eUpdated for LP4 operations on Feb. 20, 2017 (2017.051) with PR#86945.

Tables 19 and 20 have been tailored to remove regions of the target spectrum that may contain Geocoronal light. The Geocoronal light fills the aperture and has a very different XD profile which could cause problems with FUV TAs.

In 2014–5, several “hot-spots” appeared during solar maximum. The FUV LP3 subarrays were adjusted to avoid these hot-spots. Details are given in § 4.4, and the adjusted FUVB subarrays are also given in Table 20.

4.4 Trimming of COS FUV TA subarrays due to FUVB “Hot-Spot”.

A “hot-spot” appeared on the COS FUVB segment coincident with increased solar activity in 2014–15. This spot produced enough counts that it could cause mis-centering during all phases of the FUV LP3 (& LP4) spectroscopic TAs. These mis-centerings could be in significant in either the AD or XD. All affected LP3 FUVB TA subarrays were adjusted on April 20, 2015 (2015.110). See PR#80571 for futher details.

In FUVB detector coordinates, the approximate location of the hot-spot is at [X_{DET},Y_{DET}]=[14895,482].

Table 19. FUVA SA Subarrays for LP1–4

<i>OPT_ELEM</i>	<i>CENWAVE</i> (Å)	XC (2)	A1 Subarray			A2 Subarray		
			YC (3)	XS (4)	YS (6)	XC (7)	YC (8)	XS (9)
LP1								
G130M	1291	1201	6555 ^b	437 ^a	76	4078	8896 ^b	437 ^a
G130M	1300	1201	7559 ^b	437 ^a	76	4078	9900 ^b	437 ^a
G130M	1309	1201	8562 ^b	437 ^a	76	4097 ^b	10903 ^b	437 ^a
G130M	1318	1201	9465 ^b	437 ^a	76	3194 ^b	11806 ^b	437 ^a
G130M	1327	1201	10489 ^b	437 ^a	76	2170 ^b	12830 ^b	437 ^a
G160M	ALL	1201	13799	432 ^{a,b}	76
G140L	1105	1201	10458 ^c	445 ^{a,b}	76	457	14543	445 ^{a,b}
G140L	1230 ^g	1201	12216 ^c	445 ^{a,b}	76
G140L	1280	1201	12216 ^c	445 ^{a,b}	76
G140L	1105	4701 ^c	6958 ^c	445 ^{a,b}	76	457	14543	445 ^{a,b}
G140L	1230 ^g	4701 ^c	8716 ^c	445 ^{a,b}	76
G140L	1280	6201 ^c	7400 ^c	445 ^{a,b}	76
LP2 ^d								
G130M	1291	1201	472	6555	76	8896	472	4078
G130M	1300	1201	472	7559	76	9900	472	4078
G130M	1309	1201	472	8562	76	10903	472	4097
G130M	1318	1201	472	9465	76	11806	472	3194
G130M	1327	1201	472	10489	76	12830	472	2170
G160M	ALL	1201	466	13799	76
G140L	1105	4701	479	6958	76	14543	479	457
G140L	1280	6201	479	7400	76	...	34	...
G140L	1105	4701	479	6958	76	14543	479	457
G140L	1280	6201	479	7400	76
LP3 ^e								
G130M	1291	1201	409	6555	76	8896	409	4078
G130M	1300	1201	409	7559	76	9900	409	4078
G130M	1309	1201	409	8562	76	10903	409	4097
G130M	1318	1201	409	9465	76	11806	409	3194
G130M	1327	1201	409	10489	76	12830	409	2170
G160M	ALL	1201	403	13799	76
G140L	1105	4701	418	6958	76	14543	418	457
G140L	1280	6201	418	7400	76
LP4 ^f								
G130M	1291	1201	362	6555	112	8896	362	4078
G130M	1300	1201	362	7559	112	9900	362	4078
G130M	1309	1201	362	8562	112	10903	362	4097
G130M	1318	1201	362	9465	112	11806	362	3194
G130M	1327	1201	362	10489	112	12830	362	2170
G160M	ALL	1201	356	13799	112
G140L	1105	4701	372	6958	112	14543	372	457
G140L	1280	6201	372	7400	112

^aUpdated on 2009.200 with PR#63095, some early ERO and calibrations used slightly different subarrays.^bUpdated early in LP1 on Aug 27, 2009 (2009.2239) with PR#63378.^cG140L updates were made on Dec. 4, 2012 (2012.339) with PR#72193 to further optimize the G140L subarrays.^dUpdated for LP2 July 18, 2012 (2012.200) with PR#70548.^eUpdated for LP3 operations on Aug. 26, 2014 (2014.238) with PR#78747.^fUpdated for LP4 operations on Feb. 20, 2017 (2017.051) with PR#86945.^gStarting with C18, the C1230 *CENWAVE* was replaced with C1280 due to first-order light issues (see Dixon et al., 2010, PR#64041 and PR#64659).

Table 20. FUVB PSA/BOA Subarrays for LP1–4.

<i>OPT_ELEM</i>	<i>CENWAVE</i> (Å)	B1 Subarray			B2 Subarray				
(1)	(2)	XC	YC	XS	YS	XC	YC	XS	YS
LP1 ^c									
G130M	1291	5036 ^b	76	1501	483	7477 ^b	76	7773 ^b	483 ^{a,b}
G130M	1300	6039 ^b	76	1501	483	6474 ^b	76	8776 ^b	483 ^{a,b}
G130M	1309	7023 ^b	76	1501	483	5490 ^a	76	9760 ^a	483 ^{a,b}
G130M	1318	7977 ^b	76	1501	483	4536 ^b	76	10714 ^b	483 ^{a,b}
G130M	1327	7629 ^b	76	2792 ^b	483	3593 ^b	76	11657 ^b	483 ^{a,b}
G160M	ALL	13749	76	1501	477 ^{a,b}
G140L	ALL ^g
LP2 ^c									
G130M	1291	1501	522	5036	76	7773	522	7477	76
G130M	1300	1501	522	6039	76	8776	522	6474	76
G130M	1309	1501	522	7023	76	9760	522	5490	76
G130M	1318	1501	522	7977	76	10714	522	4536	76
G130M	1327	2792	522	7629	76	11657	522	3593	76
G160M	ALL	1501	515	13749	76
G140L	ALL
LP3 ^d (Pre FUVB “Hot-Spot”)									
G130M	1291	1501	460	5036	76	7773	460	7477	76
G130M	1300	1501	460	6039	76	8776	460	6474	76
G130M	1309	1501	460	7023	76	9760	460	5490	76
G130M	1318	1501	460	7977	76	10714	460	4536	76
G130M	1327	2792	460	7629	76	11657	460	3593	76
G160M	ALL	1501	453	13749	76
G140L	ALL
LP3 ^e (Post FUVB “Hot-Spot”) ^d									
G130M	1291	1501	460	5036	76	7773	460	7060 ^e	76
G130M	1300	1501	460	6039	76	8776	460	6057 ^e	76
G130M	1309	1501	460	7023	76	9760	460	5073 ^e	76
G130M	1318	1501	460	7977	76	10714	460	4119 ^e	76
G130M	1327	2792	460	7629	76	11657	460	3176 ^e	76
G160M	ALL	1501	453	13332	76
G140L	ALL
LP4 ^f									
G130M	1291	1501	419	5036	112	7773	419	7060	112
G130M	1300	1501	419	6039	112	8776	419	6057	112
G130M	1309	1501	419	7023	112	9760	419	5073	112
G130M	1318	1501	419	7977	112	10714	419	4119	112
G130M	1327	2792	419	7629	112	11657	419	3176	112
G160M	ALL	1501	416	13332	112
G140L	1105
G140L	1280

^aUpdated during SMOV (2009.201) with PR#63095.^bUpdated for LP2 operations on July 18, 2012 (2012.200) with PR#70548.^cDue to gain sag induced ‘Y-walk’, FUVB usage for ACQ/PEAKXD (NUM_POS=1) TAs was deprecated on 2011.098 with PR#67985. FUVB is still used for ACQ/SEARCH and ACQ/PEAKD TA exposures.^dUpdated for LP3 on Aug. 26, 2014 (2014.238) with PR#78747.^eUpdated for post “Hot-Spot” LP3 TA operations on April 20, 2015 (2015.110) with PR#80571.^fUpdated for LP4 on Feb. 20, 2017 (2017.051) with PR#86945. Both FUVA and FUVB are used for all LP4 ACQ/PEAKXDS (NUM_POS> 1) TA exposures. These subarrays also avoid the FUVB “Hot-Spot”.^gStarting with C18, the C1230 CENWAVE was replaced with C1280 due to first-order light issues. (see Dixon et al., 2010, PR#64041 and PR#64659.

As this is near the detector edge, we are able to avoid this hotspot by stopping the last subarray of the FUVB subarrays at $X_{DET}=14833$. For the COS FUV gratings and the FUVB TA subarrays, the impacts were:

G140L: Not affected as no FUVB TA subarrays are used for G140L

G160M: One FUVB subarray is used for each *CENWAVE* with $XC1=1501$, $XS1=13749$. These were all changed to $XS=13332$ (no change in Y).

G130M: Two *CENWAVE*-specific FUVB subarrays are used to avoid Geocoronal Ly α . The X-size (XS) of the second subarray (XS2) will be trimmed to avoid the hotspot ($XC1$, $XS1$, $XC2$ and all the Y definitions do not change).

As of March 2018, no additional hot-spots have appeared on either FUVA or FUVB that required adjustment of the TA subarrays. Due to the possibility of future hot-spots, the number of allow FUV TA subarrays per segment was increased from two to four on Sept 21, 2015 (2015.264) with PR#81263.

5 NUV Imaging TA verification

Add intro here

5.1 Baseline Bootstrapping of ACQ/IMAGE Modes

Each visit of each cycles annual TA monitoring program directly compares two ACQ/IMAGE configurations. We can bootstrap these back to PSA×MIRA to test the co-alignment of all four configurations. We call this the ‘baseline’ bootstrapping, the results of which are shown in Table 22 for C17–20 and in Table 23 for C21–C24. The values shown in this table are almost exclusively taken from the _RAWACQ.FITS FITS headers of the indicated ACQ/IMAGES. The values in these header keywords have been converted to COS USER coordinates as given by equations 1 & 2. In these header keyword names, ‘Y’ refers to XD (Y_{USER}) and ‘X’ to AD (X_{USER}).

The columns of the Tables 22 & 23 give:

1. *PROPOSID* gives the HST program id (PID).
2. *ROOTNAME* gives the IPPSSOOT of the COS exposure.
3. gives the SA×MIRROR configuration (*APERTURE*×*OPT_ELEM*) of the ACQ/IMAGE.
4. gives the measured AD median (in p) of the WCA (lamp) image, as reported in the ACQ/IMAGE *LAMPMXCR* keyword. (The header keyword name uses ' X_{USER} ' for AD).
5. gives the measured XD median (in p) of the WCA (lamp) image, as reported in the *LAMPMXCR* keyword (The header keyword name uses ' Y_{USER} ' for XD).
6. gives the measured AD centroid³¹ (in p) of the SA (PSA or BOA) target image. This is reported in the *ACQCENTX* keyword ('X' USER coordinate is AD).
7. gives the measured XD centroid (in p) of the SA image. This is reported in the *ACQCENTY* keyword ('Y' USER coordinate is XD).
8. gives the calculated AD centroid (in p) of the SA in use, as reported in the *ACQPREFX* keyword. Calculated as the WCA measured position plus the AD component of the WCA-to-SA offset from the FSW.
9. gives the calculated XD centroid (in p) of the SA in use, as reported in the *ACQPREFY* keyword. Calculated as the WCA measured position plus the XD component of the WCA-to-SA offset from the FSW.
10. gives the SA-to-WCA AD offset (in p) used in this ACQ/IMAGE (calculated as *ACQPREFX*-*ACQCENTX*) This offset, and XD counterpart, should match that given for the corresponding configuration and date in Table 21.
11. gives the SA-to-WCA XD offset (in p) used in this ACQ/IMAGE (calculated as *ACQPREFY*-*ACQCENTY*).
12. gives the AD centering slew (in '') performed by the ACQ/IMAGE, as reported in the *ACQSLEWX* keyword.
13. gives the XD centering slew (in '') performed by the ACQ/IMAGE, as reported in the *ACQSLEWY* keyword.
14. *DATE-OBS* gives the date of the observation in YEAR-MONth-DAy format.

³¹For details of the ACQ/IMAGE target centroiding algorithm, see the COS IHB (Fox et al., 2017 or Penton & Keyes, 2011)

Table 21 ACQ/IMAGE WCA-to-SA FSW Target Offsets

Direction (AD or XD)	DETector Coordinate	USER ^a Coordinate	OPT_ELEM	PSA	BOA
MIRRORA					
AD ^c	Y_{DET}	$-X_{USER}$	MIRRORA	45.3	45.5
XD ^d	X_{DET}	$-Y_{USER}$	MIRRORA	372.7	368.4
MIRRORB prior to Oct-20-2014 (2014.283)					
AD	Y_{DET}	$-X_{USER}$	MIRRORB	45.0	45.5
XD	X_{DET}	$-Y_{USER}$	MIRRORB	374.1	366.3
MIRRORB after ^b to Oct-20-2014 (2014.283)					
AD	Y_{DET}	$-X_{USER}$	MIRRORB	46.0	46.5
XD	X_{DET}	$-Y_{USER}$	MIRRORB	374.0	366.2

^a COS DETector and USER coordinates are related by equations 1 & 2. A consequence of these definitions, a given APERTURE×OPT_ELEM configurations' AD or XD WCA-to-SA offset in one coordinate system is equal to the SA-to-WCA offset in the other. For example, the AD PSA×MIRA WCA-to-PSA offset is +45.3 in detector coordinates (Y_{DET}), as is the SA-to-WCA AD offset in USER coordinates (X_{USER}).

^b Installed 2014.283 (PR#79116, "Update MIRRORB Cal Target Offsets").

^c XD offsets, measured from WCA median to SA center, stored in FSW PCTA_XIMCALTARGETOFFSET table.

^d AD offsets, measured from WCA median to SA center, stored in FSW PCTA_YIMCALTARGETOFFSET table.

The ACQ/IMAGE monitoring results are repeated in Table 24, but sorted by configuration. In this table, it is easier to identify that the correct SA-to-WCA offsets have been used. As noted in Table ??, due to the relationship between COS DETector and USER coordinates (equations 1 & 2), a given APERTURE×OPT_ELEM configurations' AD or XD WCA-to-SA offset in one coordinate system is equal to the SA-to-WCA offset in the other. For example, the XD PSA×MIRA WCA-to-PSA offset is +372.7 in detector coordinates (Y_{DET}), as is the SA-to-WCA XD offset in USER coordinates (X_{USER}).

The SA-to-WCA offsets in the PSA×MIRB section above the horizontal line were taken before the MIRB ACQ/IMAGE adjustment of November 6, 2014. On this date (2014.279), the MIRB ACQ/IMAGE wavelength calibration lamp (P2) exposure time and current were changed to compensate for increasing detector background. Specifically, The LTIMCAL lamp exposure for all MIRB ACQ/IMAGES was changed from a 30 second exposure at LOW current (3 mA) to a 12 second exposure at MEDIUM current (10 mA) with PR#78749. At the same time, the XIMCAL-TARGETOFFSET and YIMCALTARGETOFFSET FSW parameters were updated from [AD,XD]=[45.0,374.1] to [46.0,374.0] for PSA×MIRB and from [AD,XD]=[45.5,366.3] to [46.5,366.2] for BOA×MIRB in the FSW (SCRC#365). Updates tested in Visit 03 of PR#13526 on 2014.279. MIRRORB ACQ/IMAGES were restored to operations on 2014.314.

Non-repeatability of the OSM and aperture mechanisms, along with environmental factors, result in WCA lamp center offsets of up to 4p in AD and to 10p in XD in these exposures in Table 24. BOA ACQ/IMAGES move the aperture in the XD direction to obtain the WCA lamp image. Occasionally, the aperture mechanism misses the desired location by ± 1 APERXPOS step of $\sim 0.053''$. In addition, short term drift is often encountered after mechanism moves in the XD. This could be up to 2p ($\approx 0.106''$) or more, and is not correctable. These errors correspond directly to unintentional XD target offsets. However, the XD alignment requirement ($0.3''$) can accommodate this error. To date, only single-step XD offset errors have been observed in BOA

Table 22. C17–C20 PSA ACQ/IMAGE Co-alignment Measurements

PROP OSID	ROOT NAME	Configuration APERTURE × OPT_ELEM	WCA-Msrda		PSA-Msrda		PSA-Centered		SA-to-WCA		TA Centering		DATE- OBS		
			MXCR	MYCR	ACQ	CENTX	ACQ	PREFX	ACQ	AD	XD ^b	AD	SLEWX	ACQ	
(PID)	(1)	(2)	(3)	(4)	(5)	(6)	(7)	(8)	(9)	(10)	(11)	(12)	(13)	(14)	
C17															
P11878	lbc1a3s3q	PSA×MIRA	555	653	509.3	282.7	509.7	280.3	45.3	372.7	-0.010	0.056	2010-11-05		
P11878	lbc1a3s7q	PSA×MIRB	342	813	296.4	439.8	297.0	438.9	45.0	374.1	-0.015	0.021	2010-11-05		
C18															
P12399	lbt7a2ahq	PSA×MIRA	529	653	475.2	279.5	483.7	280.3	45.3	372.7	-0.200	-0.019	2011-09-12		
P12399	lbt7a2ajq	PSA×MIRB	317	813	271.2	439.3	272.0	438.9	45.0	374.1	-0.018	0.008	2011-09-12		
C19															
P12781	lbx1a2ffq	PSA×MIRA	503	650	450.0	280.6	457.7	277.3	45.3	372.7	-0.183	0.078	2012-09-24		
P12781	lbx1a2fhq	PSA×MIRB	296	811	249.8	436.0	251.0	436.9	45.0	374.1	-0.028	-0.021	2012-09-24		
C20															
P13171	lc6ka2imq	PSA×MIRA	508	650	459.7	284.0	462.7	277.3	45.3	372.7	-0.070	0.158	2013-09-01		
P13171	lc6ka2ioq	PSA×MIRB	304	811	258.2	436.5	259.0	436.9	45.0	374.1	-0.019	-0.009	2013-09-01		
P13124	lc6601rrq	PSA×MIRB	312	810	266.5	426.9	267.0	435.9	45.0	374.1	-0.012	-0.211	2013-10-24		
P13124	lc6601rvq	BOA×MIRA	524	650	479.0	284.8	478.5	281.6	45.5	368.4	0.012	0.074	2013-10-24		
P13124	lc6602y5q	BOA×MIRA	533	651	484.7	281.2	487.5	282.6	45.5	368.4	-0.066	-0.032	2013-11-01		
P13124	lc6602y9q	BOA×MIRB	326	813	279.7	442.3	280.5	446.7	45.5	366.3	-0.019	-0.102	2013-11-01		

^aNon-repeatability of the OSM and aperture mechanisms, along with environmental factors, result in lamp center offsets of up to 3 p in AD and to 52 p in XD in these exposures.

Note. — If the table caption is in the *Courier* font, this value was taken directly from the indicated *_RAWACQ.FITS* header keyword. In DETector coordinates, +AD is -Y_{DET}, +XD is -X_{DET}, in USER coordinates, +AD is +Y_{USER}, +XD is +X_{USER}.

ACQ/IMAGES. These single-step offset errors are discussed further in § 5.2

5.2 Co-alignment of ACQ/IMAGE Configurations

C20–C24 results of Tables 22 & 23 and 24 can be combined to show the measured offsets of PSA×MIRB, BOA×MIRA, and BOA×MIRB compared to the initial PSA×MIRA ACQ/IMAGE. These results are shown in Table 24. The C20–23 FGS-to-SI alignment programs contain PSA×MIRB alignment exposures, but consisted of only back-to-back PSA×MIRA & PSA×MIRB tacqIMAGES. The C21 and C24 TA monitoring programs used their contingency visits to obtain a pair of back-to-back ACQ/IMAGES for each configuration.³²

The columns of Table 25 are:

1. *PROPOSID* gives the HST program id (PID).
2. *ROOTNAME* gives the IPPSSOOT of the COS exposure.

³²The C21 contingency visit (PR#13526) was used to test the MIRB WCA lamp changes for ACQ/IMAGE, and the C24 contingency visit (PR#13526) was activated due to changes to the FGS-to-SI alignment program.

Table 23. C21–24 ACQ/IMAGE Bootstrapping Results

PROP OSID (PID) (1)	ROOT NAME (2)	Configuration <i>APERTURE</i> × <i>OPT_ELEM</i> (3)	WCA-Msrda		SA-Msrdb		SA-Centred		SA-to-WCA		TA Centering		DATE- OBS (14)
			<i>MXCR</i>	<i>MYCR</i>	<i>ACQ</i>	<i>ACQ</i>	<i>ACQ</i>	<i>ACQ</i>	<i>SLEWX</i>	<i>SLEWY</i>	<i>ACQ</i>	<i>ACQ</i>	
			<i>LAMP</i>	<i>LAMP</i>	<i>CENTX</i>	<i>CENTY</i>	<i>PREFX</i>	<i>PREFY</i>	<i>AD</i>	<i>XD</i>	<i>AD</i>	<i>XD</i>	
C21													
P13616	lci4a2e3q	PSA×MIRA	517	650	471.7	282.9	471.7	277.3	45.3	372.7	0.001	0.133	2014-10-27
P13616	lci4a2e5q	PSA×MIRB	305	809	259.7	436.1	259.0	435.0	46.0	374.0	0.016	0.027	2014-10-27
P13526	lcgq03dbq	PSA×MIRA	566	648	527.7	268.2	520.7	275.3	45.3	372.7	0.166	-0.168	2014-10-06
P13526	lcgq03dlq	PSA×MIRB	357	808	310.8	434.2	312.0	433.9	45.0	374.1	-0.029	0.006	2014-10-06
P13526	lcgq03dtq	PSA×MIRA	574	649	530.1	275.2	528.7	276.3	45.3	372.7	0.032	-0.026	2014-10-06
P13526	lcgq01q5q	PSA×MIRB	306	809	222.4	447.7	260.0	435.0	46.0	374.0	-0.888	0.298	2014-11-19
P13526	lcgq01qdq	BOA×MIRA	520	651	472.9	283.2	474.5	282.6	45.5	368.4	-0.038	0.013	2014-11-19
P13526	lcgq01qjy	PSA×MIRB	305	811	260.2	433.7	259.0	437.0	46.0	374.0	0.027	-0.078	2014-11-19
P13526	lcgq02hmq	BOA×MIRA	495	649	452.0	293.6	449.5	280.6	45.5	368.4	0.058	0.305	2014-11-17
P13526	lcgq02huq	BOA×MIRB	285	811	237.9	440.3	238.5	444.8	46.5	366.2	-0.015	-0.105	2014-11-17
P13526	lcgq02i0q	BOA×MIRA	501	651	455.7	285.3	455.5	282.6	45.5	368.4	0.006	0.063	2014-11-17
C22													
P14035	lcsla2bhq	PSA×MIRA	505	653	458.8	284.8	459.7	280.3	45.3	372.7	-0.020	0.105	2015-10-02
P14035	lcsla2bjq	PSA×MIRB	293	813	247.9	439.3	247.0	439.0	46.0	374.0	0.022	0.007	2015-10-02
P13972	lcri01fzq	PSA×MIRB	302	813	264.0	427.4	256.0	439.0	46.0	374.0	0.189	-0.273	2015-10-06
P13972	lcri01g7q	BOA×MIRA	517	651	471.0	287.2	471.5	282.6	45.5	368.4	-0.011	0.109	2015-10-06
P13972	lcri01geq	PSA×MIRB	300	812	255.5	434.1	254.0	438.0	46.0	374.0	0.036	-0.092	2015-10-06
P13972	lcri02h8q	BOA×MIRA	499	654	462.0	272.2	453.5	285.6	45.5	368.4	0.201	-0.315	2015-10-06
P13972	lcri02hgq	BOA×MIRB	286	810	240.6	444.2	239.5	443.8	46.5	366.2	0.026	0.010	2015-10-06
P13972	lcri02hmq	BOA×MIRA	504	651	457.7	284.2	458.5	282.6	45.5	368.4	-0.018	0.038	2015-10-06
C23													
P14452	ld3la2ojq	PSA×MIRA	527	654	481.0	284.5	481.7	281.3	45.3	372.7	-0.017	0.075	2016-10-02
P14452	ld3la2onq	PSA×MIRB	306	813	259.9	439.9	260.0	439.0	46.0	374.0	-0.002	0.021	2016-10-02
P14440	ld3701gtq	PSA×MIRB	297	813	246.6	442.7	251.0	439.0	46.0	374.0	-0.104	0.088	2016-10-18
P14440	ld3701lh1q	BOA×MIRA	518	651	471.7	287.1	472.5	282.6	45.5	368.4	-0.018	0.105	2016-10-18
P14440	ld3701h7q	PSA×MIRB	295	811	249.7	434.0	249.0	437.0	46.0	374.0	0.016	-0.071	2016-10-18
P14440	ld3702mzq	BOA×MIRA	509	654	480.0	299.3	463.5	285.6	45.5	368.4	0.390	0.322	2016-10-19
P14440	ld3702n9q	BOA×MIRB	295	811	248.5	446.1	248.5	444.8	46.5	366.2	0.001	0.030	2016-10-19
P14440	ld3702nhq	BOA×MIRA	516	651	470.0	285.0	470.5	282.6	45.5	368.4	-0.012	0.057	2016-10-19
C24													
P14857	ldozpb5fq	PSA×MIRA	515	654	467.3	266.2	469.7	281.3	45.3	372.7	-0.058	-0.355	2017-09-10
P14857	ldozpbfbq	PSA×MIRB	289	813	243.8	440.0	243.0	439.0	46.0	374.0	0.020	0.023	2017-09-10
P14857	ldozpbfhq	PSA×MIRA	510	653	463.9	279.8	464.7	280.3	45.3	372.7	-0.020	-0.011	2017-09-10
P14857	ldozbadhq	PSA×MIRB	299	813	237.5	397.9	253.0	439.0	46.0	374.0	-0.366	-0.967	2017-09-04
P14857	ldozbadpq	BOA×MIRA	524	651	477.9	287.4	478.5	282.6	45.5	368.4	-0.013	0.113	2017-09-04
P14857	ldozbadqv	PSA×MIRB	298	811	253.2	434.5	252.0	437.0	46.0	374.0	0.029	-0.059	2017-09-04
P14857	ldozbbgleq	BOA×MIRA	518	653	484.8	289.5	472.5	284.6	45.5	368.4	0.290	0.114	2017-09-06
P14857	ldozbbilmq	BOA×MIRB	293	811	246.7	444.3	246.5	444.8	46.5	366.2	0.006	-0.011	2017-09-06
P14857	ldozbbllsq	BOA×MIRA	514	651	467.9	285.1	468.5	282.6	45.5	368.4	-0.015	0.060	2017-09-06

^aNon-repeatability of the OSM and aperture mechanisms, along with environmental factors, result in lamp center offsets of up to 6 p in AD and > 50 p in XD in these exposures.

^bBOA ACQ/IMAGES move the aperture in the XD direction to obtain the WCA lamp image. Occasionally, the aperture mechanism misses the desired location by ± 1 APERYPOS step of $\sim 0.053''$.

Note. — If the table caption is in the *ITALICS*, this value was taken directly from the indicated *_RAWACQ.FITS* header keyword. Columns 4-11 are in units of NUV pixels (p). Columns 12 & 13 are in arcseconds (''). In DETector coordinates, +AD is $-Y_{DET}$, +XD is $-X_{DET}$, in USER coordinates, +AD is $+Y_{USER}$, +XD is $+X_{USER}$.

Table 24. ACQ / IMAGE Bootstrapping Measurements Sorted by Configuration

PROP OSID (PID) (1)	ROOT NAME (2)	HST Cycle (3)	WCA-Msrda		SA-Msrdb		SA-Center		SA-to-WCA		TA Centering		DATE OBS (14)
			LAMP MXCR AD (4)	LAMP MYCR XD (5)	ACQ MSRDX AD (6)	ACQ MSRDY XD (7)	ACQ PREFIX AD (8)	ACQ PREFIX XD (9)	AD (10)	XD (11)	AD ('') (12)	ACQ SLEWX AD ('') (13)	ACQ SLEWY XD ('') (14)
			PSA × MIRRORA										
P11878	lbcla3s3q	C17	555	653	509.3	282.7	509.7	280.3	45.3	372.7	-0.010	0.056	2010-11-05
P12399	lbtm7a2ahq	C18	529	653	475.2	279.5	483.7	280.3	45.3	372.7	-0.200	-0.019	2011-09-12
P12781	lbx1a2ffq	C19	503	650	450.0	280.6	457.7	277.3	45.3	372.7	-0.183	0.078	2012-09-24
P13171	lc6ka2imq	C20	508	650	459.7	284.0	462.7	277.3	45.3	372.7	-0.070	0.158	2013-09-01
P13616	lci4a2e3q	C21	517	650	471.7	282.9	471.7	277.3	45.3	372.7	0.001	0.133	2014-10-27
P14035	lcsla2bhq	C22	505	653	458.8	284.8	459.7	280.3	45.3	372.7	-0.020	0.105	2015-10-02
P14452	ld3la2oqj	C23	527	654	481.0	284.5	481.7	281.3	45.3	372.7	-0.017	0.075	2016-10-02
P14857	ldozpbfsq	C24	515	654	467.3	266.2	469.7	281.3	45.3	372.7	-0.058	-0.355	2017-09-10
P14857	ldozpbfhq	C24	510	653	463.9	279.8	464.7	280.3	45.3	372.7	-0.020	-0.011	2017-09-10
PSA × MIRRORB ^c													
P11878	lbcla3s7q	C17	342	813	296.4	439.8	297.0	438.9	45.0	374.1	-0.015	0.021	2010-11-05
P12399	lbtm7a2ajq	C18	317	813	271.2	439.3	272.0	438.9	45.0	374.1	-0.018	0.008	2011-09-12
P12781	lbx1a2fhq	C19	296	811	249.8	436.0	251.0	436.9	45.0	374.1	-0.028	-0.021	2012-09-24
P13171	lc6ka2ioq	C20	304	811	258.2	436.5	259.0	436.9	45.0	374.1	-0.019	-0.009	2013-09-01
P13124	lc6601rrq	C20	312	810	266.5	426.9	267.0	435.9	45.0	374.1	-0.012	-0.211	2013-10-24
P13616	lci4a2e5q	C21	305	809	259.7	436.1	259.0	435.0	46.0	374.0	0.016	0.027	2014-10-27
P14035	lcsla2bjq	C22	293	813	247.9	439.3	247.0	439.0	46.0	374.0	0.022	0.007	2015-10-02
P13972	lcri01fzq	C22	302	813	264.0	427.4	256.0	439.0	46.0	374.0	0.189	-0.273	2015-10-06
P13972	lcri01geq	C22	300	812	255.5	434.1	254.0	438.0	46.0	374.0	0.036	-0.092	2015-10-06
P14452	ld3la2onq	C23	306	813	259.9	439.9	260.0	439.0	46.0	374.0	-0.002	0.021	2016-10-02
P14440	ld3701gtq	C23	297	813	246.6	442.7	251.0	439.0	46.0	374.0	-0.104	0.088	2016-10-18
P14440	ld3701h7q	C23	295	811	249.7	434.0	249.0	437.0	46.0	374.0	0.016	-0.071	2016-10-18
P14857	ldozbadhq	C24	299	813	237.5	397.9	253.0	439.0	46.0	374.0	-0.366	-0.967	2017-09-04
P14857	ldozbadvq	C24	298	811	253.2	434.5	252.0	437.0	46.0	374.0	0.029	-0.059	2017-09-04
P14857	ldozpbfbq	C24	289	813	243.8	440.0	243.0	439.0	46.0	374.0	0.020	0.023	2017-09-10
BOA × MIRRORA													
P13124	lc6601rvq	C20	524	650	479.0	284.8	478.5	281.6	45.5	368.4	0.012	0.074	2013-10-24
P13124	lc6602y5q	C20	533	651	484.7	281.2	487.5	282.6	45.5	368.4	-0.066	-0.032	2013-11-01
P13526	lcgq01qdq	C21	520	651	472.9	283.2	474.5	282.6	45.5	368.4	-0.038	0.013	2014-11-19
P13972	lcri01g7q	C22	517	651	471.0	287.2	471.5	282.6	45.5	368.4	-0.011	0.109	2015-10-06
P13972	lcri02h8q	C22	499	654	462.0	272.2	453.5	285.6	45.5	368.4	0.201	-0.315	2015-10-06
P13972	lcri02hmq	C22	504	651	457.7	284.2	458.5	282.6	45.5	368.4	-0.018	0.038	2015-10-06
P14440	ld3701h1q	C23	518	651	471.7	287.1	472.5	282.6	45.5	368.4	-0.018	0.105	2016-10-18
P14440	ld3702mzq	C23	509	654	480.0	299.3	463.5	285.6	45.5	368.4	0.390	0.322	2016-10-19
P14440	ld3702nhq	C23	516	651	470.0	285.0	470.5	282.6	45.5	368.4	-0.012	0.057	2016-10-19
P14857	ldozbadpq	C24	524	651	477.9	287.4	478.5	282.6	45.5	368.4	-0.013	0.113	2017-09-04
P14857	ldozbbleq	C24	518	653	484.8	289.5	472.5	284.6	45.5	368.4	0.290	0.114	2017-09-06
P14857	ldozbbbsq	C24	514	651	467.9	285.1	468.5	282.6	45.5	368.4	-0.015	0.060	2017-09-06
BOA × MIRRORB ^c													
P13124	lc6602y9q	C20	326	813	279.7	442.3	280.5	446.7	45.5	366.3	-0.019	-0.102	2013-11-01
P13526	lcgq02huq	C21	285	811	237.9	440.3	238.5	444.8	46.5	366.2	-0.015	-0.105	2014-11-17
P13972	lcri02hgq	C22	286	810	240.6	444.2	239.5	443.8	46.5	366.2	0.026	0.010	2015-10-06
P14440	ld3702n9q	C23	295	811	248.5	446.1	248.5	444.8	46.5	366.2	0.001	0.030	2016-10-19
P14857	ldozbbmq	C24	293	811	246.7	444.3	246.5	444.8	46.5	366.2	0.006	-0.011	2017-09-06

^aEnvironmental factors, and non-repeatable mechanisms, results in lamp offsets up to 6 p in AD and > 50 p in XD.^bBOA ACQ / IMAGES move the aperture in the XD and can miss its WCA location by ±1 APERXPOS ∼ 0.053'' step.^cOn 2014.310, the MIRB ACQ / IMAGE lamp exposure changed in duration & current (PR#67139).

Note. — Table captions in *Courier* indicated _RAWACQ.FITS header keywords. Columns 4-11 are in units of NUV pixels (p). Columns 12 & 13 are in arcseconds (''). In DETector coordinates, +AD is -Y_{DET}, +XD is -X_{DET}, in USER coordinates, +AD is +Y_{USER}, +XD is +X_{USER}.

3. gives the SA×MIRROR Config#1 (*APERTURE*×*OPT_ELEM*) of the initial ACQ/IMAGE (Config#1). This ACQ/IMAGE centers the target for the following ACQ/IMAGE (Config#2).
 4. gives ACQ/IMAGE [AD,XD] slew (in '') as reported by *ACQSLEWX* & *ACQSLEWY*.
- 6-10 Repeat of columns 1-5 for the configuration being tested (Config#2).
- 11-15 Repeat of columns 1-5 for the repeat of Config#1 (“...” indicate data was not available).

The ACQ/IMAGE slews of the initial Config#1 exposures reflect the scatter that can be expected from HST blind pointing. For example, the C21 Config#1 ACQ/IMAGES show initial offsets ranging from [AD,XD] = [-0.888, 0.298]'' (R=0.94'') to [0.166, -0.168]'' (R=0.24''). The use of GAIA guide stars (GS), with superior astrometry, for COS began on 2017.272 (just before the FUV LP4 move on 2017.275). This shows promise to reduce the GS contribution to the COS blind pointing.

Config#2 ACQ/IMAGES start with the target centered via the Config#1 exposure and should provide a direct measure of the co-alignment of the two configurations. A 2nd Config#1 exposure follows Config#2 for all BOA configurations, and for the PSA×MIRB exposures in C21 and C24. These offsets can be averaged to determine the approximate co-alignment of the modes for each Cycle. These results are shown in Table 26. As previously discussed, the COS aperture does not always go back to the same XD positon after being moved. The keyword *APERYPOS* can be used to track and correct these single step (0.053'') offsets.

The columns of Table 26 are:

1. Config#1 gives the *APERTURE*×*OPT_ELEM* (SA×MIRROR) of the initial and confirming ACQ/IMAGE exposures.
2. Config#2 gives the *APERTURE*×*OPT_ELEM* of the ACQ/IMAGE configuration being tested. The alignment of Config#2 to Config#1 is being measured.
3. Gives the [AD,XD] slew (in '') as reported by the *ACQSLEWX* & *ACQSLEWY* from the Config#2 ACQ/IMAGE.
4. Gives the [AD,XD] slew (in '') as reported in the confirming (2nd) Config#1 ACQ/IMAGE. These slews should be in the opposite [AD,XD] direction from the Config#2 slews. For C22 and C23, there is no confirming PSA×MIRA Config#1 exposure. These are indicated by “...” in the table.
5. Gives the average of the Column 3 (Offset#1) and Column 4 (Offset#2) slews. These are calculated as Avg [AD,XD] = ([AD,XD]#1 - [AD,XD]#2)/2.
6. Gives the [AD,XD] offset correction based upon knowledge of the COS AD (*APERXPOS*) and X (*APERYPOS*) aperture position. All *APERXPOS* positions were nominal (22.1), but the *APERYPOS* positions were nominal (126.1) ±1 step. The parity of the correction is that a change of -1 *APERYPOS* step requires a positive *ACQSLEWY* correction of +0.053'' (19 *APERYPOS* steps per '').
7. Gives estimated co-alignment of Config#2 to Config#1. Uncertainties associated with each ACQ/IMAGE configuration are based upon measurement errors are given in Table 2.

Table 27 collects these results individually for C20–C24 ACQ/IMAGES, and as a group. In order to summarize the results, the table used a “From” and “To” arrangement where the co-alignment is presented with the “From” ACQ/IMAGE configuration represented for the 1st column. This is identical to the Config#1, used in previous tables. The “To” configurations are given by the columns 2-5 and represent the Config#1 of previous tables. Tables are given for each Cycle, and then as an average over C20–24.

The columns of Table 27 are:

1. Base Configuration gives the config ($APERTURE \times OPT_ELEM$, or SA \times MIRROR) is the “To” configuration in the Config#1 To Config#2, or Config#2 as used other tables. Columns 2-4 give the “From” or Config#1 ACQ/ IMAGE $APERTURE$ and MIRROR configuration.
2. PSA \times MIRA as the “From” configuration (Config#1).
3. PSA \times MIRB as the “From” configuration (Config#1).
4. BOA \times MIRA as the “From” configuration (Config#1).
5. BOA \times MIRB as the “From” configuration (Config#1).
6. Gives the measurement uncertainty for the “To” mode in NUV pixels as given in Table 2.
7. Gives the measurement uncertainty in " as given in Table 2. Note that for convenience, a mean plate scale was assumed so that this uncertainty applies both to AD and XD.
8. Gives the estimate co-alignment of Config#2 to Config#1. Uncertainties associated with each ACQ/ IMAGE configuration based upon measurement errors are given in Table 2.

The NUV AD TA requirements are strictest at $0.041''$, while the strictest FUV requirement is $0.106''$. The co-alignment results allow us to compare the centering of all ACQ/ IMAGE configurations to PSA \times MIRA, and is therefore a measure of our NUV imaging TA precision. Averaged over C20–24:

- PSA \times MIRB was aligned with PSA \times MIRA to [AD, XD] \sim [0.002, 0.015] \pm 0.012".
- BOA \times MIRA was aligned with PSA \times MIRA to [AD, XD] \sim [-0.021, 0.082] \pm 0.014".
- BOA \times MIRB was aligned with PSA \times MIRA to [AD, XD] \sim [-0.016, 0.047] \pm 0.016".

In each case, C21 showed the worst co-alignment:

- PSA \times MIRB was aligned with PSA \times MIRA to [AD, XD] \sim [-0.031, 0.016] \pm 0.024".
- BOA \times MIRA was aligned with PSA \times MIRA to [AD, XD] \sim [-0.063, 0.088] \pm 0.024".
- BOA \times MIRB was aligned with PSA \times MIRA to [AD, XD] \sim [-0.074, 0.030] \pm 0.024".

As all three C21 measurements occurred in different visits, it is unlikely that this is a simple GS issue skewed these results. However, as the four cycle averages are less than $\frac{1}{2}$ of the most restrictive TA requirement, and are all at or below the $1.5 \times$ the measurement error, NUV imaging TA appears to have been functioning nominally, if not exceptionally, over C20–24.

5.3 WCA Lamp Images (aka, Lamp Family Portraits)

The four panels of Figures 1–4 show a ‘family portrait’ of the available COS PtNe Lamp (**P1** or **P2**) + MIRROR (MIRA or MIRB) combinations possible with ACQ/ IMAGE. Panel titles give the lamp and mirror configuration, along with the lamp current setting (in milli-amps, mA) and the exposure times. The images and subarrays are in ‘detector’ coordinates, as used on-board COS. The images show the observed counts/pixel/s (cps) as given by the colorbar on the bottom. The red dashed boxes show the given cycles’ ACQ/ IMAGE WCA subarrays. At the top of the subarrays, text provides the count rate in the brightest pixel (BP) in units of cps. The blue histogram on the bottom edge shows the cross-dispersion (XD) lamp profile in detector ‘ X_{DET} ’ coordinates, while the green histogram on the left edge shows the along-dispersion (AD) lamp profile in detector ‘ Y_{DET} ’ coordinates. The cross-hairs show the median location of the given configurations’ lamp events within the TA subarray. PtNe#2 (**P2**) lamp was used for all ACQ/ IMAGES during C20–24, and was operated at LOW current (6 mA) for MIRA images and LOW current (3 mA) or MEDium

Table 25. ACQ / IMAGE Co-alignment Measurements

PROPOSID (PID)	ROOT NAME	Configuration ^a #1 [X,Y] ('')	ACQSLEW YPOS	APER PID	ROOT NAME	Config ^a #2 [X,Y] ('')	ACQSLEW YPOS	APER PID	ROOT NAME	Config ^{a,c} #1 [X,Y] ('')	ACQSLEW YPOS	APER PID		
(1)	(2)	(3)	(4)	(5)	(6)	(7)	(8)	(9)	(10)	(11)	(12)	(13)	(14)	(15)
C20 ^d														
P13171	lc6ka2imq	PSA × MIRA	[-0.070, 0.158]	127.1	P13171	lc6ka2ioq	PSA × MIRB	[-0.019, -0.009]	127.1
P13124	lc6601rrq	PSA × MIRB	[-0.012, -0.211]	127.1	P13124	lc6601rvq	BOA × MIRA	[0.012, 0.074]	127.1
P13124	lc6602y5q	BOA × MIRA	[-0.066, -0.032]	126.1	P13124	lc6602y9q	BOA × MIRB	[-0.019, -0.102]	126.1
C21 ^b														
P13616	lci4a2e3q	PSA × MIRA	[0.001, 0.133]	127.1	P13616	lci4a2e5q	PSA × MIRB	[0.016, 0.027]	127.1
P13526	lcgq03dbq	PSA × MIRB	[-0.166, -0.168]	127.1	P13526	lcgq03dlq	PSA × MIRB	[-0.029, 0.006]	127.1	P13526	lcgq03dtq	PSA × MIRA	[0.032, -0.026]	127.1
P13526	lcgq01qsq	PSA × MIRB	[-0.888, 0.298]	127.1	P13526	lcgq01dqq	BOA × MIRA	[-0.038, 0.013]	126.1	P13526	lcgq01ljq	PSA × MIRB	[0.027, -0.078]	126.1
P13526	lcgq02hmq	BOA × MIRA	[0.058, 0.305]	127.1	P13526	lcgq02huq	BOA × MIRB	[-0.015, -0.105]	126.1	P13526	lcgq02ifq	BOA × MIRA	[0.006, 0.063]	126.1
C22														
P14035	lcsla2bhq	PSA × MIRA	[-0.020, 0.105]	125.1	P14035	lcsla2bjq	PSA × MIRB	[0.022, 0.007]	125.1
P13972	lcri01fzq	PSA × MIRB	[0.189, -0.273]	125.1	P13972	lcri01g7q	BOA × MIRA	[-0.011, 0.109]	126.1	P13972	lcri01geq	PSA × MIRB	[0.036, -0.092]	126.1
P13972	lcri02h8q	BOA × MIRA	[0.201, -0.315]	125.1	P13972	lcri02hq	BOA × MIRB	[0.026, 0.010]	126.1	P13972	lcri02hmq	BOA × MIRA	[-0.018, 0.038]	126.1
C23														
P14452	ld3la2ojq	PSA × MIRA	[-0.017, 0.075]	125.1	P14452	ld3la2onq	PSA × MIRB	[-0.002, 0.021]	125.1
P14440	ld3701gtq	PSA × MIRB	[-0.104, 0.088]	125.1	P14440	ld3701h1q	BOA × MIRA	[-0.018, 0.105]	126.1	P14440	ld3701h7q	PSA × MIRB	[0.016, -0.071]	126.1
P14440	ld3702mzq	BOA × MIRA	[0.390, 0.322]	125.1	P14440	ld3702n9q	BOA × MIRB	[0.001, 0.030]	126.1	P14440	ld3702nhq	BOA × MIRA	[-0.012, 0.057]	126.1
C24														
P14857	ldozpbff5q	PSA × MIRA	[-0.058, -0.355]	125.1	P14857	ldozpbfbq	PSA × MIRB	[0.020, 0.023]	125.1	P14857	ldozpbfhq	PSA × MIRA	[-0.020, -0.011]	125.1
P14857	ldozbadhq	PSA × MIRB	[-0.366, -0.967]	125.1	P14857	ldozbadpq	BOA × MIRA	[-0.013, 0.113]	126.1	P14857	ldozbadvq	PSA × MIRB	[0.029, -0.059]	126.1
P14857	ldozbbfq	BOA × MIRA	[0.290, 0.114]	125.1	P14857	ldozbbfq	BOA × MIRB	[0.006, -0.011]	126.1	P14857	ldozbbfsq	BOA × MIRA	[-0.015, 0.060]	126.1

^aEach row tests the co-alignment of two ACQ / IMAGE configurations. The first “Configuration#1” exposure centers the target, then the “Configuration#2” exposure measures the co-alignment. A second Configuration#1 ACQ / IMAGE provides a second co-alignment measurement of the BOA configuration #2s.

^bDuring C21, both the FGS-to-SI (P13636) and TA monitoring program (P13526) executed PSA × MIRA and PSA × MIRB back-to-back ACQ / IMAGES. P13526 contained an additional PSA × MIRA exposure as part of the MIRB re-enablement effort. Both programs provided consistent results, but the more complete P13526 dataset is used in the analysis of this ISR.

^cDuring C20 no confirming PSA × MIRA ACQ / IMAGES were obtained in the COS TA monitoring program (P13124).

Note. — FGS-to-SI alignment programs (P13616, P14035, & P14452) contain a single pair of ACQ / IMAGES, while the COS TA programs contain a third Configuration#1 ACQ / IMAGE.

Table 26. Initial ACQ/IMAGE Co-alignment Measurements

Configuration #1 (1)	Configuration #2 (2)	Offset#1 [AD,XD] ('') (3)	Offset#2 [AD,XD] ('') (4)	Avg Offset (5)	APERYPOS Correction [AD,XD] ('') (6)	Est. Offset [AD,XD] ('') (7)
C21						
PSA×MIRA	PSA×MIRB	[-0.029, 0.006]	[0.032,-0.026]	[-0.031, 0.016]	[0.000,0.000]	[-0.031, 0.016]
PSA×MIRB	BOA×MIRA	[-0.038, 0.013]	[0.027,-0.078]	[-0.033, 0.046]	[0.000,0.053]	[-0.033, 0.072]
BOA×MIRA	BOA×MIRB	[-0.015,-0.105]	[0.006, 0.063]	[-0.011,-0.084]	[0.000,0.053]	[-0.011,-0.058]
C22						
PSA×MIRA	PSA×MIRB	[0.022, 0.007]	... ^a	[0.022, 0.007]	[0.000, 0.000]	[0.022, 0.007]
PSA×MIRB	BOA×MIRA	[-0.011, 0.109]	[0.036,-0.092]	[-0.024, 0.101]	[0.000,-0.053]	[-0.024, 0.074]
BOA×MIRA	BOA×MIRB	[0.026, 0.010]	[-0.018, 0.038]	[0.022,-0.014]	[0.000,-0.053]	[0.022,-0.040]
C23						
PSA×MIRA	PSA×MIRB	[-0.002, 0.021]	... ^a	[-0.002, 0.021]	[0.000, 0.000]	[-0.002, 0.021]
PSA×MIRB	BOA×MIRA	[-0.018, 0.105]	[0.016,-0.071]	[-0.017, 0.088]	[0.000,-0.053]	[-0.017, 0.062]
BOA×MIRA	BOA×MIRB	[0.001, 0.030]	[-0.012, 0.057]	[0.007, 0.122]	[0.000,-0.053]	[0.007, 0.095]
C24						
PSA×MIRA	PSA×MIRB	[0.020, 0.023]	[-0.020,-0.011]	[0.020, 0.017]	[0.000, 0.000]	[0.020, 0.017]
PSA×MIRB	BOA×MIRA	[-0.013, 0.113]	[0.029,-0.059]	[-0.021, 0.086]	[0.000,-0.053]	[-0.021, 0.060]
BOA×MIRA	BOA×MIRB	[0.006,-0.011]	[-0.015, 0.060]	[0.011,-0.036]	[0.000,-0.053]	[0.011,-0.062]

^aFor C22 and C23, no confirming PSA×MIRA Configuration#1 exposures were acquired.

Table 27. C20–C24 ACQ/IMAGE Co-Alignment Results

Base Configuration (1)	PSA ×MIRA [AD,XD]'' (2)	PSA ×MIRB [AD,XD]'' (3)	BOA ×MIRA [AD,XD]'' (4)	BOA ×MIRB [AD,XD]'' (5)	Measurement Uncertainty ^a (p) ('') (6) (7)	
C20						
PSA×MIRA	[1,1]	[0.019,0.009]	[0.007,-0.065]	[0.026,0.037]	0.850	0.020
PSA×MIRB	[-0.019,-0.009]	[1,1]	[-0.012,-0.074]	[0.007,0.028]	1.041	0.024
BOA×MIRA	[-0.007,0.065]	[0.012,0.074]	[1,1]	[0.019,0.102]	1.201	0.028
BOA×MIRB	[-0.026,-0.037]	[-0.007,-0.028]	[-0.019,-0.102]	[1,1]	1.343	0.032
C21						
PSA×MIRA	[1,1]	[0.031,-0.016]	[0.063,-0.088]	[0.074,-0.030]	0.850	0.020
PSA×MIRB	[-0.031,0.016]	[1,1]	[0.033,-0.072]	[0.043,-0.014]	1.041	0.024
BOA×MIRA	[-0.063,0.088]	[-0.033,0.072]	[1,1]	[0.011, 0.058]	1.201	0.028
BOA×MIRB	[-0.074,0.030]	[-0.043,0.014]	[-0.011,-0.058]	[1,1]	1.343	0.032
C22						
PSA×MIRA	[1,1]	[-0.022,-0.007]	[0.002,-0.081]	[-0.021,-0.041]	0.850	0.020
PSA×MIRB	[0.022,0.007]	[1,1]	[0.024,-0.074]	[0.002,-0.034]	1.041	0.024
BOA×MIRA	[-0.002,0.081]	[-0.024,0.074]	[1,1]	[-0.022,0.040]	1.201	0.028
BOA×MIRB	[0.021, 0.041]	[-0.002,0.034]	[0.022,-0.040]	[1,1]	1.343	0.032
C23						
PSA×MIRA	[1,1]	[0.002,-0.021]	[0.023,-0.081]	[0.013,-0.019]	0.850	0.020
PSA×MIRB	[-0.002,0.021]	[1,1]	[0.021,-0.060]	[0.011, 0.002]	1.041	0.024
BOA×MIRA	[-0.023,0.081]	[-0.021, 0.060]	[1,1]	[-0.011,0.062]	1.201	0.028
BOA×MIRB	[-0.013,0.019]	[-0.011,-0.002]	[0.011,-0.062]	[1,1]	1.343	0.032
C24						
PSA×MIRA	[1,1]	[-0.020,-0.017]	[-0.003,-0.079]	[-0.001, -0.100]	0.850	0.020
PSA×MIRB	[0.020,0.017]	[1,1]	[0.017,-0.062]	[0.019,-0.083]	1.041	0.024
BOA×MIRA	[0.003,0.079]	[-0.017,0.062]	[1,1]	[0.002,-0.021]	1.201	0.028
BOA×MIRB	[0.001,0.100]	[-0.019, 0.083]	[-0.002, 0.021]	[1,1]	1.343	0.032
C20–C24						
PSA×MIRA	[1 , 1]	[-0.002,-0.015]	[0.021,-0.082]	[0.016,-0.047]	0.425	0.010
PSA×MIRB	[0.002,0.015]	[1,1]	[0.024,-0.067]	[0.019,-0.032]	0.520	0.012
BOA×MIRA	[-0.021,0.082]	[-0.024,0.067]	[1,1]	[-0.005,0.035]	0.601	0.014
BOA×MIRB	[-0.016,0.047]	[-0.019,0.032]	[0.005,-0.035]	[1,1]	0.672	0.016

^aAn average of the AD and XD platescales was used to estimate the uncertainty (in '') in column 7.

Note. — To determine the co-alignment of ACQ/IMAGE Config#2 To Config#1, Config#2 is the base configuration. Use that row at the desired column (of Config#1) to determine the co-alignment. The alignment order is that if a Config#1 ACQ/IMAGE is followed by a Config#2 ACQ/IMAGE, one should expect the given ACQSLEWX and ACSLEWY. Final co-alignment averages, and uncertainties, over C20–24 are shown in **bold**.

current (10 mA) for the MIRB, depending on the Cycle. Note the separate MIRB images in about a 2:1 ratio, and the asymmetric (toward -XD) scattered light.

See the figure captions for specific details about each cycles' family portrait.

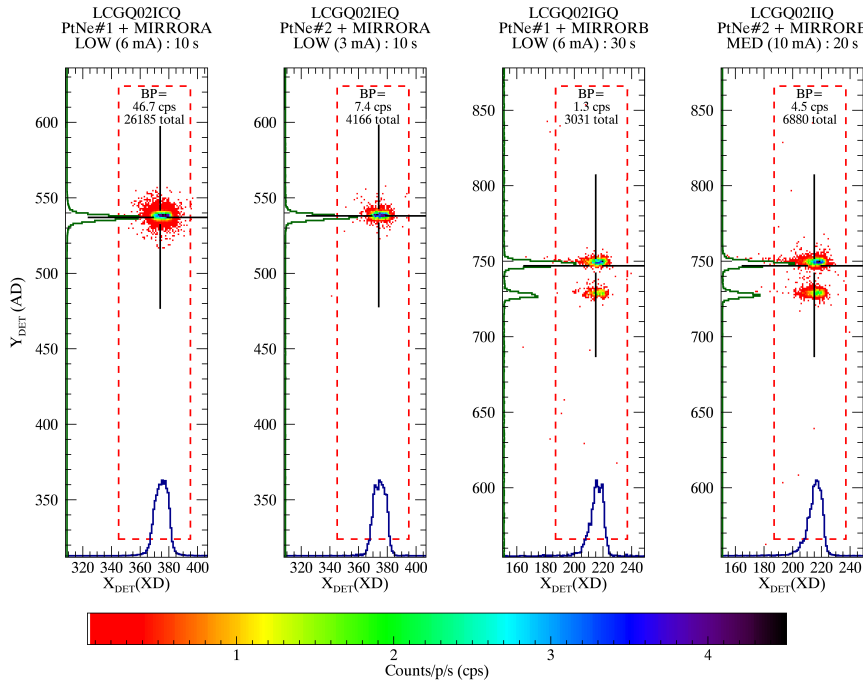


Figure 1 Cycle 21 (P13526 PtNe Lamp 'Family Portrait' counts per second per pixel (cps) NUV images of the internal PtNe lamps (**P1** & **P2**) through the WCA using either MIRRORA (MIRA, left 2 panels) or MIRRORB (MIRB, right 2 panels). The titles give the exposure *ROOTNAME*, configuration, exposure time and lamp current. Cross hairs show median locations and dashed lines show the LTAIMCAL TA subarrays. The insert text gives the Brightest Pixel (BP) in cps and the total counts in the subarray. AD and XD profiles are given along each axis, and the color bar at the bottom applies to all four images. Note the separate MIRB images in about a 2:1 ratio, and the asymmetric (toward -XD) profile and scattered light. All panels are in detector (DET) coordinates.

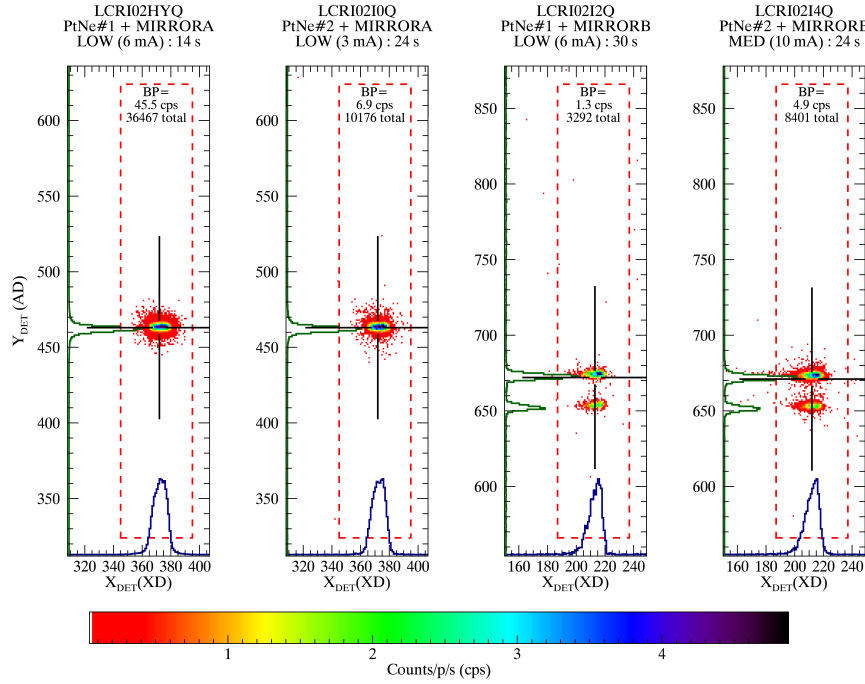


Figure 2 Cycle 22 PtNe Lamp ‘Family Portrait’ (see Fig 1). Note that during both the MIRA and MIRB images, the lamp image is about -50 p from the C21 AD location (Y_{DET}). This is common, and the TA subarrays must be large enough to account for this offset.

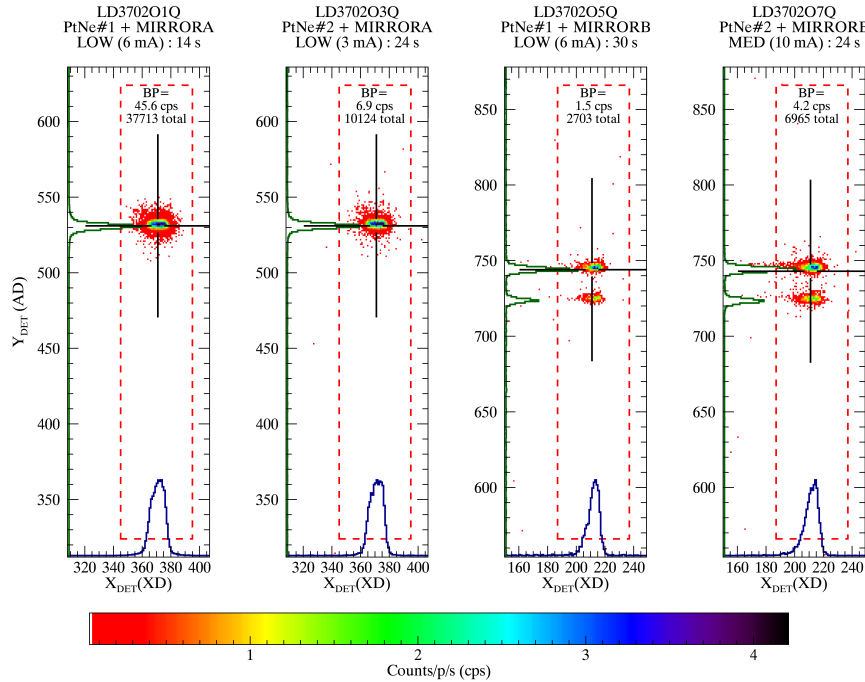


Figure 3 Cycle 23 PtNe Lamp ‘Family Portrait’ (see Fig 1 & Fig 2). Note that during all images, the lamp image is about +50 p from the C22 AD location (Y_{DET}), and has returned to its C21 AD position.

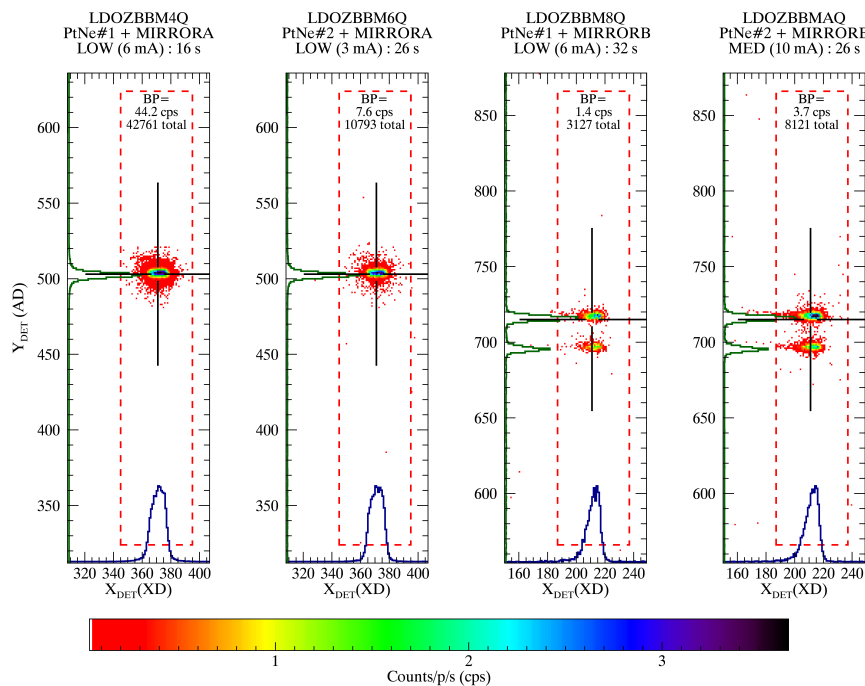


Figure 4 Cycle 24 PtNe Lamp ‘Family Portrait’ (see Fig 1–Fig 3). Note that during all images, the lamp image has returned to its C21 position.

6 SIAF Verification

6.1 COS SIAF History

The pre-SM4 COS Science Instrument Aperture File (SIAF) is described in detail in Mallo, 2008. The active COS entries in the 2018 SIAF, and the [V2,V3] aperture positions are given in Table 29. The changes since SMOV to the COS SIAF, and the continuing Fine Guidance Sensor (FGS) re-alignment efforts are documented in Table 28. This table includes all NUV LP1 and FUV LP1–4 entries. Each LP contains entries for the BOA, PSA, BOA when the PSA is being used, and PSA when the BOA is being used.

The COS SIAF “Aperture Names” start with the “L”, and are followed by either an “N” (NUV), “F” (FUV), or “APT” indicating that the aperture is only used in APT and not for observations. “APT” in the APT entries are immediately followed by an “N” or “F”. The SA (BOA or PSA) or MAC then follows. MAC represents the APT/SPSS³³ MACro aperture used for bright object checking. Finally, FUV entries end in a number giving the LP#, while the NUV “offset” apertures end with “OF”. An illustration of the active COS SIAF entries is given in Figure 5. As described in the individual FUV LP enabling ISRs, the location of each LP aperture is determined by first selecting the desired XD location on the FUV detector segments. After this selection, an AD aperture scan, using POS_TARGs in APT, determines the SIAF entry adjustment corresponding to the desired LP [V2,V3] aperture center. As shown in Figure 5, this alignment procedure produces a series of aperture locations that are at an $\approx 44.2^\circ$ angle to the -V3 (U3) axis.

The orientation of the COS AD and XD directions in relation to the HST mechanical [V2,V3] coordinates and U-frame are shown in Figure 6. The HST U-frame of $[U2,U3]=[-V2,-V3]$ and is used by APT and SPSS. Converting the orientation shown in Figure 5 to the nomenclature of the SIAF, the COS FUV apertures are aligned as follows: $\beta_x = 135.8^\circ$, $\beta_y = 45.8^\circ$, and parity=+1. As shown in Figure 5, for COS:

$$AD = [+V2, -V3] \quad (13)$$

$$XD = [+V2, +V3] \quad (14)$$

$$V2 = [+AD, +XD] \quad (15)$$

$$V3 = [-AD, +XD] \quad (16)$$

The NUV coordinate system orientation was measured during SMOV (Hartig et al., 2010 and Goudfrooij et al., 2010). This NUV angle was determined to be $0.52 \pm 0.01^\circ$ from +Y POS_TARG in the +X POS_TARG direction ($\beta_x = 135.5^\circ$, $\beta_y = 45.5^\circ$). The COS SIAF currently uses $\beta_x = 135^\circ$, $\beta_y = 45^\circ$ for both NUV and FUV. All conversions between [AD,XD] and [V2,V3] in this ISR use the current SIAF values for β_x and β_y . The conversion between [V2,V3] and [AD,XD] in terms of β_x and β_y are :³⁴

$$V2 = S_{AD} \cdot \sin(\beta_x) \cdot XD + S_{XD} \cdot \sin(\beta_y) \cdot XD \quad (17)$$

$$V3 = S_{XD} \cdot \cos(\beta_x) \cdot XD + S_{XD} \cdot \cos(\beta_y) \cdot XD \quad (18)$$

Where, S_{AD} is the AD plate scale (0.02352"/p), S_{XD} is the XD plate scale (0.02362"/p), and the aperture center was taken as the reference point.

³³SPSS=Science Planning and Scheduling System

³⁴See <http://www.stsci.edu/hst/observatory/apertures/siaf.html>

Table 28. History of COS SIAF Changes and FGS Alignment Activities

YEAR.DAY	STScI PR# ^a	Entries Changed ^b	Comment
2001.001	N/A	Original 10 ^c	Estimates for all COS apertures from Ground Testing
2009.054	61897	None	FGS1R Alignment Update
2009.215	63138	Original 10	On-orbit positions based upon SMOV alignment
2010.055	64538	Original 10	Update following December 2009 re-alignment
2010.263	65904	None	FGS2R2 Distortion/Scale Update
2011.172	68498	Original 10 + 16 New entries ^d	Update original 10 to match June 2011 FGS realignment LP2 prep. 2 x copies of 8 original non-MACro apertures. 8 (4 FUV, 4 NUV) have an 'A' (ALTERNATE) added to the end. 8 (4 FUV, 4 NUV) have a 'B' (BEST) added to end.
2011.206	68299	None	FGS2R2 Allowed to be Dominant in GS Pairs
2012.086	70792	LF*A	Initial correction to 4 LP2 FUV LP*Alternate entries
2012.100	70903	LF*A	LP2 correction to 4 FUV LP*Alternate entries.
2012.135	71160	LF*A	PR#70903 adjustment incorrectly applied, corrected.
2012.205	71568	LF*A and LF*B	Swap FUV A and B entries. After, LF*A=LP1 & LP*B=LP2
2013.205	75035	None	FGS re-alignment update loaded to HST
2014.055	76982	All Entries	SIAF update to match FGS re-alignment (all apertures) $\Delta[V2,V3] = [0.077, -0.070]$ "
2014.188	78255	LF*A	LP3 initial estimates installed in LF*A
2014.245	78801	LF*A	LP3 Final Refinement
2014.265	78775	LF*A and LF*B	LP3 Move Best/Alternate Swap: LP1=Original, LP2=LF*A & LP3=LF*B. Activated 2014.351 (SIAF entries use 2014.265)
2015.327		None	COS stopped using FGS2R2 as DOMinant FGS
2016.095	83878	None	New FGS2R2 Calibration installed on HST FGS2R2 DOM GS still OFF for COS, but on for STIS
2016.123		None	Based upon STIS data, FGS2R2 for DOM GS re-enabled for COS
2016.151	84188	Add 32 LP1-8 entries LF* 1,2,3 updated LF* 4,5,6,7,8	Install new LP# nomenclature Original, Alternate, and Best copied to LP1, LP2 & LP3 LP4-8 entries set to LP3 values
2016.346	86315	LF*4	Initial LP4 Estimates
2017.058	86877	LF*4	LP4 Position Update ($\Delta[V2,V3]=[0.0255, -0.0255]$)

^aProblem Report #s refer to the SCIOPSDB delivery PRs.^bTrailing characters not part of the original nomenclature are shown in **bold**.^cThe original 5 NUV SIAF entries were LNMAC, LNBOA, LNPSA, LAPTNPSAOOF & LAPTNBOAOOF. The original 5 FUV entries were LFMAC, LFBOA, LFPSA, LAPTFPSAOOF & LAPTFBOAOOF.^dThe 8 new Alternate entries were LNBOAA, LNPSAA, LFBOAA, LFPSAA, LAPTFPSAFA, LAPTFBOAFA, LAPTNPSAFA & LAPTNBOAFA. The 8 new Best entries are identical to the Alternates, but end with **B** instead of **A**. The penultimate letter, "O", in the offset apertures has been removed in create room for the trailing **A** or **B**.

Table 29. Active COS SIAF^a Entries

SIAF APERNAME	YEAR.DAY Activated	V2 (")	V3 (")
NUV LP1			
LNMAC	2014.055	+232.7230	-237.5150
LNBOA	2014.055	+232.7230	-237.5150
LNPSA	2014.055	+232.7230	-237.5150
LAPTNBOAOF	2014.055	+223.3488	-246.8892
LAPTNPSAOF	2014.055	+242.0972	-228.1408
FUV LP1			
LFMAC	2014.055	+232.7230	-237.5150
LFBOA1	2016.151	+232.7230	-237.5150
LFPSA1	2016.151	+232.7230	-237.5150
LAPTFBOAF1	2016.151	+223.3488	-246.8892
LAPTFPSAF1	2016.151	+242.0972	-228.1408
FUV LP2			
LFBOA2	2016.151	+235.1580	-235.0100
LFPSA2	2016.151	+235.1580	-235.0100
LAPTFBOAF2	2016.151	+225.7838	-244.3842
LAPTFPSAF2	2016.151	+244.5322	-225.6358
FUV LP3			
LFBOA3	2016.151	+230.9137	-239.2749
LFPSA3	2016.151	+230.9137	-239.2749
LAPTFBOAF3	2016.151	+221.5395	-248.6491
LAPTFPSAF3	2016.151	+240.2879	-229.9007
FUV LP4			
LFBOA4	2017.031	+229.1328	-241.0575
LFPSA4	2017.031	+229.1328	-241.0575
LAPTFBOAF4	2017.031	+219.7586	-250.4317
LAPTFPSAF4	2017.031	+238.5070	-231.6833

^aSIAF = Science Instrument Aperture File.

Note. — COS SIAF “Aperture Names” (APERNAME) start with the “L”, and are followed by either an “N” (NUV), “F” (FUV), or “APT” indicating that the aperture is only used in APT and not for observations. “APT” in the APT entries are immediately followed by an “N” or “F”. The SA (BOA or PSA) or MAC then follows. MAC represents the APT/SPSS MACro aperture used for bright object checking. Finally, FUV entries end in a number giving the LP#, while the NUV “offset” apertures end with “OF”.

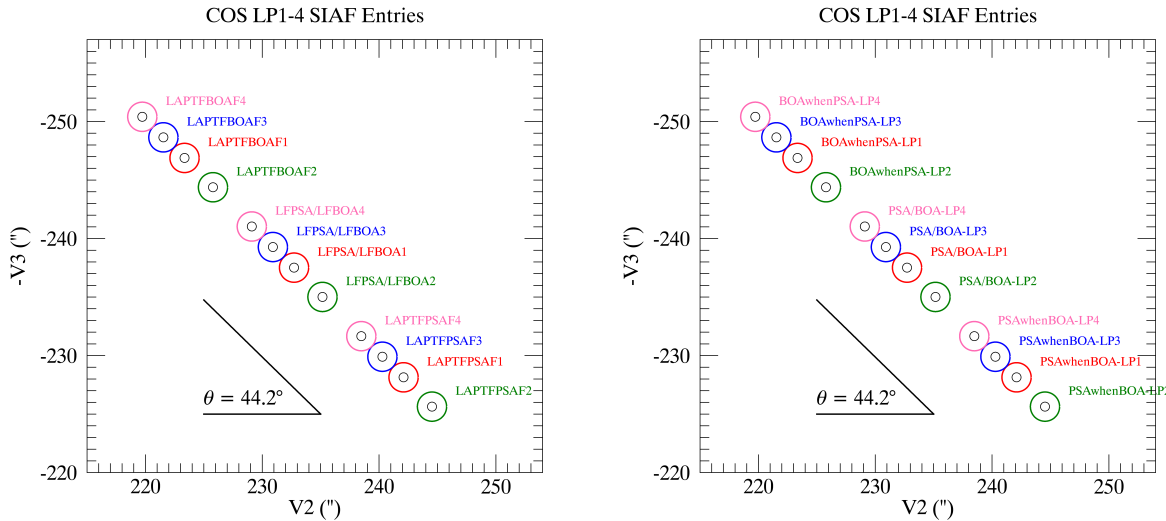


Figure 5 Illustration of the COS SIAF Entries. All FUV LP1 entries are shown in **RED**, LP2 entries are shown in **GREEN**, LP3 entries are shown in **BLUE**, and the LP4 entries are shown in **MAGENTA**. The NUV SIAF entries are coincident with the **LP1** FUV entries. The left panel shows the actual SIAF entry names, while the right panel gives a more readable translation.

6.2 C17–C23 COS to SIAF Alignment

The FGS-to-SI programs provide the opportunity to estimate the co-alignment of the COS SIAF entry to the actual center of the COS SAs. The FGS-to-SI programs concludes with two cos ACQ/IMAGES and a target that is approximately centered in the COS aperture. By comparing the [V2,V3] position after the first of these ACQ/IMAGES (the Configuration#1 or Config#1 PSA×MIRA ACQ/IMAGE), a direct comparison is possible. Table 30 gives these results for both the Spring and the Fall C17–C23 FGS-to-SI alignment programs.

The columns of Table 30 are:

1. *PROPOSID* gives the HST program id (PID).
2. *YEAR.DAY* gives the Year and day of the year of the observation.
3. *DATE-OBS* gives the observation date as reported in the fits header in DY-Mon-YEAR format.
4. gives HST [V2,V3] coordinates (in '') of the initial HST pointing before the (Config#1) PSA×MIRA ACQ/IMAGE.
5. gives HST [V2,V3] coordinates (in '') of the intermediate HST pointing after the (Config#1) PSA×MIRA ACQ/IMAGE and before the (Config#2) PSA×MIRB ACQ/IMAGE.
6. gives HST [V2,V3] “Miss-Distances” (in '') of the initial HST pointing before the (Config#1) PSA×MIRA ACQ/IMAGE and are the Initial Pointing coordinates subtracted from the *LNPSA* SIAF entry active at the time of the observation.
7. gives HST [V2,V3] “Miss-Distances” (in '') of the intermediate HST pointing after the PSA×MIRA ACQ/IMAGE.
8. “SIAF Dates” gives the dates the [V2,V3] SIAF entry in the following “SIAF Entry” column was active.
9. “SIAF Entry” gives the [V2,V3] entries that were active at the time of the observations of this row.

Table 30. C17–C23 FGS-to-SI Program Initial Pointing Determinations

<i>PROP OSID</i>	HST Cycle	YEAR .DAY	<i>DATE- OBS</i>	Initial Pointing [V2,V3] ("")	Intermediate Pointing [V2,V3] ("")	Initial Miss-Distance [V2,V3] ("")	Intermediate Miss-Distance [AD,XD] ("")	SIAF Dates ^a	Active SIAF Entry
PID (1)	(2)	(3)	(4)	(5)	(6)	(7)	(8)	(9)	10
P11878	C17	2009.338	04-Dec-2009	[232.790,-237.459]	[232.556,-237.544]	[0.018, 0.052]	[-0.216,-0.033]	3-Aug-2009	[232.772,-237.511]
P11878	C17	2010.074	15-Mar-2010	[232.316,-237.864]	[232.480,-237.453]	[-0.456,-0.353]	[-0.292, 0.058]	...	[232.772,-237.511]
P11878	C17	2010.110	20-Apr-2010	[232.346,-237.835]	[232.480,-237.458]	[-0.426,-0.324]	[-0.292, 0.053]	...	[232.772,-237.511]
P11878	C17	2010.309	05-Nov-2010	[232.633,-237.514]	[232.604,-237.561]	[-0.139,-0.003]	[-0.168,-0.050]	...	[232.772,-237.511]
P12399	C18	2011.070	11-Mar-2011	[232.459,-237.857]	[232.645,-237.438]	[-0.313,-0.346]	[-0.127, 0.073]	20-Jun-2011	[232.772,-237.511]
P12399	C18	2011.255	12-Sep-2011	[232.578,-237.378]	[232.734,-237.507]	[-0.068, 0.067]	[0.088,-0.062]	21-Jun-2011	[232.646,-237.445]
P12781	C19	2012.087	27-Mar-2012	[232.489,-237.821]	[232.622,-237.515]	[-0.157,-0.376]	[-0.024,-0.070]	...	[232.646,-237.445]
P12781	C19	2012.268	24-Sep-2012	[232.603,-237.386]	[232.678,-237.570]	[-0.043, 0.059]	[0.032,-0.125]	...	[232.646,-237.445]
P13171	C20	2013.061	02-Mar-2013	[232.597,-237.554]	[232.647,-237.590]	[-0.049,-0.109]	[0.001,-0.145]	...	[232.646,-237.445]
P13171	C20	2013.244	01-Sep-2013	[232.783,-237.353]	[232.723,-237.515]	[0.137, 0.092]	[0.077,-0.070] ^b	23-Feb-2014	[232.646,-237.445]
P13616	C21	2014.055	06-Apr-2014	[232.547,-237.465]	[232.535,-237.497]	[-0.176, 0.050]	[-0.188, 0.018]	24-Feb-2014	[232.723,-237.515]
P13616	C21	2014.300	27-Oct-2014	[232.841,-237.465]	[232.745,-237.558]	[0.118, 0.050]	[0.022,-0.043]	...	[232.723,-237.515]
P14035	C22	2015.104	14-May-2015	[232.617,-237.464]	[232.519,-237.568]	[-0.106, 0.051]	[-0.204,-0.053]	...	[232.723,-237.515]
P14035	C22	2015.275	02-Oct-2015	[232.865,-237.381]	[232.807,-237.471]	[0.142, 0.134]	[0.084, 0.044]	...	[232.723,-237.515]
P14452	C23	2016.092	01-Apr-2016	[232.643,-237.512]	[232.742,-237.485]	[-0.080, 0.003]	[0.019, 0.030]	...	[232.723,-237.515]
P14452	C23	2016.277	03-Oct-2016	[232.785,-237.429]	[232.747,-237.494]	[0.062, 0.086]	[0.024, 0.021]	...	[232.723,-237.515]

^aDates in this column show the dates that the [V2,V3] SIAF entries in this and the following rows were active.

^bThese exposures, and the offsets measured here, were used to adjust the COS SIAF entries on 2014.055 (STScI PR#76982).

As shown in Table 31, from 2009.215–2011.171 the average SIAF to PSA ACQ/IMAGE pointing residual was [-0.169,-0.141]" in [AD,XD] ($\Delta[V2,V3]=[-0.044,-0.215]''$). In June 2011, an FGS re-alignment solution was uploaded to HST and a COS SIAF adjustment was performed of $\Delta[AD,XD]=[0.136,0.139]$ (2011.173). During this time period (2011.172–2014.054) the average SIAF to PSA ACQ/IMAGE pointing residual was [0.091,-0.042]" in [AD,XD] ($\Delta[V2,V3]=[-0.071,0.041]''$). In Feb 2014, a new FGS re-alignment solution was uploaded to HST, and a COS SIAF adjustment of [0.070,-0.077]" was initiated (2014.055). From 2014.055–2016.276, the average SIAF to PSA ACQ/IMAGE pointing residual was [-0.031,-0.027]" in [AD,XD] ($\Delta[V2,V3]=[0.038,0.065]''$). Further details about the SIAF coordinates to COS PSA center alignment can be determined by reviewing the average ACQ/IMAGE slews as a function of time and DOMinant FGS. These “Blind Pointing” details are beyond the scope of this ISR, but will be presented elsewhere.

Table 31. C17–C23 SIAF vs PSA×MIRA ACQ/IMAGE Residuals

<i>PROP OSID</i> (PID)	HST Cycle (1)	DATE-OBS [V2,V3] ('')	Post ACQ/ IMAGE SIAF Residual [AD,XD] ('')	Pre ACQ/ IMAGE SIAF Residual [AD,XD] ('')	Post ACQ/ IMAGE SIAF Residual [AD,XD] ('')	SIAF Dates ^a (7)	Active SIAF Entry (8))
P11878	C17	04-Dec-2009	[-0.216,-0.033]	[-0.024, 0.049]	[-0.129,-0.176]	3-Aug-2009	[232.772,-237.511]
P11878	C17	15-Mar-2010	[-0.292, 0.058]	[-0.073,-0.572]	[-0.247,-0.165]	...	[232.772,-237.511]
P11878	C17	20-Apr-2010	[-0.292, 0.053]	[-0.072,-0.530]	[-0.244,-0.169]	...	[232.772,-237.511]
P11878	C17	05-Nov-2010	[-0.168,-0.050]	[-0.096,-0.100]	[-0.083,-0.154]	...	[232.772,-237.511]
P12399	C18	11-Mar-2011	[-0.127, 0.073]	[-0.023,-0.466]	[-0.141,-0.038]	20-Jun-2011	[232.772,-237.511]
2009.215–2011.171			Avg Residual =	[-0.169,-0.141]			
P12399	C18	12-Sep-2011	[0.088,-0.062]	[-0.095,-0.001]	[0.106, 0.018]	21-Jun-2011	[232.646,-237.445]
P12781	C19	27-Mar-2012	[-0.024,-0.070]	[0.155,-0.377]	[0.033,-0.066]	...	[232.646,-237.445]
P12781	C19	24-Sep-2012	[0.032,-0.125]	[-0.072, 0.011]	[0.111,-0.066]	...	[232.646,-237.445]
P13171	C20	02-Mar-2013	[0.001,-0.145]	[0.042,-0.112]	[0.103,-0.102]	...	[232.646,-237.445]
P13171	C20	01-Sep-2013	[0.077,-0.070]	[0.032, 0.162]	[0.104, 0.005]	23-Feb-2014	[232.646,-237.445]
2011.172–2014.054			Avg Residual =	[0.091,-0.042]			
P13616	C21	06-Apr-2014	[-0.188, 0.018]	[-0.160,-0.089]	[-0.146,-0.120]	24-Feb-2014	[232.723,-237.515]
P13616	C21	27-Oct-2014	[0.022,-0.043]	[0.048, 0.119]	[0.046,-0.015]	...	[232.723,-237.515]
P14035	C22	14-May-2015	[-0.204,-0.053]	[-0.111,-0.039]	[-0.107,-0.182]	...	[232.723,-237.515]
P14035	C22	02-Oct-2015	[0.084, 0.044]	[0.006, 0.195]	[0.028, 0.091]	...	[232.723,-237.515]
P14452	C23	01-Apr-2016	[0.019, 0.030]	[-0.059,-0.054]	[-0.008, 0.035]	...	[232.723,-237.515]
P14452	C23	03-Oct-2016	[0.024, 0.021]	[-0.017, 0.105]	[0.002, 0.032]	...	[232.723,-237.515]
2014.055 – 2016.276			Avg Residual =	[-0.031,-0.027]			

^aDates in this column show the dates that the [V2,V3] SIAF entries in this and the following rows were active.^bThese exposures, and the offsets measured here, were used to adjust the COS SIAF entries on 2014.055 (STScI PR#76982).

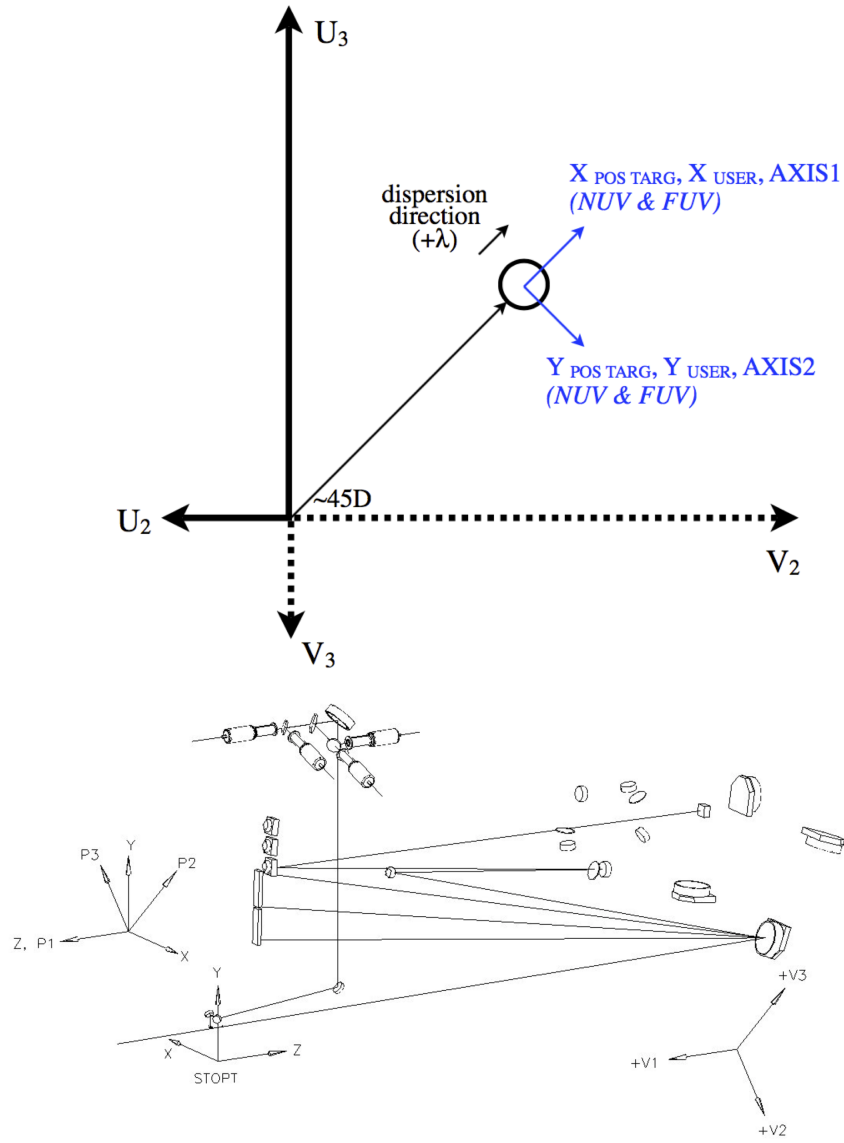


Figure 6 The upper panel shows the COS aperture orientation versus the $[V_2, V_3]$ telescope coordinate system (Lallo 2008). The U ($[U_2, U_3] = [-V_2, -V_3]$) frame is used during the proposal process in APT and SPSS. The lower panel (Osbourne, 2004) shows all the pre-launch COS coordinate systems. From left to right, the “P” physical coordinate system is aligned with the COS enclosure, and shares a common origin with the $[X, Y, Z]$ “DET” ector coordinates. The X , Y , and Z axes of the STOPT (Space Telescope OPTical) coordinate system are shown slightly below and aft of these. The HST $[V_1, V_2, V_3]$ coordinate system is shown on the right.

7 COS TA Slew Accuracy

The COS telemetry used in the SIAF analysis provides the opportunity to determine the accuracy of the commanded COS ACQ/IMAGE slews. As all COS TA slews use the identical HST commanding, these results should be valid for all COS TAs.

Table 32 compares the slew directions and distances as reported by the HST telemetry (in [V2,V3]) to those commanded by the initial PSA×MIRA ACQ/IMAGE slews (in [AD,XD]³⁵). during the FGS-to-SI program visits. In one case (visit ‘A1’ of P13171), the telemetry before the PSA×MIRA ACQ/IMAGE was not available and the instead the slews of the following PSA×MIRB ACQ/IMAGE were used. Equations 13–16 convert from [V2,V3] to [AD,XD].

1. *PROPOSID* gives the HST program id (PID).
2. *ROOTNAME* gives the IPPSSOOT of the COS exposure. In all cases but one, the spring C20 exposure of P13171, this corresponds to the initial PSA×MIRA ACQ/IMAGE. Due to missing telemetry, for Spring C20 we have used LC6KA1I3Q, the secondary (Config#2) PSA×MIRB ACQ/IMAGE.
3. *DATE-OBS* gives the date of the observation in YEAR-MOnth-DAy format.
4. gives the [V2,V3] position difference (in '') before and after the ACQ/IMAGE exposure as reported by HST telemetry.
5. gives the [AD,XD] position difference (in '') before and after ACQ/IMAGE exposure.
6. gives the [AD,XD] position difference (in '') before and after ACQ/IMAGE exposure as reported by the COS header keywords [*ACQPREFX,ACQPREFY*].
7. gives the [AD,XD] position difference (in '') between the HST telemetry and COS header keyword reported slews.
8. “SIAF Entry” gives the [V2,V3] entries that were active at the time of the observations of this row.

These results indicate that, on average, the observed HST slews agree with the ACQ/IMAGE commanded slews to $\Delta[\text{AD},\text{XD}] = [-0.002, -0.006]''$, with an RMS difference of $[\text{AD},\text{XD}] = [0.003, 0.010]''$.

³⁵The COS [AD,XD] slews are reported in the [*ACQPREFX,ACQPREFY*] fits header keyword.

Table 32. C17–23 FGS-to-SI Program Pointing Accuracy

<i>PROPOSID</i>	<i>ROOT</i>	<i>DATE</i>	Slew - HST ^b	Slew - HST ^b	Slew - COS ^c	Slew Diff ^d	Active SIAF Entry	
<i>PID</i>	<i>NAME</i>	<i>OBS</i>	[V2,V3] ('')	[AD,XD] ('')	[AD,XD] ('')	[AD,XD] ('')	[V2,V3] ('')	
(1)	(2)	(3)	(4)	(5)	(6)	(7)	(8)	
P11878	C17	lbclaa6xaq	04-Dec-2009	[0.234, 0.085]	[0.105, 0.226]	[0.108, 0.108]	[-0.003, 0.001]	[232.772,-237.511]
P11878	C17	lbc104g0q	15-Mar-2010	[-0.164,-0.411]	[0.175,-0.407]	[0.174, 0.174]	[0.001, 0.000]	[232.772,-237.511]
P11878	C17	lbclaa2nbq	20-Apr-2010	[-0.134,-0.377]	[0.172,-0.361]	[0.174, 0.174]	[-0.002, 0.001]	[232.772,-237.511]
P11878	C17	lbclaa3s3q	05-Nov-2010	[0.029, 0.047]	[-0.013, 0.054]	[-0.010,-0.010]	[-0.003,-0.002]	[232.772,-237.511]
P12399	C18	lbtm7a1lsq	11-Mar-2011	[-0.186,-0.419]	[0.165,-0.428]	[0.168, 0.168]	[-0.003,-0.002]	[232.772,-237.511]
P12399	C18	lbtm7a2ahq	12-Sep-2011	[-0.156, 0.129]	[-0.202,-0.019]	[-0.200,-0.200]	[-0.002,-0.038]	[232.646,-237.445]
P12781	C19	lbtm1a1f9q	27-Mar-2012	[-0.133,-0.306]	[0.122,-0.310]	[0.128, 0.128]	[-0.006,-0.003]	[232.646,-237.445]
P12781	C19	lbtm1a2ffq	24-Sep-2012	[-0.075, 0.184]	[-0.183, 0.077]	[-0.183,-0.183]	[-0.000,-0.001]	[232.646,-237.445]
P13171	C20	lc6ka1i3q ^e	02-Mar-2013	[-0.050, 0.036]	[-0.061,-0.010]	[-0.060,-0.060]	[-0.001, 0.000]	[232.646,-237.445]
P13171	C20	lc6ka2imq	01-Sep-2013	[0.060, 0.162]	[-0.072, 0.157]	[-0.070,-0.070]	[-0.002,-0.001]	[232.646,-237.445]
P13616	C21	lc14a1dcq	06-Apr-2014	[0.012, 0.032]	[-0.014, 0.031]	[-0.013,-0.013]	[-0.001, 0.002]	[232.723,-237.515]
P13616	C21	lc14a2e3q	27-Oct-2014	[0.096, 0.093]	[0.002, 0.134]	[0.001, 0.001]	[0.001, 0.001]	[232.723,-237.515]
P14035	C22	lcsla1i4q	14-May-2015	[0.098, 0.104]	[-0.004, 0.143]	[-0.004, 0.004]	[0.000, 0.002]	[232.723,-237.515]
P14035	C22	lcsla2bhq	02-Oct-2015	[0.058, 0.090]	[-0.023, 0.105]	[-0.020,-0.020]	[-0.003,-0.000]	[232.723,-237.515]
P14452	C23	ld3la1coq	01-Apr-2016	[-0.099,-0.027]	[-0.051,-0.089]	[-0.046,-0.046]	[-0.005,-0.002]	[232.723,-237.515]
P14452	C23	ld3la2oqj	03-Oct-2016	[0.038, 0.065]	[-0.019, 0.073]	[-0.017,-0.017]	[-0.002,-0.002]	[232.723,-237.515]
Avg Diff = [0.003,0.010]								

^aDates that this, and the following rows, were active with the given SIAF entries.^bDue to timing offsets of the post-observation analysis, this is the config#2 PSA×MIRB ACQ/ IMAGE. All other rows correspond to the initial PSA×MIRA ACQ/ IMAGE.^cHST slew during the initial ACQ/ IMAGE, as measured by the HST telemetry in [V2,V3] and converted by equations?? & ??.^dHST slew during the initial ACQ/ IMAGE, as reported by the COS header keywords [AD,XD]=[ACQSLEWX,ACQSLEWY].^eDue to timing offsets of the post-observation analysis, this is the config#2 PSA×MIRB ACQ/ IMAGE. All other rows correspond to the initial PSA×MIRA ACQ/ IMAGE.

8 Spectroscopic TA Verification

After the series of ACQ/IMAGES that start each visit, the target should be accurately centered. We take advantage of this to monitor certain aspects of COS spectroscopic TAs.

COS spectroscopic TAs consist of up to three stages ACQ/SEARCH, PEAKD, and PEAKXD. The COS spectroscopic ACQ/SEARCH and PEAKD algorithms do not use any FSW patchable constants, and do not flash the internal calibration lamps. The only monitoring required for these TA phases is to ensure that the mechanisms were in their proper positions and that the TA subarrays defined in the HST ground commanding are proper for the mechanism positions used during the TAs. As discussed in § 4, the majority of the details will be addressed for each FUV LP in its enabling ISR, or have already been verified for the LP1 positions in Penton & Keyes (2011).

COS NUV (LP1) and FUV LP2–4 spectroscopic TA in the XD direction uses ACQ/PEAKXD and requires the use of the XD WCA-to-PSA offsets with the nominal NUM_POS=1 algorithm. These offsets are contained for both the NUV and FUV channels in the FSW patchable constant table PCTA_CALTARGETOFFSET, and are provided for reference for all COS LPs in Table 33. This ISR only attempts to verify that these offsets were appropriate for all data obtained during the annual monitoring programs.

Each FUV *CENWAVE* uses a unique OSM1 rotation, whereas all NUV TAs use the same OSM1 rotation independent of *CENWAVE*. However, each NUV *CENWAVE* uses a different OSM2 rotation during TA. Each FUV *CENWAVE* has its own set of TA subarrays (up to four per segment), while the NUV TA subarrays are not *CENWAVE* specific, but are grating specific.

The verification process for ACQ/PEAKXD is simple, take a normal spectrum with a target signal-to-noise ratio of least 50 for the entire spectrum (2500 target counts), and directly measure the WCA-to-SA offset and compare it the FSW value. For NUV exposures, this is almost always STRIPE=B, and for the FUV, only events from FUVA are used at LP2–4. TA subarrays are used to mask out any detector hot-spots or Geocoronal light that could interfere with the centering process. These spectra are also compared to the TA subarrays to verify that they satisfactory.

LTAPKXD uses the measured target location and known WCA-to-SA offset to calculate the required centering slew. This requires converting from NUV pixels and FUV rows to arcseconds on the sky. Table 34 gives the COS FSW platescale values³⁶. All NUV spectroscopic LTAPKXDs use the same plate scale value of 0.02384"/p, stored in PCTA_NUVMILLIARCSECSPERPIXELXDISP. Each NUV grating and *CENWAVE* has a slightly different plate scale, but the difference is small enough to ignore for COS TAs, see COS-11-0014B § 2.5 (Penton 2001B).

8.1 NUV Spectroscopic TA verification

The P2 WCA lamp and target XD locations for all NUV spectroscopic exposures are given in Table 8.1. As shown in the two rightmost “ $|\Delta|$ ” columns, all measured WCA-to-PSA offsets were within 3 p in XD of their FSW values. This equates to a $< 0.07''$ XD offset due to TA for all NUV monitoring exposures over C20–24. A visual inspection of the spectra showed all NUV spectra to continue to be well centered in the ACQ/PEAKXD, ACQ/PEAKD, and ACQ/SEARCH NUV spectroscopic subarrays.

³⁶Stored in the PCTA_FUVMILLIARCSECSPERPIXELXDISP table

Table 33 LTAPKXD WCA-to-PSA offsets

<i>OPT_ELEM</i>	LP1	LP2	LP3
FUV ¹			
G130M	-898	-943	-892
G140L	-884	-950	-857
G160M	-898	-933	-901
NUV ²			
G185M	3742
G225M	3746
G230L	3734
G285M	3749

FSW patchable constant PCTA_CALTARGETOFFSETSCALE determines the FSW scaling (currently set to 10). FUV offsets are “negative” due to the parity of HST slews relative to the COS coordinate system.

¹ Divide the FUV numbers by -10 to get the number of XD rows between the PSA and WCA spectra for a target centered in the aperture.

² Divide the NUV numbers by 10 to get the NUV WCA-to-PSA offset.

Table 34 LTAPKXD Plate Scales

<i>OPT_ELEM</i>	LP1	LP2	LP3
FUV ¹			
G130M	-11086	-11400	-9550
G140L	-10549	-11839	-9800
G160M	-9881	-11178	-9040
NUV ²			
ALL	2384

The FSW patchable constant PCTA_MILLIARCSECSPERPIXELSCALE determines the FSW scaling (currently set to 100). FUV plate scales are “negative” due to the parity of HST slews relative to the COS coordinate system.

¹ Divide FUV numbers by 100 to get FUV plate scale in mas/row.

² Divide NUV numbers by 100 to get NUV plate scale in mas/p.

8.2 FUV Spectroscopic TA verification

The P2 WCA lamp and target XD locations for all centered FUV spectroscopic exposures is given in Table 8.1.³⁷ Explain the last three columns: All FUV monitoring verifications ($|\Delta| = |WtP - eWtp|$) exceeded both the $\pm 0.3''$ requirement, but spectra taken near the end of the LP2 lifetime, and all G140L spectra, exceeded the $\pm 0.1''$ goal. A visual inspection showed all FUV spectra continue to be well centered in the FUV spectroscopic TA subarrays.

³⁷The POS_TARG offset spectra are not included in this table as they are beyond the scope of this ISR. These results will be presented elsewhere.

Table 35. NUV Spectroscopic ACQ/PEAKXD Monitoring

<i>ROOTNAME</i>	<i>DATE-OBS</i>	<i>OPT_ELEM</i>	LP	WCA ^a (p)	PSA ^b (p)	WtP ^c (p)	eWtP ^d (p)	$ \Delta $ ^e (p)	$ \Delta $ ^f ($''$)
(1)	(2)	(3)	(4)	(5)	(6)	(7)	(8)	(9)	(10)
C21 (P13526)									
lcgq02i2q	2014-11-17	G185M	1	366.0	742.0	376.0	374.20	1.80	0.04
lcgq02i4q	2014-11-17	G225M	1	370.0	747.0	377.0	374.60	2.40	0.06
lcgq01r6q	2014-11-19	G285M	1	355.0	728.0	373.0	374.90	1.90	0.04
lcgq01qlq	2014-11-19	G230L	1	374.0	748.0	374.0	373.40	0.60	0.01
C22 (P13972)									
lcri02hqq	2015-10-06	G185M	1	367.0	742.0	375.0	374.20	0.80	0.02
lcri02hoq	2015-10-06	G225M	1	371.0	747.0	376.0	374.60	1.40	0.03
lcri01giq	2015-10-06	G285M	1	351.0	726.0	375.0	374.90	0.10	<0.01
lcri01ggq	2015-10-06	G230L	1	374.0	747.0	373.0	373.40	0.40	0.01
C23 (P14440)									
ld3702noq	2016-10-19	G185M	1	366.0	743.0	377.0	374.20	2.80	0.07
ld3702nmq	2016-10-19	G225M	1	370.0	747.0	377.0	374.60	2.40	0.06
ld3701hbq	2016-10-18	G285M	1	352.0	727.0	375.0	374.90	0.10	<0.01
ld3701h9q	2016-10-18	G230L	1	375.0	748.0	373.0	373.40	0.40	0.01
C24 (P14857)									
ldozbblwq	2017-09-06	G185M	1	366.0	743.0	377.0	374.20	2.80	0.07
ldozbbluq	2017-09-06	G225M	1	370.0	747.0	377.0	374.60	2.40	0.06
ldozbadzq	2017-09-04	G285M	1	352.0	727.0	375.0	374.90	0.10	<0.01
ldozbadxq	2017-09-04	G230L	1	374.0	748.0	374.0	373.40	0.60	0.01

^aXD centroid of the WCA spectrum. For NUV spectra, this is the median calibration lamp location.

^bXD centroid of the target spectrum taken through the PSA, using the same centroid method as the WCA.

^cWtP is absolute value of XD location difference of measured WCA and PSA spectra ($WtP = |PSA - WCA|$)

^deWtP = Expected WCA-to-PSA offset from FSW table XIMCALTARGETOFFSET (see Table 33).

^eOffset of WtP from a perfectly centered target measured in XD rows.

^fOffset of WtP in arcseconds ($''$). Note that the platescales are different for each grating, as shown in Table 34.

Note. — All spectra taken at FP-POS=3. All verifications ($|\Delta| = |WtP - eWtp|$) easily exceeded both the $\pm 0.3''$ requirement and the $\pm 0.1''$ goal.

Table 36. FUV Spectroscopic ACQ/PEAKXD Monitoring

<i>ROOTNAME</i>	<i>DATE-OBS</i>	<i>OPT_ELEM</i>	<i>LP</i>	WCA ^a (p)	PSA ^b (p)	WtP ^c (p)	eWtP ^d (p)	$ \Delta $ ^e ($''$)	$ \Delta $ ^f ($''$)
(1)	(2)	(3)	(4)	(5)	(6)	(7)	(8)	(9)	(10)
C21 (P13526)									
lcgq01r8q	2014-11-19	G130M	2	602.15	508.31	-93.84	-92.80	1.04	0.12
lcgq01raq	2014-11-19	G140L	2	608.76	513.48	-95.28	-93.50	1.78	0.20
lcgq02i6q	2014-11-17	G160M	2	596.07	503.35	-92.71	-91.80	0.91	0.11
C22 (P13972)									
lcri01gkq	2015-10-06	G130M	3	537.32	448.98	-88.34	-89.20	0.86	0.08
lcri01h6q	2015-10-06	G140L	3	544.55	457.36	-87.20	-85.70	1.50	0.15
lcri02hsq	2015-10-06	G160M	3	531.78	442.13	-89.65	-90.10	0.45	0.04
C23 (P14440)									
ld3701hdq	2016-10-18	G130M	3	536.33	447.41	-88.92	-89.20	0.28	0.03
ld3701hfq	2016-10-18	G140L	3	543.43	455.95	-87.48	-85.70	1.78	0.17
ld3702nqq	2016-10-19	G160M	3	531.09	440.96	-90.13	-90.10	0.03	0.00
C24 (P14857)									
ldozbae1q	2017-09-04	G130M	3	535.26	445.66	-89.61	-89.20	0.41	0.04
ldozbae3q	2017-09-04	G140L	3	541.76	454.25	-87.51	-85.70	1.81	0.18
ldozbblyq	2017-09-06	G160M	3	530.84	440.75	-90.09	-90.10	0.01	0.00

^aXD centroid of the WCA spectrum. For FUV spectra, this is mean lamp photon location.

^bXD centroid of the target spectrum taken through the PSA, using the same centroid method as the WCA.

^cWtP is absolute value of XD location difference of measured WCA and PSA spectra ($WtP = |PSA - WCA|$)

^deWtP = Expected WCA-to-PSA offset from FSW table XIMCALTARGETOFFSET (see Table 33).

^eOffset of WtP from a perfectly centered target measured in XD rows.

^fOffset of WtP in $''$. Note that the platescales are different for each FUV grating and LP, as shown in Table 34.

Note. — All spectra taken at FP-POS=3. All FUV verifications ($|\Delta| = |WtP - eWtp|$) exceeded both the $\pm 0.3''$ requirement, but spectra taken near LP2 lifetime end, and all G140L spectra, exceeded the $\pm 0.1''$ goal.

9 Results and Conclusion

The main results of the HST Cycles 20–24 COS TA monitoring programs are as follows:

SIAF: All COS NUV ACQ/IMAGEs use identically-valued SIAF entries (*LFPSA* & *LFBOA*), although the changed twice over C18–C24. The exposures in the FGS-to-SI Alignment programs gave great estimates of the accuracy of the existing NUV LP1 *LFPSA/LFBOA* SIAF entries as they performed a PSA×MIRA ACQ/IMAGE. For C20–24, this results of this ISR indicate that the NUV SIAF entry was accurate to :

- 2009.215–2011.171 $\Delta[\text{AD},\text{XD}] \sim [-0.169,-0.141]''$ ($\Delta[\text{V2},\text{V3}]=[-0.044,-0.215]''$).
- 2011.172–2014.054 $\Delta[\text{AD},\text{XD}] \sim [0.091,-0.042]''$ ($\Delta[\text{V2},\text{V3}]=[-0.071,0.041]''$),
- 2014.055–2016.276 $\Delta[\text{AD},\text{XD}] \sim [-0.031,-0.027]''$ ($\Delta[\text{V2},\text{V3}]=[0.038,0.065]''$),

SIAF entry offsets affect the “blind pointing” of COS, but the COS TA modes are designed to center any target within the aperture to the center, so small offsets do not affect the final COS post-TA pointing. Long term SIAF monitoring is used to track any mechanical drift in the location of the COS aperture mechanism or any changes to the FGS-to-SI alignment that will need adjusting. The last such adjustment was in C22 (February 24, 2014; 2014.055, PR#76982), while COS FUV observations were at LP2. At this time, all COS entries (NUV and FUV) were adjusted in [V2,V3] by [0.077, -0.070]”.

Spectroscopic TA Subarrays: Visual inspection of NUV and FUV images, and a comparison of the NUV and FUV spectra XD centroids, indicate that all spectroscopic TA subarrays were appropriately defined for C20–C24. However, NUV PtNe lamp (WCA) monitoring should be continued, as OSM1 and OSM2 secular drift continues to move the WCA lamp images in the AD direction, and XD aperture offsets are common, especially when switching to and from NUV and FUV. Combined with the increased detector background of the NUV channel, some of the approved NUV central wavelength settings for COS TA have loss viability, for further details see § 2.6 of the C25 COS IHB (Fox et al., 2017). Hot-spot monitoring must be continued for both FUVA and FUVB as COS TAs are particularly susceptible to contamination from variable localized detector background.

NUV Imaging TAs and Subarrays: C20–C24 ACQ/IMAGE tests indicate that the following average co-alignment between ACQ/IMAGE configurations to PSA×MIRA ACQ/IMAGE to within $[\text{AD},\text{XD}] \approx [0.010,0.020]''$, with a measurement error of approximately 0.014”.

- PSA×MIRB was aligned with PSA×MIRA to $[\text{AD}, \text{XD}] \sim [\textbf{0.002},\textbf{0.015}] \pm \textbf{0.012}''$.
- BOA×MIRA was aligned with PSA×MIRA to $[\text{AD}, \text{XD}] \sim [\textbf{-0.021},\textbf{0.082}] \pm \textbf{0.014}''$.
- BOA×MIRB was aligned with PSA×MIRA to $[\text{AD}, \text{XD}] \sim [\textbf{-0.016},\textbf{0.047}] \pm \textbf{0.016}''$.

Larger XD alignment errors due to a frequent ± 1 p XD (*APERYPOS*) step mechanism position errors (1 step $0.053''$). As shown in the PtNe lamp ‘family portraits’ of Figures 1–4, and used during the LTAIMCAL portion of ACQ/IMAGE, the COS PtNe lamps are still performing well although their positions on the detector must continue to be monitored as there is considerable AD (± 50 p) and XD (± 5 p) non-repeatability. No changes of concern were observed in the PtNe lamp count rates between C20–C24.

HST+COS TA Slew Accuracy: As determined from C17–C24 observations FGS-to-SI programs, slews commanded by ACQ/IMAGES move very close to their expected positions. The average measured offset was $\Delta[\text{AD,XD}]=[-0.002,-0.006]''$, with an RMS difference of $[\text{AD,XD}]=[0.003,0.010]''$.

NUV Spectroscopic TAs: Spectroscopic TAs for all NUV gratings in all Cycles met both the $0.3''$ requirement and the $0.1''$ goal.

FUV Spectroscopic TAs: C20–C24 spectroscopic TAs for all FUV gratings met the $0.3''$ requirement and the G130M and G160M gratings achieved the $0.1''$ goal for C20–C24. However, spectra taken near the end of the LP2 lifetime, and all G140L spectra, did not achieve the $\pm 0.1''$ goal.

Through constant monitoring, and periodic FSW, ground commanding, and operations updates, HST+COS TA has performed remarkably well during Cycles 17–24. The STScI Team thanks the GSFC and STScI personal for their outstanding cooperation and contributions in these efforts

NUV detector background has been the biggest source of concern for NUV TAs, while FUV gain-sag induced Y-walk, hot-spots, and inherent detector geometric distortions were the biggest concerns of FUV TAs at LP1–3. At FUV LP4, Y-walk will not be as big a concern as the NUM.POS=1 ACQ/PEAKXD is not affected by either Y-walk or geometric distortions.

With continued monitoring, and occasional corrective actions, COS TAs should continue their excellent performance in future HST Cycles.

10 Acknowledgements

The author would like to thank the following Instrument Development Team (IDT), GSFC and STScI personal for their contributions to supporting COS over the years:

- GFSC : Larry Dunham, Mike Kelly, Olivia Lupie, Faizan Naqvi, Beverly Serrano, Scott Swain, Ben Teasdel, & Morgan Van Arsdell.
- STScI : John Bacinski, George Chapman, Colin Cox, Joshua Goldberg, Matt Lallo, Sean Lockwood, Karla Peterson, Merle Reinhart, Mary Romelfinger, David Sahnow, Alan Welty, Thomas Wheeler, James White, & Brian York.
- IDT : James Green, Jason McPhate, & Steven Osterman.

11 Change History for COS ISR 2018-XX

Version 0.01: 30-March-2018 Original Draft Document for Review

Version 0.02: 04-April-2018 NUV Image Verification Section partially debuts with tweaks to tables and text (no external comments)

Version 0.03: 12-April-2018 At direction for management, removed all notes to reviewers. All sections not complete have been removed (no external comments)

Version 0.10: 17-April-2018 After careful re-evaluation of all FGS-to-SI telemetry, numerous errors were discovered and corrected. This allows the SIAF and SLEW accuracy sections to become

Instrument Science Report HST+COS 2018-XX

viable, and they have been re-inserted and drastically updated. This version is ready for external review.

Note to reviewers: I will be documenting updates here, until Version 1.0 is released. At that time, these will be removed for the Version 1.0 declaration.

12 References

- Dixon, W. V., et al. 2010, COS Instrument Handbook (IHB), Version 2.0 (Baltimore, STScI)
- Keyes, T., & Penton, S. 2010, COS ISR 2010-14 (v1), “HST+COS Target Acquisition Guidelines, Recommendations, and Interpretation”
- Fix, M. B., 2018, COS ISR 2018-03 (v1) (COS NUV Dark Monitor Summary)
- Fox, A. J., et al. 2017, COS Instrument Handbook (IHB), Version 9.0 (Baltimore, STScI)
- Fox, A. J., et al. 2015, COS Data Handbook (DHB), Version 3.0 (Baltimore, STScI)
- Goudfrooij, P., Burgh, E., Aloisi, A., Hartig, G., and Penton, S., 2010, COS 2010-10(v2), “SMOV: COS NUV Imaging Performance”
- Hartig, G., Delker, T., & Keyes, T., 2010, COS ISR 2010-04 (v1) “SMOV: COS NUV On-orbit Optical Alignment”
- Holland, S. T., et al. 2014, COS Instrument Handbook (IHB), Version 6.0 (Baltimore: STScI)
- Lallo, M., 2008, TEL ISR 2008-02, “The COS Pre-flight Aperture Model and SIAF.dat File” Osbourne, B. J., 2004, BATC SE-02 (IN0090-903), “COS Systems Hanbook and User’s Manuel” (Boulder, CO: BATC)
- Penton, S., 2001A, COS-11-0024A, “TAACOS: Phase I NUV Report”
- Penton, S., 2001B, COS-11-0014B, “Recommended TA FSW and Operations Changes Based upon the TAACOS Phase I Reports for the FUV and NUV Channels”
- Penton, S., 2002, COS-11-0016A, “TAACOS: Phase I FUV Report”
- Penton, S., 2010, “The 2010 STScI Calibration Workshop : COS: On-Orbit Performance of Target Acquisitions”
- Penton, S., & Keyes, T., 2011, COS TIR 2010-03, “On-Orbit Target Acquisitions with HST+COS”
- Penton, S., 2016, COS ISR 2016-09, “Cycle 22 HST+COS Target Acquisition Monitoring Summary” (P13972)
- Penton, S., 2017, COS ISR 2017-18, “Cycle 23 HST+COS Target Acquisition Monitoring Summary” (P14440)
- Penton, S., COS ISR 2018-22, “HST+COS LP2 Target Acquisition Enabling” (LENA3, P12797)
- Penton, S., COS ISR 2018-33, “HST+COS LP3 Target Acquisition Enabling” (FENA4, P13636)
- Penton, S. & White, J. 2018, COS ISR 2018-44, “HST+COS LP4 Target Acquisition Enabling” (P14907)
- Proffitt, C., et al., 2013, COS ISR 2013-03 “Second COS FUV LP: Verification of Aperture and FUV Spectrum Placement (FENA2, P12795)”
- Roman-Duval, J., 2015, COS ISR 2015-02, “Summary of the COS Cycle 20 Calibration Program” (P13124)
- Rose, S., et al., 2017, HST Cycle 25 Phase II Proposal Instructions (V25.0)
- Sahnow, D., & Penton, S., COS ISR 201X-YY, “COS Aperture and Spectrum Placement at LP3” (LENA1, P13634)
- Sahnow, D., & Penton, S., COS ISR 201X-ZZ, “COS Aperture and Spectrum Placement at LP4” (P14875)
- Sana, H., et. al., 2015, COS ISR 2015-06, “Summary of the COS Cycle 21 Calibration Program” (P13526)
- Smith, H., et al., 2004, “Hubble Space Telescope COS Contract End Item (CEI) Specification” (NASA STE-63, HST #TM-025984) (2004)
- Sonnentrucker, P., et. al., 2016, COS ISR 2016-03, “Summary of the COS Cycle 22 Calibration Program” (P13972)
- Taylor, J., 2017, COS ISR 2017-13, “Cycle 23 COS/NUV Spectroscopic Sensitivity Monitor” (P14441)